


Spring 2019

# Coupling Metaproteomics with Taxonomy to Determine Responses of Bacterioplankton to Organic Perturbations in the Western Arctic Ocean

Molly P. Mikan  
*Old Dominion University*

Follow this and additional works at: [https://digitalcommons.odu.edu/oeas\\_etds](https://digitalcommons.odu.edu/oeas_etds)

 Part of the [Biogeochemistry Commons](#), [Biology Commons](#), [Microbiology Commons](#), and the [Oceanography Commons](#)

---

## Recommended Citation

Mikan, Molly P. "Coupling Metaproteomics with Taxonomy to Determine Responses of Bacterioplankton to Organic Perturbations in the Western Arctic Ocean" (2019). Doctor of Philosophy (PhD), dissertation, Ocean/Earth/Atmos Sciences, Old Dominion University, DOI: 10.25777/p8gg-tr58  
[https://digitalcommons.odu.edu/oeas\\_etds/85](https://digitalcommons.odu.edu/oeas_etds/85)

This Dissertation is brought to you for free and open access by the Ocean, Earth & Atmospheric Sciences at ODU Digital Commons. It has been accepted for inclusion in OEAS Theses and Dissertations by an authorized administrator of ODU Digital Commons. For more information, please contact [digitalcommons@odu.edu](mailto:digitalcommons@odu.edu).

COUPLING METAPROTEOMICS WITH TAXONOMY TO DETERMINE RESPONSES OF  
BACTERIOPLANKTON TO ORGANIC PERTURBATIONS IN THE WESTERN ARCTIC  
OCEAN

by

Molly P. Mikan

B.S. December 2004, Colorado State University

M.S. December 2012, North Carolina State University

A Dissertation Submitted to the Faculty of  
Old Dominion University in Partial Fulfillment of the  
Requirements for the Degree of

DOCTOR OF PHILOSOPHY

OCEANOGRAPHY

OLD DOMINION UNIVERSITY

May 2019

Approved by:

H. Rodger Harvey (Director)

Brook L. Nunn (Member)

P. Dreux Chappell (Member)

David Gauthier (Member)

## ABSTRACT

# COUPLING METAPROTEOMICS WITH TAXONOMY TO DETERMINE RESPONSES OF BACTERIOPLANKTON TO ORGANIC PERTURBATIONS IN THE WESTERN ARCTIC OCEAN

Molly P. Mikan  
Old Dominion University, 2019  
Director: Dr. H. Rodger Harvey

Understanding how the functionality of marine microbial communities change over time and space, and which taxonomic groups dominate distinct metabolic pathways, are essential to understanding the ecology of these microbiomes and the factors contributing to their regulation of elemental cycles in the oceans. The primary goal of this dissertation was to investigate the community metabolic and taxonomic responses and the degradation potential of two compositionally distinct marine microbiomes within the shallow shelf ecosystem of the Chukchi Sea after rapid fluctuations in algal organic matter availability. Novel bioinformatics tools were collaboratively developed and used together with community proteomics (metaproteomics) to characterize and quantify changes in bacterial community functioning and taxonomic composition over time. 16S rRNA sequencing was employed to confirm bacterial taxonomic dynamics. These approaches were linked to particulate analyses for lipids and amino acids in order to track temporal changes in organic substrate composition. Results obtained using these improved methodological standards and the multidisciplinary approach demonstrated that organic perturbations within these systems stimulated changes to microbial taxonomic composition and functionality. The removal of organic particles seen within the control initiated a divergence between the two microbiomes while substrate abundance, as algal inputs, led to a convergence in community function. Despite the functional and taxonomic overlap seen as dominant features characterizing the responses to rapid influxes of algal organic matter, unique metabolic traits differentiated the major bacterial groups of each microbiome. This was most apparent in the recycling of nitrogen and carbon as well as substrate acquisition, suggesting that conditions which select for certain bacterial groups in the western Arctic Ocean may impact local chemical gradients. The large dataset of information obtained from this dissertation provides

insight into the timing and characterization of Arctic bacterial community responses to environmental perturbations and in turn how they influence changes in substrate composition through selective degradation of labile lipid classes. In addition, this work demonstrates the applicability of trait-based methodologies to inform on how environmental conditions may drive niche formation within complex microbial communities.

Copyright, 2019, by Molly P. Mikan, All Rights Reserved.

This dissertation is dedicated to my husband, daughter and son, and to my parents. This finished body of work would never have been completed without their continuous love, support and patience.

## ACKNOWLEDGMENTS

I express sincere appreciation for everyone that contributed to the design, analysis and completion of this dissertation. In particular, I am especially grateful for my academic advisor, H. Rodger Harvey, whose sustained support and kindness guided me throughout the many segmented stages of this dissertation. Collaboration with a group of talented scientists from the University of Washington, Genome Sciences Department (Emma Timmins-Schiffman, Michael Riffle, Damon H. May, William S. Noble and Brook L. Nunn) was essential for the development of bioinformatics tools vital to my research. This group demonstrated that a gathering of the minds and fearless approach to tackle inherent limitations within a scientific discipline can result in powerful outcomes; through this collaboration, we raised the standards for applying metaproteomic techniques to complex and uncultured natural bacterial communities. Additionally, Ian Salter assisted with experimental design, collection of samples and long hours of filtering seawater while at sea aboard the USCGC Healy, all while providing a dose of good humor. Lab work completed for this research was possible because of the expertise of so many different people, including Brook Nunn (metaproteomics and tandem mass spectrometry), Ian Salter (16S rRNA sequencing), Fred Dobbs (microbial techniques) and many members of the Harvey lab group (amino acids and lipids analysis). Last, but not least, a thank you to my academic committee members (H. Rodger Harvey, P. Dreux Chappell, Dave Gauthier and Brook L. Nunn), who provided important feedback that improved this final product.

## NOMENCLATURE

*Functional traits*: “Morphological, physiological, phenological, or behavioral features measured on organisms that can ultimately be linked to their performance.” Violle et al. [1]

*Functional-trait ecology*: An ecosystem-based approach recognizing that “the health of an ecosystem may depend not only on the number of species present, but also on the diversity of their traits.” Cernansky [2]

*Functional redundancy*: “The ability of one microbial taxon to carry out a process at the same rate as another under the same environmental conditions.” Allison and Martiny [3]

*Strict functional redundancy*: “The coexistence of organisms that share the exact same set of functions and that can readily replace each other.” Galand et al. [4]

*Metabolic plasticity*: “The potential [of bacterioplankton populations] to achieve similar ecosystem process rates [in response to environmental disturbances].” Lindh et al. [5]

*Community resilience*: “The rate at which microbial composition returns to its original composition after being disturbed.” Allison and Martiny [3]

*Community resistance*: “The degree to which microbial composition remains unchanged in the face of a disturbance.” Allison and Martiny [3]

*Replacement effect*: “Replacement of OTUs, leading to changes in community composition and functioning.” Lindh et al. [5]

*Priming effect*: “Short-term changes in the turnover rate of [soil] organic matter induced by the addition of carbon and/or nutrients [to soil].” Bird et al. [6]

*Insurance hypothesis*: “Any long-term effects of biodiversity that contribute to maintain or enhance ecosystem functioning in the face of environmental fluctuations.” Yachi and Loreau [7]



## TABLE OF CONTENTS

	Page
LIST OF TABLES .....	xi
LIST OF FIGURES .....	xii
Chapter	
1. INTRODUCTION AND OVERVIEW .....	1
2. METAPROTEOMICS REVEAL THAT RAPID PERTURBATIONS IN ORGANIC MATTER INPUTS STIMULATE FUNCTIONAL RESTRUCTURING IN ARCTIC OCEAN MICROBIOMES .....	6
2.1 Introduction .....	6
2.2 Methods .....	8
2.2.1 Seawater sample collection .....	8
2.2.2 Shipboard incubation set-up with organic amendments .....	11
2.2.3 16S rRNA: DNA extraction, library construction, and sequencing .....	11
2.2.4 16S rRNA: Bioinformatic and Statistical Analyses .....	14
2.2.5 Metagenomics: sample preparation and data analysis .....	14
2.2.6 Metaproteomics: sample preparation and data analysis .....	15
2.2.7 Peptide-based Gene Ontology (GO) enrichment analysis .....	15
2.3 Results & Discussion .....	17
2.3.1 Peptide and 16S rRNA taxonomic assignments .....	17
2.3.2 Temporal changes in community functions .....	27
2.3.3 Changes in community function under contrasting organic matter perturbations .....	36
2.3.4 Bacterial classes of Bering Strait community functions .....	38
2.4 Conclusions .....	50
3. ORGANIC MATTER PERTURBATIONS DRIVE COMPOSITIONAL AND FUNCTIONAL SHIFTS IN ARCTIC OCEAN MICROBIOMES .....	51
3.1 Introduction .....	51
3.2 Additional Methods .....	53

Chapter.....	Page.....
3.2.1 Hierarchical clustering.....	53
3.2.2 Beta-diversity statistics.....	53
3.2.3 Alpha-diversity statistics .....	54
3.2.4 Test of linearity.....	57
3.3 Results.....	57
3.3.1 Comparative taxonomic composition of the Bering Strait and Chukchi Sea .....	57
3.3.2 Organic perturbations, community composition and bacterial abundance over time ..	64
3.3.3 Alpha diversity .....	65
3.3.4 Peptide and Gene ontology (GO) identification.....	68
3.3.5 Comparative proteomic responses between microbiomes: Bering Strait community functions .....	68
3.3.6 Comparative proteomic responses between microbiomes: Chukchi Sea community functions .....	74
3.4 Discussion .....	75
3.5 Conclusions .....	84
4. SELECTIVE LOSS OF ALGAL BIOMARKERS BY DISTINCT ARCTIC OCEAN MICROBIOMES AND EVIDENCE OF ENZYME ACTIVITY THROUGH METAPROTEOMICS .....	87
4.1 Introduction.....	87
4.2 Additional Methods.....	88
4.2.1 Particulate organic carbon and nitrogen .....	88
4.2.2 Lipid extraction and analysis.....	89
4.2.3 Particulate amino acids.....	89
4.2.4 Enzyme profiles and taxonomic assignments.....	90
4.3 Results.....	90
4.3.1 Changes in fatty acid composition.....	90
4.3.2 Particulate neutral lipids .....	98
4.3.3 Biomarkers.....	98
4.3.4 Particulate amino acids.....	107
4.3.5 Bacterial enzyme profiles .....	107
4.4 Discussion .....	115
4.5 Conclusions .....	121

Chapter .....	Page
5. CONCLUSIONS.....	123
REFERENCES .....	127
APPENDICES .....	138
SUPPLEMENTAL MATERIALS.....	152
VITA.....	153

## LIST OF TABLES

Table	Page
1. Bacterial and particulate measurements.....	12
2. Mass spectrometry & gene ontology data.....	28
3. Changing functions in Bering Strait microbiome .....	30
4. Changing functions in Chukchi Sea microbiome with algal inputs.....	48
5. Functional differences between microbiomes .....	71
6. Fatty acid distributions.....	93
7. Changes in fatty acid concentrations .....	97
8. Neutral lipid distributions .....	100
9. Changes in neutral lipid concentrations .....	104
10. Lipid biomarkers.....	105
11. Distributions of lipid biomarkers .....	106
12. Amino acid concentrations .....	108
13. Enzyme Commission number data .....	110
14. Hydrolase distributions .....	113

## LIST OF FIGURES

Figure	Page
1. Sample location map.....	9
2. Water column profiles.....	10
3. Peptide spectra taxonomic categorization.....	18
4. DAG example .....	19
5. Bacterial taxonomic classes over time.....	21
6. 16S rRNA genera.....	23
7. Functional shifts in the Bering Strait microbiome over time.....	29
8. Bacterial classes associated with changing community functions.....	39
9. Chukchi Sea bacterial classes for Bering Strait functions .....	46
10. Chukchi Sea functional shifts under algal substrate inputs .....	47
11. Shepherd plot .....	55
12. Histogram.....	56
13. NMDS.....	58
14. Bray-Curtis dissimilarity trends.....	59
15. Initial compositions of bacterial communities.....	61
16. High temporal resolution of 16S rRNA bacterial classes .....	66
17. Boxplot of Shannon diversity indices.....	67
18. Heatmap of GO functions differentiating microbiomes. ....	70
19. Structure-function relationship .....	83
20. Fatty acid concentrations over time. ....	92
21. Neutral lipid concentrations over time.....	99
22. Amino acid distributions.....	109
23. Enzyme commission category distributions .....	111
24. Bacterial ester hydrolases .....	114

## CHAPTER 1

### 1. INTRODUCTION AND OVERVIEW

Microbes regulate major biogeochemical cycles within the global ocean, with profound impacts to ocean-atmosphere exchange, primary productivity and carbon sequestration (e.g., [8-10]). Identifying the factors that regulate the structuring and functionality of *in situ*, and largely uncultured, complex marine microbial communities (i.e., microbiomes) has been a fundamental research goal for decades (e.g., [11]). Standard measures of microbial activity such as bacterial production, enzymatic activity and compositional changes to substrates within the environment (e.g., [12-15]) have historically been used to show that taxonomically distinct communities are not functionally uniform, supporting evidence that some microbes are better equipped to respond to stimulus by initiating specific chemical transfers and/or reactions (e.g., [16-20]). Recent progress has indicated that the organic matter environment (e.g., chemical composition and concentration) is an essential regulatory factor influencing microbial community composition and activity, which simultaneously alters both the abundance and composition of organic matter substrates used for growth and energy production (e.g., [17, 19, 21, 22]). Linking bacterial activity to ecosystem function and unraveling the taxonomic identity of the microbes that dominate distinct community functions remains a primary research goal in marine microbial ecology.

The advancement of -omic methodologies (genomics, transcriptomics, proteomics, and metabolomics) has provided molecular-level insights into the physiological diversity of microbes, which have been used to identify specific responses to environmental stimuli with implications to oceanic biogeochemical cycles (e.g., [23-28]). In particular, the application of tandem mass spectrometry to identify and quantify protein profiles within natural systems has exponentially increased over the past decade. Due to the tight cellular regulation of protein synthesis and internal degradation, protein abundances reflect the metabolic status of a single cell or community of organisms [29]. Provided that proteins dominate the majority of functions

within the cell, protein abundances can serve as useful proxies for cellular function, informing on the response and adaptation to environmental conditions [30, 31].

Each of the -omic technologies contains some inherent limitations, especially when applied to complex communities within natural systems [32]. As traditional (medical) proteomics techniques were developed with single organisms or target molecules in mind, the transfer of this powerful methodology to analyze complex communities of organisms (i.e., metaproteomics) reveals a range of bioinformatic challenges, many of which have yet to be dissected and overcome. The methodological constraints are further amplified when employing metaproteomics techniques to track communities of organisms whose genomic profiles may, or may not, be categorized. This latter concern is prevalent in environmental microbial communities, where it is thought that a myriad of organisms remain uncharacterized. In addition, these methods are all known to produce astounding amounts of data, lending to additional bioinformatics hurdles that require statistical checks and verification of data quality prior to reporting. Thus, methodological consistency between research groups, reproducibility of results and unbiased analysis must be considered in order to compose robust ecological conclusions from this type of data across oceanic regions.

The first steps of this dissertation were spent in collaboration with an interdisciplinary team of scientists to coalesce oceanography, biochemistry, bioinformatics, and computer sciences with the goal to construct, test, and apply rigorous methodological standards to the processing of complex microbial metaproteomics data. These collaborative efforts improved methodological standards [33-36], a critical contribution to the field of environmental metaproteomics. These methodological advancements benefit microbial ecology research efforts by providing the framework to identify and quantify statistically significant changes to functions over time (or differences between communities or treatments), in addition to allowing identification and quantification of taxonomic associations with those functions. Specifically, these are important features applicable to the development of trait-based approaches in the study of systems ecology.

Integrating the new innovative metaproteomics methods with standard methods to identify bacterial community composition (16S rRNA sequencing) and organic geochemistry,

this dissertation addresses important topics in the field of marine microbial ecology, including 1) functional responses of complex microbial communities to rapid organic substrate perturbations, 2) how the organic environment restructures the compositional and functional properties of microbiomes and 3) the enzymatic capacity of microbiomes to alter the organic geochemistry of substrates. Direct measures of bacterial community composition and metabolism in parallel with select particulate organic matter (POM) composition profiles were tracked over time, providing a rare opportunity to investigate how bacterioplankton respond to perturbations in their organic environment and how these community dynamics in turn influence changes in POM composition. Such reactions occur continually in the global oceans but the relationship between organic chemical composition and microbial functional and structural responses is poorly known. The geographic focus was the western Arctic Ocean (specifically within the Chukchi Sea) where both the seasonal timing of primary production and the important role of microbial recycling might provide valuable insight into nutrient and carbon cycling.

In the first research chapter of this dissertation (Chapter 2) I examined metaproteomes from two Arctic microbiomes collected from the Bering Strait subsurface chlorophyll maximum and the Chukchi Sea bottom water over a short shipboard incubation to track the functional and taxonomic responses of these communities to rapid perturbations of the organic environment (by first removing POM  $>1.0 \mu\text{m}$  in size and then simulating algal bloom conditions compared to a control treatment where POM was removed without subsequent algal inputs). Using a novel peptide-based enrichment analysis, significant changes ( $p\text{-value} < 0.01$ ) in biological and molecular functions associated with carbon and nitrogen recycling were observed. Under both organic matter conditions, Bering Strait surface water core microbiomes increased peptides correlated to protein synthesis, carbohydrate degradation and cellular redox processes while decreasing C1 metabolism within the first day. Taxonomic examinations of the functional progression revealed that the core microbiome collectively responded to algal substrate inputs by synthesizing carbon prior to select bacterial groups utilizing and re-allocating nitrogen intracellularly. Incubations of Chukchi Sea bottom water microbiomes showed similar, but temporally delayed, functional responses to identical conditions. This has important implications for the timing and magnitude of measured microbial responses to organic perturbations within the Arctic Ocean and provides unbiased analysis of how community-level functional composition could contribute to predicting biogeochemical gradients in the ocean.



Throughout the global ocean, the base of the food web is characterized by tight biological connections dominated by primary producers and heterotrophic bacterioplankton. In the highly productive, shallow shelf ecosystem of the Chukchi Sea, however, frequent temporal uncoupling can occur due to changes in sea ice dynamics and nutrient availability in a warming climate. How potential changes in primary productivity substrate availability will impact oxidation by *in situ* heterotrophic bacterioplankton is partially dependent on the activity of the community (i.e., taxonomic composition and function). The second research chapter (Chapter 3) describes the integration of 16S rRNA and metaproteomics datasets to investigate the responses of the two compositionally distinct Arctic bacterial communities following organic matter perturbation, revealing that rapid shifts in substrate availability influenced taxonomic and metabolic changes to both microbiomes. In particular, I revealed that the addition of algal organic substrates led to a convergence of metabolic functioning between the two microbiomes while the controlled incubation conditions (resource limitation as POM removal) drove taxonomic composition and function to become more distinct. An important outcome was that time and environment differentiated traits between microbiomes (i.e., surface water bacteria access carboxylic acid more rapidly under algal substrate abundance) and taxonomic composition can influence what traits are expressed (i.e., a non-dominant bacterial class, Planctomycetia, reduces nitrate to produce energy), possibly leading to the formation of unique niches within a natural community after organic matter perturbations. Lastly, results gathered from this work that may benefit modeling efforts incorporating trait-based mechanisms with taxonomic associations are discussed.

Taxonomic composition of microbial communities may be influenced by the availability of organic matter and nutrients (e.g., [19, 37, 38]) yet how compositionally distinct microbiomes impact changes to organic composition during degradation and the timeframe over which this occurs remains unclear. In the third research chapter (Chapter 4), temporal changes to the composition of POM injected into the incubations were tracked with lipid and amino acid analyses to address the question of degradation efficiencies. In addition, I sought to link these compositional shifts within the particulate substrates with bacterial enzymatic profiles and taxonomy derived from the metaproteomic datasets. As evidence for bacterial enzymatic expression increased and bacteria became more abundant, selective losses of lipid classes occurred even as bulk particulate measures increased. These results collaboratively indicate that

select portions of the substrates were bioavailable over this time frame, as they were susceptible to enzymatic attack and degradation by the Arctic Ocean bacterioplankton. The results also demonstrated some distinction in degradation potential of the labile lipids depending on the origin of the microbial community. An important observation was that the surface water community appeared more effective at recycling fatty acids than the bottom water community while the latter microbiome decreased an algal pigment to a greater degree over the ten day incubation period. Regardless of these differences in the scale of degradation, a common order of lipid class loss occurred over time. Increases of bacterial enzymes specific to ester hydrolysis occurred prior to the decreases in lipid concentrations, suggesting a link between these two datasets.

## CHAPTER 2

2. METAPROTEOMICS REVEAL THAT RAPID PERTURBATIONS IN ORGANIC  
MATTER INPUTS STIMULATE FUNCTIONAL RESTRUCTURING IN ARCTIC OCEAN  
MICROBIOMES<sup>1</sup>

## 2.1 Introduction

In the surface ocean, primary production driven by phytoplankton growth dynamics is the essential process for the transfer of carbon from inorganic to organic pools and structures the food web for higher trophic consumers. While a fraction of this organic material (OM) supports upper trophic levels, the microbial loop recycles the majority of OM in the water column with only a small fraction eventually sequestered in the deep oceanic sediments [10]. Linking microbial functionality to biogeochemical cycling has remained a primary objective of microbial ecology for decades. This functionality is predominantly regulated by a complex mixture of Bacteria, Archaea, and Eukarya. In particular, the bacterioplankton component differs in their uptake ability of organic matter [16, 39]. This differential response of bacteria to organic substrates has led to the observation that the heterotrophic community, and the associated core metabolic genes, may be structured by organic substrate availability [38]. As the complexity and often trace-level concentrations of thousands of metabolites make them a challenge to track in the ocean, researchers are exploring the use of technologies to track the physiological response of the microbial community to the changing chemical compositions in order to understand the local chemical environment as well as the dynamic relationship between microbiota and their environment [18, 26, 38, 40].

Since proteins carry out the majority of molecular functions and are tightly regulated within the cell, their characterization, quantification, and timing of expression can serve as a biologically relevant proxy for the organism's current phenotype. Consequently, changes in a metaproteome (i.e., community proteome) in response to changes in local environmental

---

<sup>1</sup> A manuscript version of this chapter is being submitted to the ISME Journal, March 2019

conditions should reflect temporally relevant metabolic strategies of a natural microbiome. Several studies have successfully linked bacterial metabolic responses to important biogeochemical cycles, with some reporting high taxonomic resolution [23, 24, 40-43]. These discovery-style metaproteomic analyses have shown insights into the physiological responses of oceanic bacteria, revealing shifts in order- or genus-level taxonomy and detailed functionality through time (e.g., [24, 41]). Nevertheless, as most metaproteomic pipelines are adaptations of traditional single-species proteomic approaches, there are inherent complications that emerge when multiple species are analyzed in a single sample [44, 45], in particular the assignment of an identified peptide to multiple protein sequences from the provided genome [46, 47]. In the case of a native oceanic microbiome where many species are present and few are cultured, a single peptide can be conserved across many proteins which may differ not only in predicted functions, but map to proteins across multiple species, genera, families, or even phyla [34, 48-51].

Using a novel metaproteomics approach, I report the response of two Arctic microbial communities to rapid changes in organic availability within short-term shipboard incubations. Before experimental manipulations were initiated, metagenomes of the native microbial population were completed to generate a site-specific reference database for peptide identification [34]. Then, a mass spectrometry-based metaproteomics analysis was completed on incubation samples to track temporal functional responses and 16S rRNA sequencing was completed to resolve taxonomic distributions of the microbial populations through time. To track microbial responses to organic matter input and minimize artifacts associated with bottle effects, experimental incubations were short term (10 days) and carried out at near *in situ* temperatures (0°C). To address the critical need to identify and trace relevant metabolic strategies of the microbiome expressed as proteins, a novel peptide-based strategy was developed that avoids protein inference and instead, using a site-specific metagenome, creates a lowest common ancestor assignment for each peptide on a functional and taxonomic tree. This new approach was coupled to a biological enrichment strategy to identify statistically significant shifts in community function through the quantification and comparison of all peptides associated with a function through time, thereby allowing unbiased reporting of all peptides identified [36]. Once those changing functions were revealed, each functional shift was followed by a detailed taxonomic analysis using the peptide data and supported by taxonomic assignments through 16S rRNA sequencing.

With this methodology, the accuracy in reporting functions distributed among different taxonomic groups of a mixed community is increased, the statistical robustness is enhanced and the resolution is more amenable to large scale functional modeling efforts. The simultaneous measurement of expressed metabolic responses to rapid OM perturbation without limiting the analysis to specific processes or taxonomic groups allowed the comprehensive metabolic response of the entire Arctic microbial community to be determined over time. With this novel method I demonstrate that natural Arctic microbiomes undergo functional restructuring related to carbon (C) and nitrogen (N) cycling shortly after rapid perturbations to their organic substrate environments thereby revealing implications for broader biogeochemical cycles.

## 2.2 Methods

### 2.2.1 Seawater sample collection

Seawater was collected from the subsurface chlorophyll maximum (SCM) of the Bering Strait and from the bottom waters of the Chukchi Sea (Figure 1) as described in May et al. [33]. Water was collected from different depths and sites to target microbiomes that were expected to be taxonomically distinct based upon physicochemical parameters (Figure 2). Waters were filtered by sequential size fractionation through 10.0  $\mu\text{m}$  and 1.0  $\mu\text{m}$  filters to isolate the free-living bacteria from eukaryotic grazers  $> 1.0 \mu\text{m}$  in size and to remove particulate organic matter (POM) before incubation. Initial genomic content from the Bering Strait and Chukchi Sea were collected in order to establish a site-specific metagenomics database for peptide identification. For the metagenome, 7 L of 1.0  $\mu\text{m}$  filtered water from each station was isolated onto 0.2  $\mu\text{m}$  polycarbonate (PC) filters (Whatman Nuclepore), immediately frozen in liquid nitrogen and stored at  $-80 \text{ }^\circ\text{C}$  until DNA extraction.

**Figure 1 - Sample location map.** Map showing locations of water sampling from the Bering Strait (BSt; 7m; 65° 43.44" N, 168° 57.42" W) and the Chukchi Sea (CS; 55.5 m; 72° 47.624" N, 164° 53.89" W).

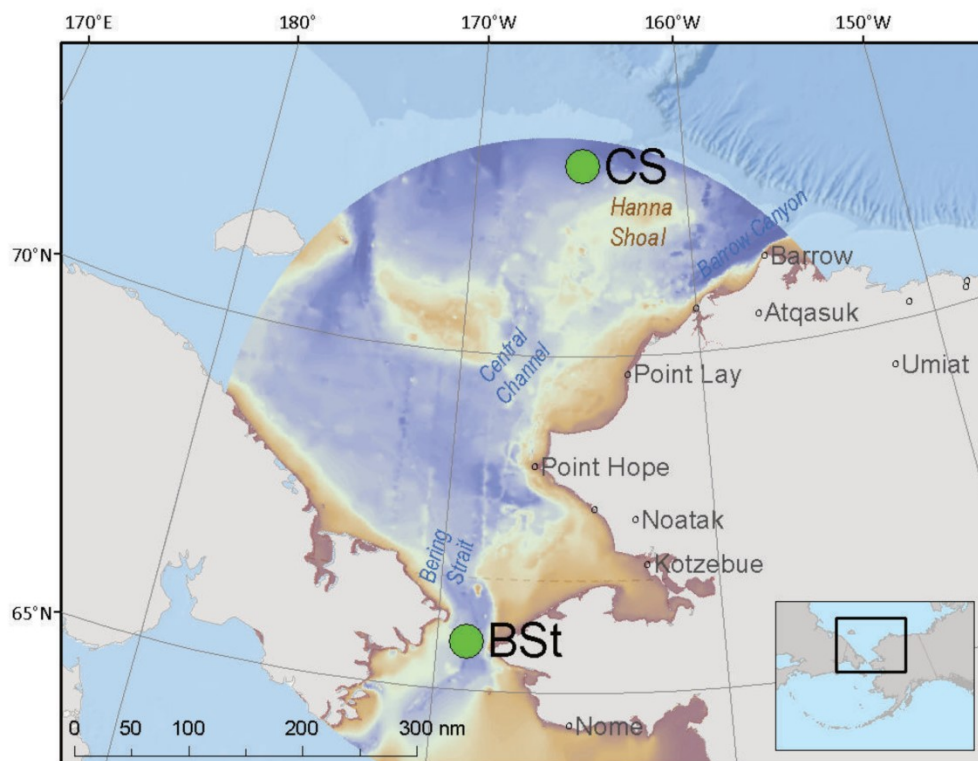
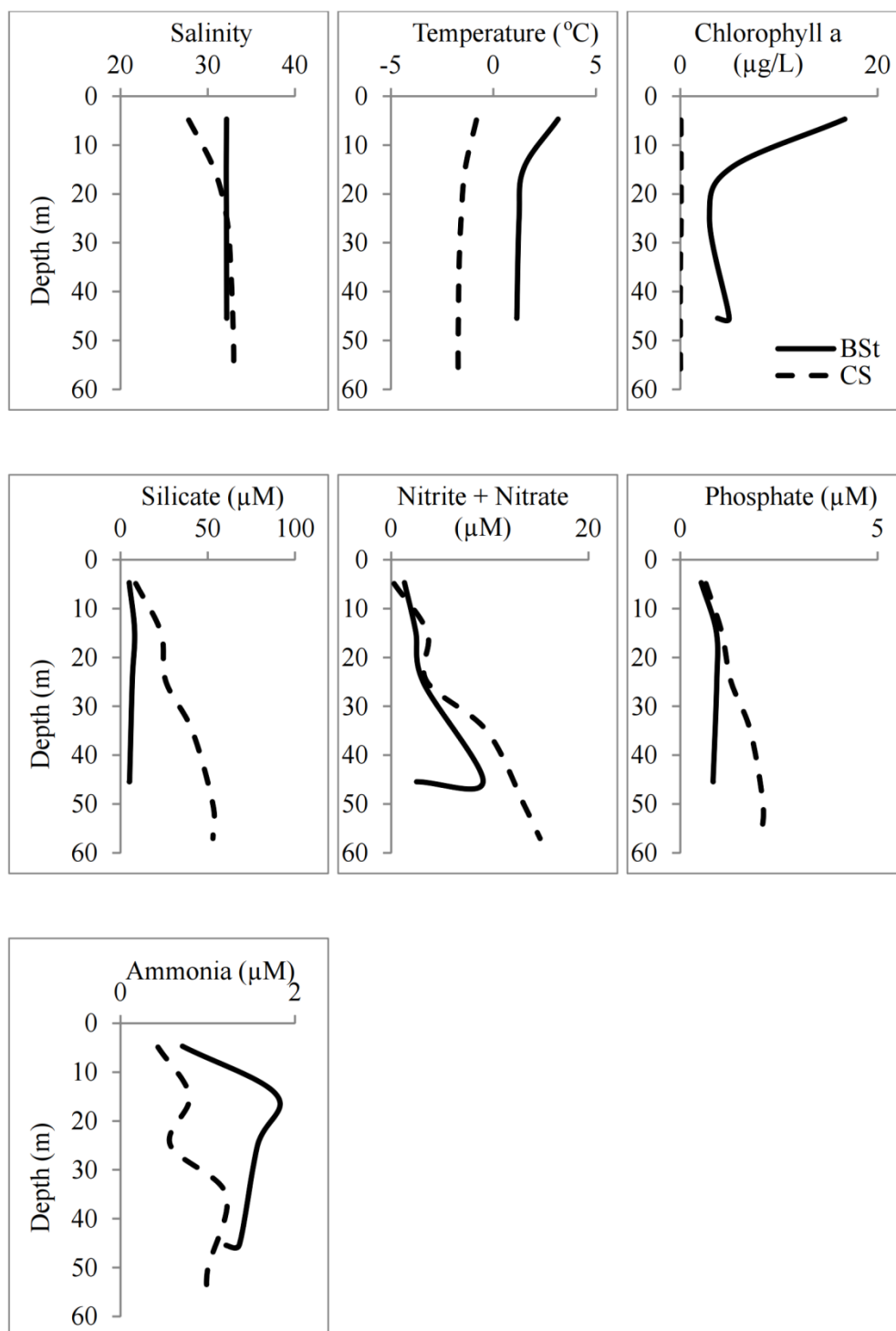


**Figure 2 – Water column profiles.** Salinity, Temperature, Chlorophyll a and nutrient concentrations from the water column of the Bering Strait (BSt) (solid line) and Chukchi Sea (CS) stations (dashed line). Water was collected from 7 m in the BSt (integrated chlorophyll a: 226.88 mg/m<sup>2</sup>) and 55.5 m from the CS (integrated chlorophyll a: 2.64 mg/m<sup>2</sup>). Data was provided by Lee Cooper: <http://arcticstudies.org/hannashoal/data.html>.



### 2.2.2 Shipboard incubation set-up with organic amendments

To examine bacterial community response to organic amendments, 60 L of 1.0  $\mu\text{m}$  prefiltered seawater from the Bering Strait and 60 L of 1.0  $\mu\text{m}$  prefiltered seawater from the Chukchi Sea were incubated shipboard for ten days at 0 °C in the dark. The first 40 L of seawater from each station were distributed among two, 20 L carboys to act as biological replicates. Each was supplemented with *in situ* algal organic matter (aOM) between 5.0-10.0  $\mu\text{m}$  in size (Table 1). The organic matter substrate was collected, filtered and then concentrated from the subsurface chlorophyll maximum of the Bering Strait and was considered to be primarily of algal origin based on C/N ratios  $\sim$ 5 at day 0 (Table 1). Before addition, the algal substrate was frozen to kill cells and encourage cell lysis and release of bioavailable dissolved organic matter (DOM) to the bacterial community. Before subsampling, water from each biological replicate was collected, and then mixed prior to filtration. 20 L of the 1.0  $\mu\text{m}$  prefiltered seawater from each station received no aOM input after POM  $>1.0 \mu\text{m}$  was removed to examine bacterial responses to incubation conditions and residual DOM, thus functioning as the control treatment (POM removal). At the initial time of sampling and on days 1, 6 and 10 of the incubation experiments, a total of 1.8 L of water were passed through a 1.0  $\mu\text{m}$  filter, collected onto duplicate or triplicate 0.2  $\mu\text{m}$  PC filters, flash frozen in liquid nitrogen and stored at -80 °C for bacterial metaproteomics analysis. Bacterial abundance and compound analysis method details (total hydrolysable amino acids, organic carbon & nitrogen) can be found in Supplementary text 1.

### 2.2.3 16S rRNA: DNA extraction, library construction, and sequencing

Methods for 16S rRNA isolation and amplicon sequencing followed Fadeev et al. [52]. Briefly, samples of bacterial DNA were isolated from filter membranes in a combined chemical and mechanical procedure using the PowerWater DNA Isolation Kit prior to using it as the template for PCR amplification (MO BIO Laboratories, Inc., Carlsbad, CA, USA). Library preparation was performed according to instructions provided by Illumina: 16S Metagenomic Sequencing Library Preparation (Illumina, Inc., San Diego, CA, USA). 16S rRNA sequences were obtained on the Illumina MiSeq platform in a  $2 \times 300$  bp paired-end run as well as in a  $2 \times 250$  bp paired-end run on the Illumina HiSeq platform (CeBiTec Bielefeld, Germany).



**Table 1 – Bacterial and particulate measurements.** Bering Strait (BSt) and Chukchi Sea (CS) bacterial and particulate organic matter (POM) measurements from the 10 day incubation experiments. BDL = below detection limit. sd = standard deviation. Dark grey cell = estimated value (see details in Supplementary text 1). aOM input = algal organic matter input; POM removal = control treatment where POM >1.0 µm was removed without aOM input. THAA = total hydrolysable amino acids. ON = organic nitrogen; OC = organic carbon. PC = 0.2 µm polycarbonate filters (Whatman Nuclepore). GF/F = glass fiber filters (Whatman).

Station	Analysis	Filter	Initial	aOM input			
				day 0	day 1	day 6	day 10
Bering Strait, 7 m (65° 43.44' N, 168° 57.42' W)	<u>bacterial measurements</u>						
	cell counts (cells/ml)	0.2 µm PC < 10 µm	5.02E+05				2.46E+06
	cell counts (cells/ml)	0.2 µm PC < 1 µm	2.02E+05				
	bacterial ON (µg/l)	GF/F	59.9	30			64
	bacterial OC (µg/l)	GF/F	209	BDL			193
	bacterial THAA (µg/l) (sd)	GF/F			16.9 (15.4)		25.0 (2.1)
	<u>POM measurements</u>						
	POC (mg/l) (sd)	GF/F		0.24 (0.02)	0.27 (0.02)	0.34 (0.01)	0.33 (0.00)
	PON (mg/l) (sd)	GF/F		0.05 (0.01)	0.05 (0.01)	0.07 (0.00)	0.08 (0.00)
	particulate C/N			4.80	5.40	4.86	4.13
particulate THAA (µg/l) (sd)	GF/F			89.56 (36.29)		176.50 (50.20)	
Chukchi Sea, 55.5 m (72° 47.624' N, 164° 53.89' W)	<u>bacterial measurements</u>						
	cell counts (cells/ml)	0.2 µm PC < 10 µm	5.14E+05	3.18E+05		1.28E+06	2.22E+06
	cell counts (cells/ml)	0.2 µm PC < 1 µm	2.07E+05				
	bacterial ON (µg/l)	GF/F	24.5	23.2			54.5
	bacterial OC (µg/l)	GF/F	BDL	BDL			107
	bacterial THAA (µg/l) (sd)	GF/F			12.4 (2.5)		66.8 (1.2)
	<u>POM measurements</u>						
	POC (mg/l) (sd)	GF/F		0.20 (0.00)	0.20 (0.00)	0.31 (0.00)	0.26 (0.01)
	PON (mg/l) (sd)	GF/F		0.04 (0.00)	0.04 (0.00)	0.07 (0.00)	0.06 (0.00)
	particulate C/N			5.00	5.00	4.43	3.33
particulate THAA (µg/l) (sd)	GF/F			55.90 (2.50)		150.26 (0.43)	

Table 1 – continued.

Station	Analysis	Filter	Initial	POM removal			
				day 0	day 1	day 6	day 10
Bering Strait, 7 m (65° 43.44" N, 168° 57.42" W)	<u>bacterial measurements</u>						
	cell counts (cells/ml)	0.2 µm PC < 10 µm	5.02E+05				1.23E+06
	cell counts (cells/ml)	0.2 µm PC < 1 µm	2.02E+05				
	bacterial ON (µg/l)	GF/F	59.9	24.5			34.1
	bacterial OC (µg/l)	GF/F	209	BDL			BDL
	bacterial THAA (µg/l) (sd)	GF/F					
	<u>POM measurements</u>						
	POC (mg/l) (sd)	GF/F					
	PON (mg/l) (sd)	GF/F					
	particulate C/N						
particulate THAA (µg/l) (sd)	GF/F						
Chukchi Sea, 55.5 m (72° 47.624" N, 164° 53.89" W)	<u>bacterial measurements</u>						
	cell counts (cells/ml)	0.2 µm PC < 10 µm	5.14E+05			2.82E+05	
	cell counts (cells/ml)	0.2 µm PC < 1 µm	2.07E+05				
	bacterial ON (µg/l)	GF/F	24.5	16.3			16.3
	bacterial OC (µg/l)	GF/F	BDL	BDL			BDL
	bacterial THAA (µg/l) (sd)	GF/F					
	<u>POM measurements</u>						
	POC (mg/l) (sd)	GF/F					
	PON (mg/l) (sd)	GF/F					
	particulate C/N						
particulate THAA (µg/l) (sd)	GF/F						

#### 2.2.4 16S rRNA: Bioinformatic and Statistical Analyses

Methods for 16S rRNA sequencing followed methods detailed in Fadeev et al. [52]. Briefly, the raw paired-end reads were primer-trimmed using cutadapt [53], quality trimmed using trimmomatic v0.32 [54] and merged using PEAR v0.9.5 [55]. Clustering into operational taxonomic units (OTUs) was done with Swarm algorithm using default parameters (v2.0) [56]. One representative sequence per OTU was taxonomically classified using SINA (SILVA Incremental Aligner; v1.2.11; Silva reference database release 128) at a minimum alignment similarity of 0.9, and a last common ancestor consensus of 0.7 [57]. OTUs which were not taxonomically assigned as bacteria or occurred with only a single sequence in the whole data set were excluded from further analysis. Pearson correlation (*rcorr* function, Hmisc package in R) was used to test for linear correlation of relative abundance data between genera composing >5% of total abundances.

#### 2.2.5 Metagenomics: sample preparation and data analysis

To produce a protein sequence database from which all peptide tandem mass spectra could be correlated, a metagenome was completed by combining filtered bacteria present at the initial time points from both the Bering Strait and Chukchi Sea. DNA from filters collected from initial Bering Strait and Chukchi Sea waters were extracted for bacterial metagenome sequencing following the protocol in Wright et al. [58]; this was followed by library preparation using the Kapa Hyper Kit, as previously described [33]. Libraries were quality checked and then sequenced on an Illumina HiSeq 2500 (PE100) in one lane. Raw sequencing reads were deposited in the NCBI Short Read Archive under accession number SRP071900. MOCAT was used to process raw reads, remove human contaminating sequences, assemble the reads and generate protein sequences [59]. This generated a protein FASTA file with 459,118 protein sequences and >41 million unique tryptic peptide sequences from which all peptide tandem mass spectra can be correlated and scored (metagenome predicted protein database is available at ProteomeXchange: PXD008780).

### 2.2.6 Metaproteomics: sample preparation and data analysis

Metaproteomic sample preparation and liquid chromatography and tandem mass spectrometry (LC-MS/MS) followed methods detailed in Timmins-Schiffman et al. [34]. Briefly, filters were sliced (2 mm<sup>2</sup>) and submerged in 100 µl of 6 M urea and 600 µl of 50 mM NH<sub>4</sub>HCO<sub>3</sub>. Cells were lysed with a sonicating probe (5 x 20s) and between sonication events each filter was flash-frozen in liquid nitrogen to reduce protease activity. The lysate was removed and proteins were reduced and alkylated using dithiothreitol (DTT) and iodoacetamide (IAM), respectively. Samples were then digested with Trypsin (1:20 enzyme to protein) for 12 hours at room temperature on a shaker. Resulting peptides were desalted with C18 centrifugal spin columns, dried down and resuspended in 2% ACN, 0.1% formic acid prior to analysis with a nanoAcquity UPLC (Waters Corp, Milford, MA) inline with a Q-Exactive-HF (Thermo Fisher Scientific, Waltham, MA). Prior to injection into the LC-MS/MS, biological replicates were combined due to low protein concentrations and then were analyzed in duplicate on the Q-Exactive in random order using a 90 minute gradient (5%-30% ACN, 0.1% formic acid, 300 nl/min), data dependent acquisition (DDA) top 20, with an MS1 scan range of 400-1000 m/z. The mass spectrometry proteomics data can be found at ProteomeXchange Consortium via the PRIDE [60] partner repository (<https://www.ebi.ac.uk/pride/archive/projects/PXD008780>). All database searches were performed using Comet [61] version 2015.01 rev. 2 against concatenated target and decoy versions of the Bering Strait/Chukchi Sea metagenome-derived proteome, as previously described [34]. Prior to further analysis, Comet results for technical replicates were combined. Peptide-spectrum matches were retained at a 1% false discovery rate (FDR) based on target-decoy competition optimized by the Percolator algorithm [62, 63]. Mass spectrometry samples from the Chukchi Sea control incubation at day 1 were compromised and excluded from analysis. Analysis using the traditional proteomic pipeline (i.e., trans-proteomic pipeline – TPP [64]), that includes protein inference and grouping on all identified peptides revealed that 35% of all identified peptides correlated to >1 protein sequence in the Bering Strait/Chukchi Sea metagenome-derived proteome.

### 2.2.7 Peptide-based Gene Ontology (GO) enrichment analysis

The abundance of Gene Ontology (GO) functional categories for molecular functions, biological processes and cellular components [65, 66] were quantified using the method

described by Riffle et al. [36]. Briefly, each peptide was associated with all metagenome proteins containing it, and then those proteins were matched by BLAST to UniProtKB/TrEMBL (downloaded April 28, 2015), keeping the top matches with maximum e-value  $1E-10$ . The GO annotations of each top match (and their ancestors) were used to construct a directed acyclic graph (DAG) containing all GO terms associated with the peptide, and the spectral count for each GO term was increased by the spectral count of the peptide. Once all peptides were processed, the spectral count for each term was then divided by the total spectral count to obtain the relative abundance.

To determine the relative contribution of each taxon to each GO term, every peptide was assigned the taxon representing the lowest common ancestor (LCA) of all of the top BLAST hits for the metagenome proteins containing the peptide (in-house Python script; released as open software 2018: MetaGOmics [36]). The spectral counts for the LCA and all ancestor taxa were incremented by the spectral count for each respective peptide, and after all peptides were examined this spectral count was divided by the spectral count for the GO term. This produced a proportion of all spectra for a GO annotation that was unambiguously contributed by each taxon. At most, the relative contribution of all taxa at the same taxonomic level (e.g., class) would be 1 if all peptides for that GO term resulted in a LCA at the class level or more granular. Although tables with all the taxonomic distributions for the functions across all time points and incubations were provided (Datasets 1-4), one taxonomic level must be selected in order to compare datasets at a functional level. Here functional changes at the class level are reported in order to utilize as much of the peptide evidence as was possible without being too broad on the classification level. Using class level resolution, 85% of the total peptide spectrum matches (PSMs) were utilized in the Bering Strait incubations (2,276,392 PSMs) (Figure 3). Reporting at the genus or family level, however, would have resulted in a 53% or 33% loss in total available peptide data, respectively. When peptides could not be matched to a taxon or they were matched to a LCA less granular than class (e.g., phylum), the relative contributions at the class level added up to less than 1. When this occurred, the difference was assigned to an Unclassified taxonomic group. After this calculation, non-bacterial PSM counts were removed from further analysis (Appendix 1).

An enrichment analysis of GO functions was performed using methods described previously [36]. Briefly, each pair of mass spectrometry runs was compared against one another, first performing Laplace-correction on the spectral count of each GO term, and the  $\log_2$  fold change calculated for the relative abundance of each GO term (Figure 4). For this study, sequential time points within each experiment were compared (i.e., initial Bering Strait sample compared to day 1, day 1 compared to day 6, and day 6 compared to day 10). Terminal GO terms (those most specific in the DAG) with Bonferroni-corrected p-value  $< 0.01$  from a two-tailed test of proportions were considered significant and were included in the enrichment analysis. All source code for calculating GO spectral counts, taxonomic analysis, and comparing results between samples is available at <https://github.com/metagomics/mmikan-metaproteomics-2018>.

## 2.3 Results & Discussion

### 2.3.1 Peptide and 16S rRNA taxonomic assignments

Within the Bering Strait and Chukchi Sea microbiomes, metaproteomics data identified peptides correlating to 30 and 25 bacterial classes, respectively (Appendix 2), and 16S rRNA OTUs corresponded to 53 and 63 classes, respectively (Appendix 3). Alphaproteobacteria, Flavobacteriia (referred to as Flavobacteria) and Gammaproteobacteria bacterial classes represented greater than 75% of the metaproteomics identifications in the Bering Strait and 66% in the Chukchi Sea over the 10 day incubations (Figure 5). From the 16S rRNA identifications, these three classes also had similarly high contributions at over 91% and 86% of abundances, respectively, demonstrating that these major classes dominated both the expressed functions and taxonomic distributions irrespective of OM perturbation. These comparisons demonstrate that a peptide-based analysis complements traditional 16S rRNA sequencing for identifying dominant taxonomic classes within a complex community, as well as providing active functions at the time of collection. An important caveat, however, is that the two methods for taxonomic identification were not identical, indicating that structure of a microbiome does not necessarily equal community function (e.g., [23, 67-69]).

**Figure 3 – Peptide spectra taxonomic categorization.** Distribution of taxonomic assignments that can be reported for all peptide spectrum matches (PSMs) passing confidence threshold for A) Bering Strait and B) Chukchi Sea metaproteomics data. Note that in both figures, more PSMs were assigned a species-level designation than a genus level designation. This is counterintuitive and results from the inconsistencies found within the taxonomic databases. Many taxonomic assignments were missing genus-level information and because this was an automated data processing step, manual interpretations were not completed to retain reproducibility.

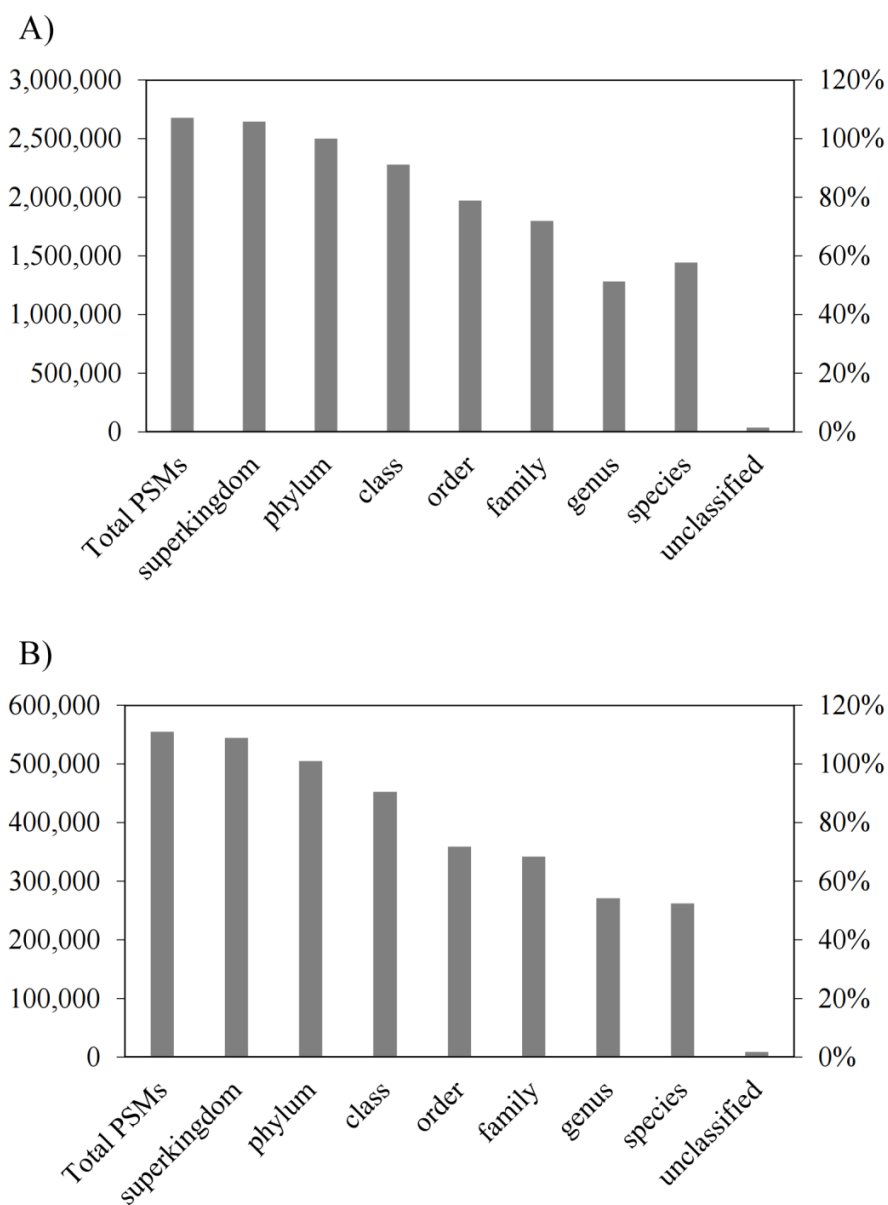
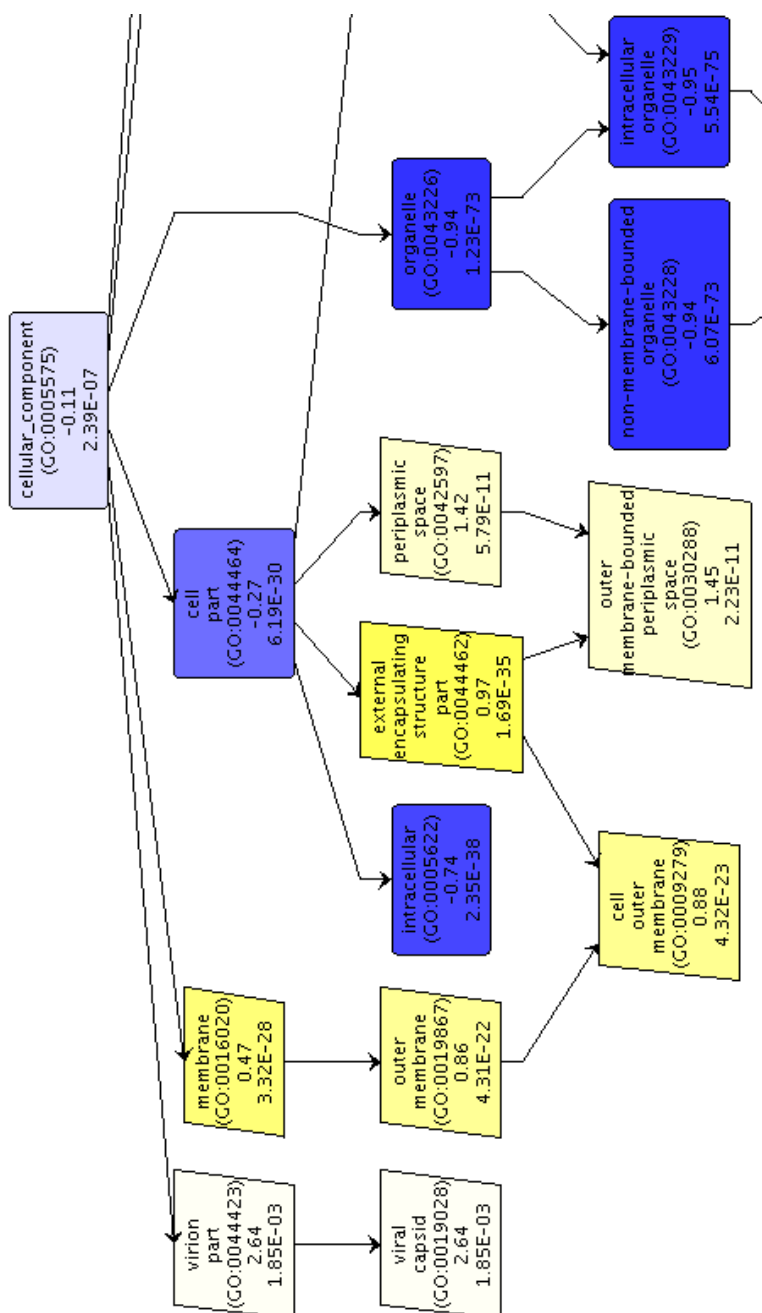


**Figure 4 - DAG example.** Example of part of a Gene Ontology (GO) directed acyclic graph (DAG) displaying cellular component functional changes within the Bering Strait (BSt) microbiome between day 1 and day 6 under algal organic matter input (aOM). The GO accession number is shown in parentheses, followed by  $\log_2$  fold changes and a two-tailed test of proportions p-value (Bonferroni corrected) for each term. Blue shading represents terms with a decrease in function over time and yellow shading represents terms with an increase in function over time. Terminal GO terms with a p-value  $< 0.01$  were considered significant, and were included in the enrichment analysis.





To increase the community taxonomic resolution, 16S rRNA OTUs were also organized into genera comprising >5% of total abundances (Figure 6; Dataset 5). This resulted in eleven genera dominating bacterial abundances in both the Bering Strait and Chukchi Sea microbiomes throughout the incubations. At the genus level, the 16S rRNA revealed less compositional stability under OM perturbation compared to temporal changes at the class level. For example, the consistently high abundances of Gammaproteobacteria within the Chukchi Sea incubation concealed inverse changes between Gammaproteobacterial genera *Balneatrix* spp. and the unclassified *Oceanospirillales* spp. within the control incubation ( $r = -0.97$ ,  $p < 0.01$ ).

Incubation results also documented that community taxonomic restructuring was dependent on the native initial microbiome (i.e., Chukchi Sea or Bering Strait), the OM treatment and time after perturbation (Figure 6). For example, *Polaribacter* spp. increased after the addition of algal-derived OM (aOM input) within both the Bering Strait and Chukchi Sea, displaying inverse relationships with *Pelagibacter* spp. (referred to as SAR11) ( $r = -0.98$ ,  $p < 0.01$ ), the unclassified *Oceanospirillales* spp. ( $r = -0.89$ ,  $p < 0.01$ ) and the sum of all other genera that contributed less than 5% abundances ('Other') ( $r = -0.72$ ,  $p < 0.01$ ). This suggests that Arctic *Polaribacter* spp. effectively outcompete other genera when labile substrates become abundant. Differences in the proteomic response time after perturbation was apparent between the two microbiomes, with largest changes in bacterial restructuring after aOM input delayed within the Chukchi Sea incubation (restructuring occurred between days 2 and 4 rather than between days 0 and 2 as in the Bering Strait microbiome). Class-level analysis of metaproteomics data corroborated a temporal offset in Flavobacterial activity between microbiomes after an influx of algal substrates (Figure 5). Within the Chukchi Sea, unclassified *Oceanospirillales* spp. and *Pelagibacter* spp. dominated the initial community, but declined late in the incubation within the control (6-10 days after POM removal) while *Balneatrix* spp., *Colwellia* spp. and *Acinetobacter* spp., plus those genera that contributed less than 5% abundances ('Other'), appeared to benefit from POM removal within the control. Opportunistic genera and, in particular, less abundant microbes in the Arctic Ocean, can have the metabolic flexibility to fill dynamic niches by accessing complex OM under substrate limitation [70], which may explain the observed shift in the taxonomic distribution after POM removal.

**Figure 5 - Bacterial taxonomic classes over time.** Changes in A) Bering Strait (BSt) and B) Chukchi Sea (CS) bacterial community taxonomic classes under variable organic matter conditions (aOM input = algal organic matter input; POM removal = control treatment where particulate organic matter (POM) >1.0  $\mu\text{m}$  was removed without aOM input) during shipboard experiments over ten days seen as the relative abundance contribution of major taxonomic classes (>1%) from the BSt proteome dataset (protein) and by 16S rRNA sequencing (rRNA). Symbol \* = class comprises >1% of proteome dataset but <1% of 16S rRNA dataset and symbol ^ = class comprises >1% of 16S rRNA dataset but <1% of proteome dataset. Mass spectrometry samples from the Chukchi Sea incubations at day 1 within the control were compromised and excluded from analysis.

A)

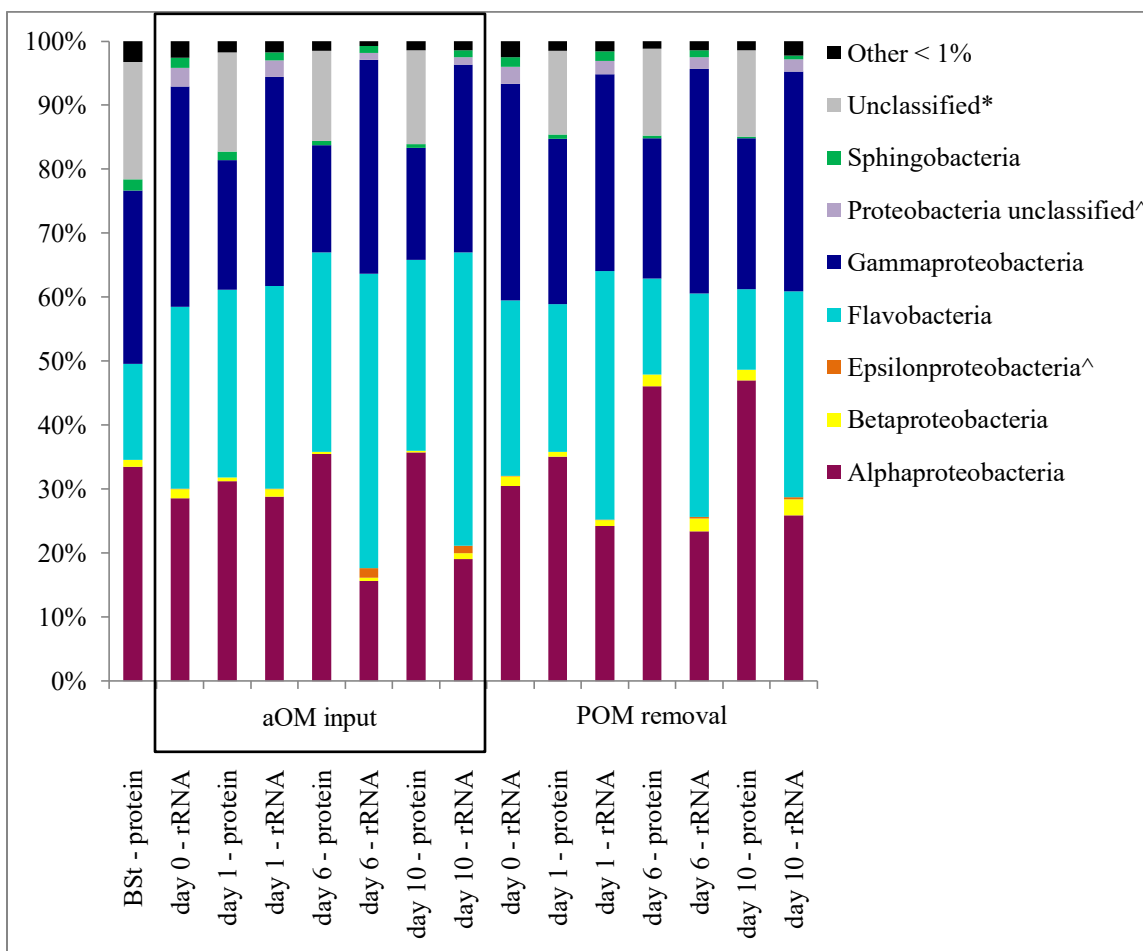
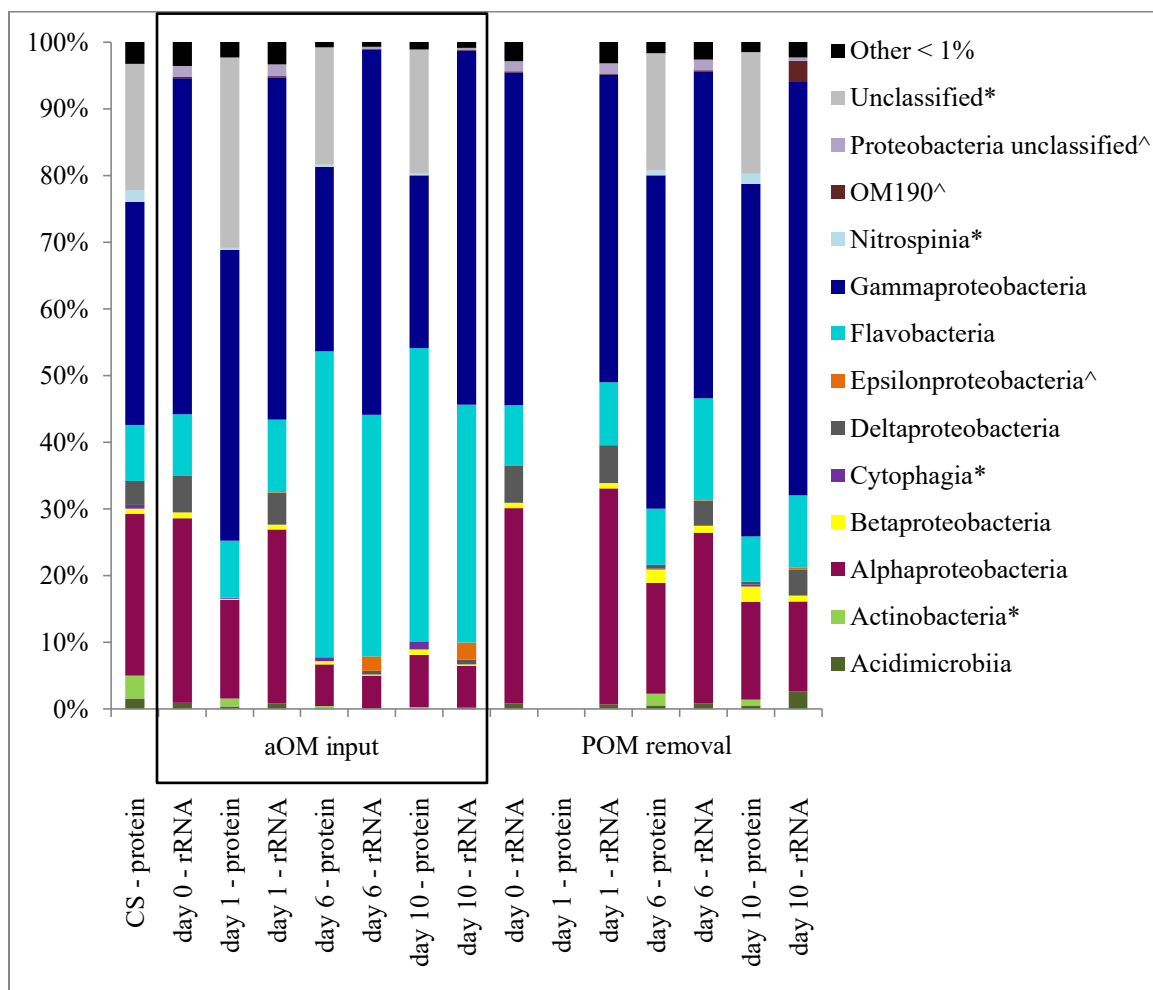


Figure 5 – continued.

B)



**Figure 6 - 16S rRNA genera.** Dominant bacterial genera in the A-B) Bering Strait (BSt) and C-D) Chukchi Sea (CS) microbiomes under each organic perturbation (aOM input = algal organic matter input; POM removal = control treatment where particulate organic matter (POM) >1.0  $\mu\text{m}$  was removed without aOM input). Genera with at least 5% of relative abundance at any time within the experiments were represented, and otherwise were combined into the ‘Other’ category comprising 347 genera. Genera with similarity percentages (SIMPER %): *Polaribacter* spp. (11.5%) and *Owenweeksia* spp. (3%) belong to Class Flavobacteria; Genera *Balneatrix* spp. (11.5%), unclassified *Oceanospirillales* spp. (10.5%), unclassified *Colwelliaceae* spp. (3%), *Colwellia* sp. (2.5%), *Pseudoalteromonas* spp. (0.5%), SAR92 clade (3%) and *Acinetobacter* spp. (0.5%) belong to Class Gammaproteobacteria; Genera *Pelagibacter* spp. (SAR11 clade) (6%) and *Sulfitobacter* spp. (4.5%) belong to Class Alphaproteobacteria. All data are included in Database 5.

A)

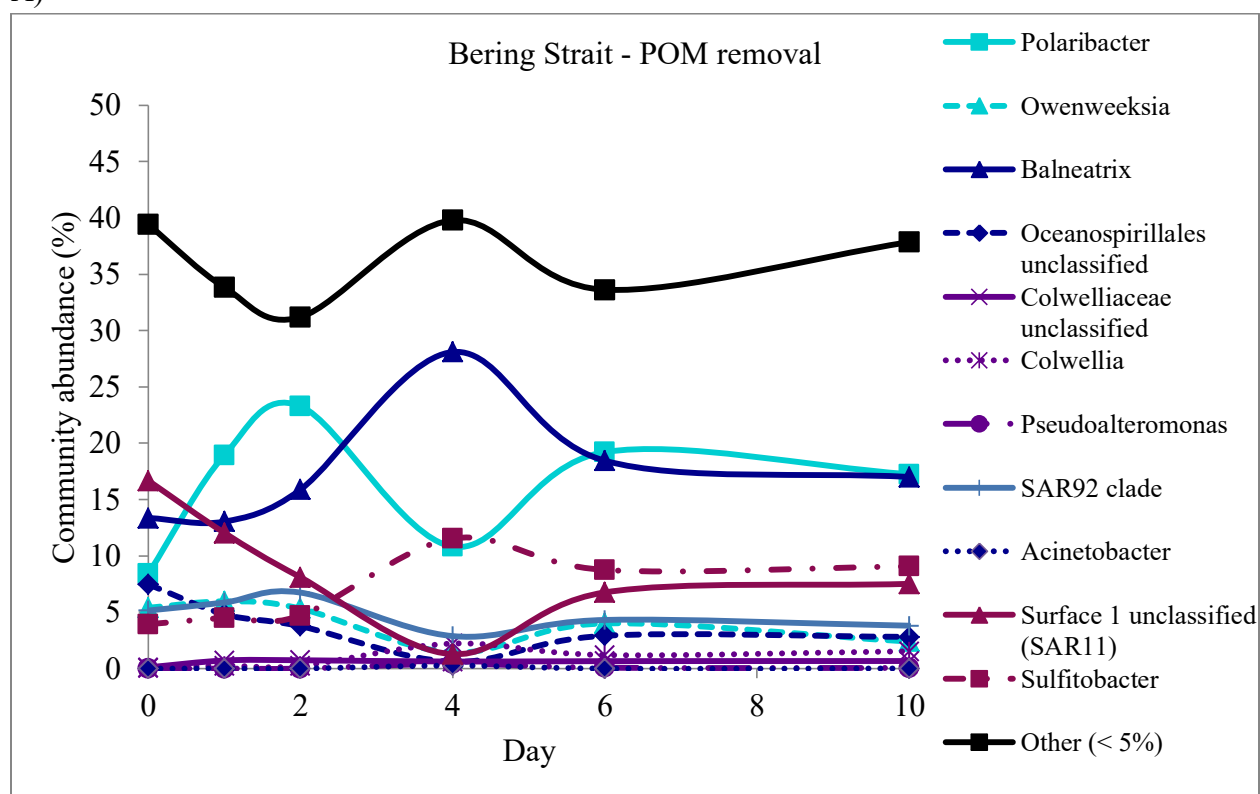


Figure 6 – continued.

B)

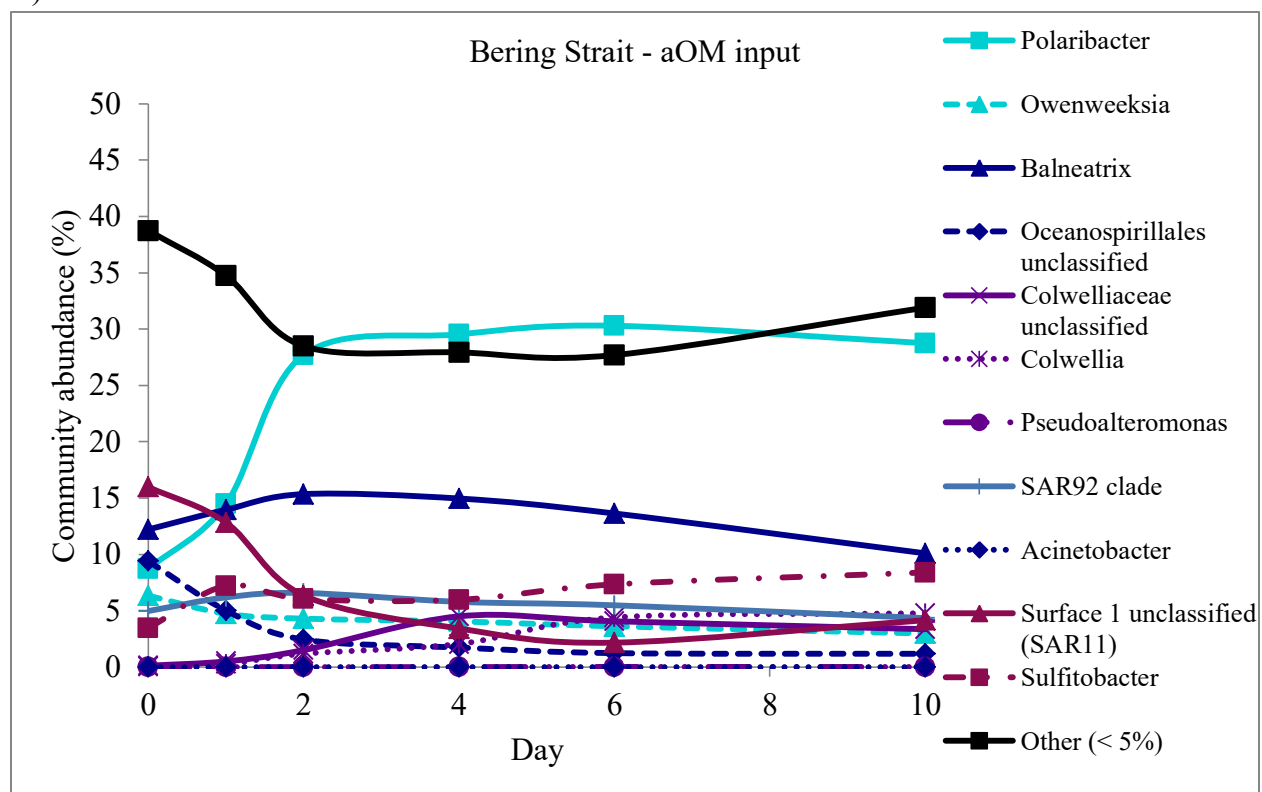


Figure 6 – continued.

C)

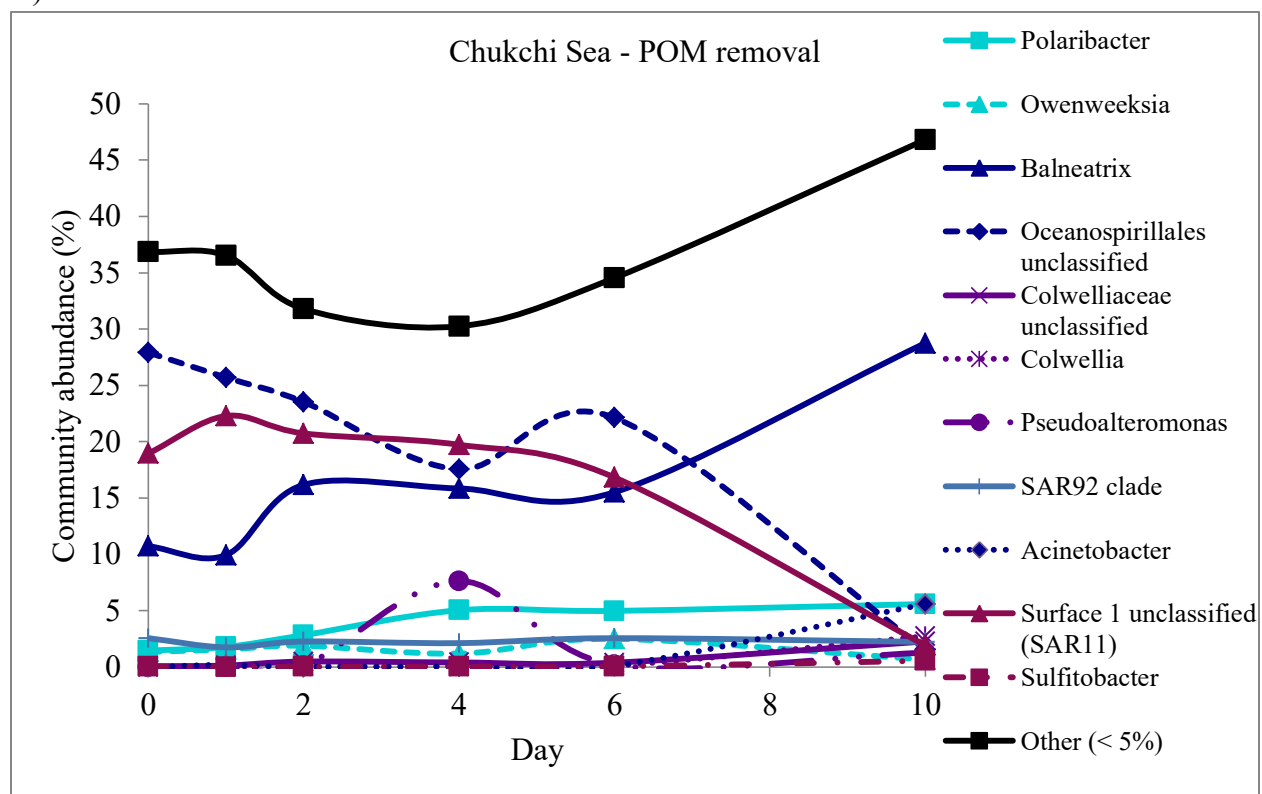
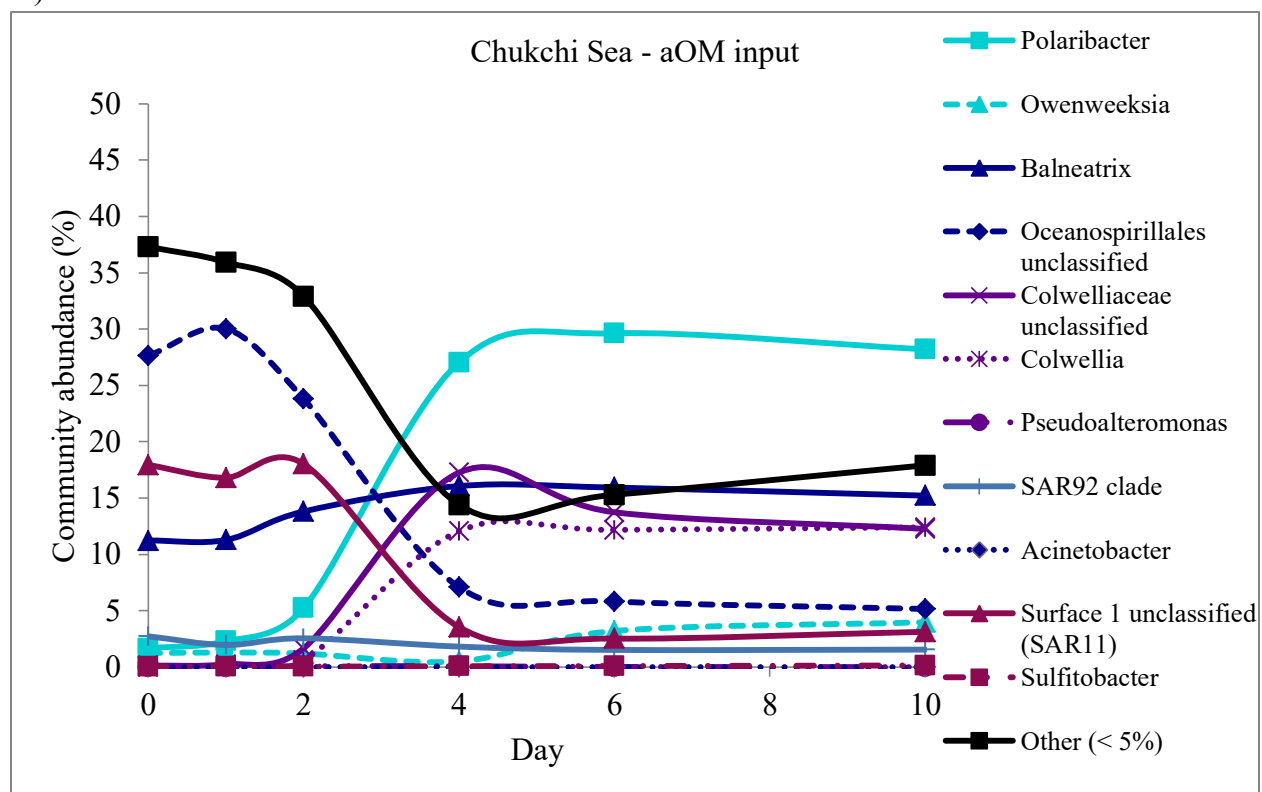


Figure 6 – continued.

D)



### 2.3.2 Temporal changes in community functions

Within the Bering Strait and Chukchi Sea microbiomes, tens of thousands of PSMs matched to thousands of Gene Ontology (GO) functions (Table 2), which were identified at high functional and taxonomic resolution. The goal, however, was to discover significantly changing functions through time in an unbiased, data-driven process. In order to report the greatest percent of the peptide data (Figure 3), GO functional assignments and class-level taxonomic information were extracted to compare the temporal progression of functions and the bacterial classes associated with those functions. In the Bering Strait microbiome, the peptide-based enrichment analysis of terminal GO terms between time points identified 71 functions with significant changes in abundance ( $p$ -value  $< 0.01$ ); these 71 functions self-organized into 7 hierarchical clusters that uncover time-dependent functions acting on the cycling of carbon and nitrogen after OM perturbations (Figure 7; Table 3). As was also seen with the taxonomic data, shifts in microbial functionality predominantly occurred within the first 6 days after OM perturbation, with smaller changes between day 6 to day 10 (Supplementary text 1). This indicates that under both OM scenarios, the Bering Strait bacterial community structure and its proteome remodeling occurred soon after perturbation (i.e., within 6 days) and then was largely maintained to the end of the incubation at day 10.

Over the 10 day incubation period, Bering Strait bacterial abundances increased 12-fold from initial abundances under aOM input conditions compared to only a 6-fold increase when POM was removed within the control (Table 1). This is consistent with the close correspondence often seen between bacterial abundances and labile substrate availability from phytoplankton blooms (e.g., [19]). Community-wide proteome remodeling occurred under both OM addition and the control (Figure 7), likely a response to nutrient resource fluctuations or limitations due to rapid increases in bacterial abundances [26, 69, 71], ‘bottle effects’ or grazing pressure of organisms  $< 1.0 \mu\text{m}$  in size [72]. Consistent with greater increases in cell abundances, aOM input treatment resulted in a greater number of significantly changing Bering Strait bacterial functions over the incubation period ( $n=64$ ) compared to the control where POM was removed ( $n=50$ ) (Figure 7, Table 3). Although 24 functional terms were shared between experimental conditions, the timing and degree of the remaining responses were highly variable, demonstrating that OM



**Table 2 - Mass spectrometry & gene ontology data.** Total number of peptides, peptide spectrum matches (PSM), PSMs matching Gene Ontology (GO) terms, and total GO terms per time point for A) Bering Strait (BSt) and B) Chukchi Sea (CS) bacterial incubations. BSt and CS = initial bacterial community sample. aOM input = algal organic matter input; POM removal = control treatment where particulate organic matter (POM) >1.0  $\mu\text{m}$  was removed without aOM input. n.d. = no data (mass spectrometry samples from the Chukchi Sea incubations at day 1 within the control were compromised and excluded from analysis).

A)

Treatment	Time	peptides	PSMs	GO PSMs	GO terms
	BSt	3038	5435	5008	1091
aOM input	day 1	5162	10028	9588	1418
	day 6	5960	11611	11192	1767
	day 10	5929	11557	11101	1770
POM removal	day 1	5235	9503	9025	1522
	day 6	6496	12722	12133	1768
	day 10	5858	11365	10793	1622

B)

Treatment	Time	peptides	PSMs	GO PSMs	GO terms
	CS	1408	2297	2027	744
aOM input	day 1	292	422	396	540
	day 6	3953	7545	7243	1570
	day 10	3990	7388	7047	1552
POM removal	day 1	n.d.	n.d.	n.d.	n.d.
	day 6	2133	3759	3439	1036
	day 10	2524	4386	3946	1157

**Figure 7 - Functional shifts in the Bering Strait microbiome over time.** Heatmap of Bering Strait (BSt) Gene Ontology (GO) functions with significant peptide spectrum match (PSM)  $\log_2$  fold changes (Bonferroni-corrected p-value < 0.01 from a two-tailed test of proportions) between time points per experiment. Column 1: initial BSt microbiome sample (indicated here as day 0) compared to day 1 with algal organic matter inputs (aOM), column 2: day 1 to day 6 with aOM, column 3: BSt to day 1 within the control (particulate organic matter, POM, removal), column 4: day 1 to day 6 with the control (POM removal). Color shading indicates the degree of  $\log_2$  fold change as seen in the Color Key. Functions (with  $\log_2$  fold changes) are outlined in Table 3.

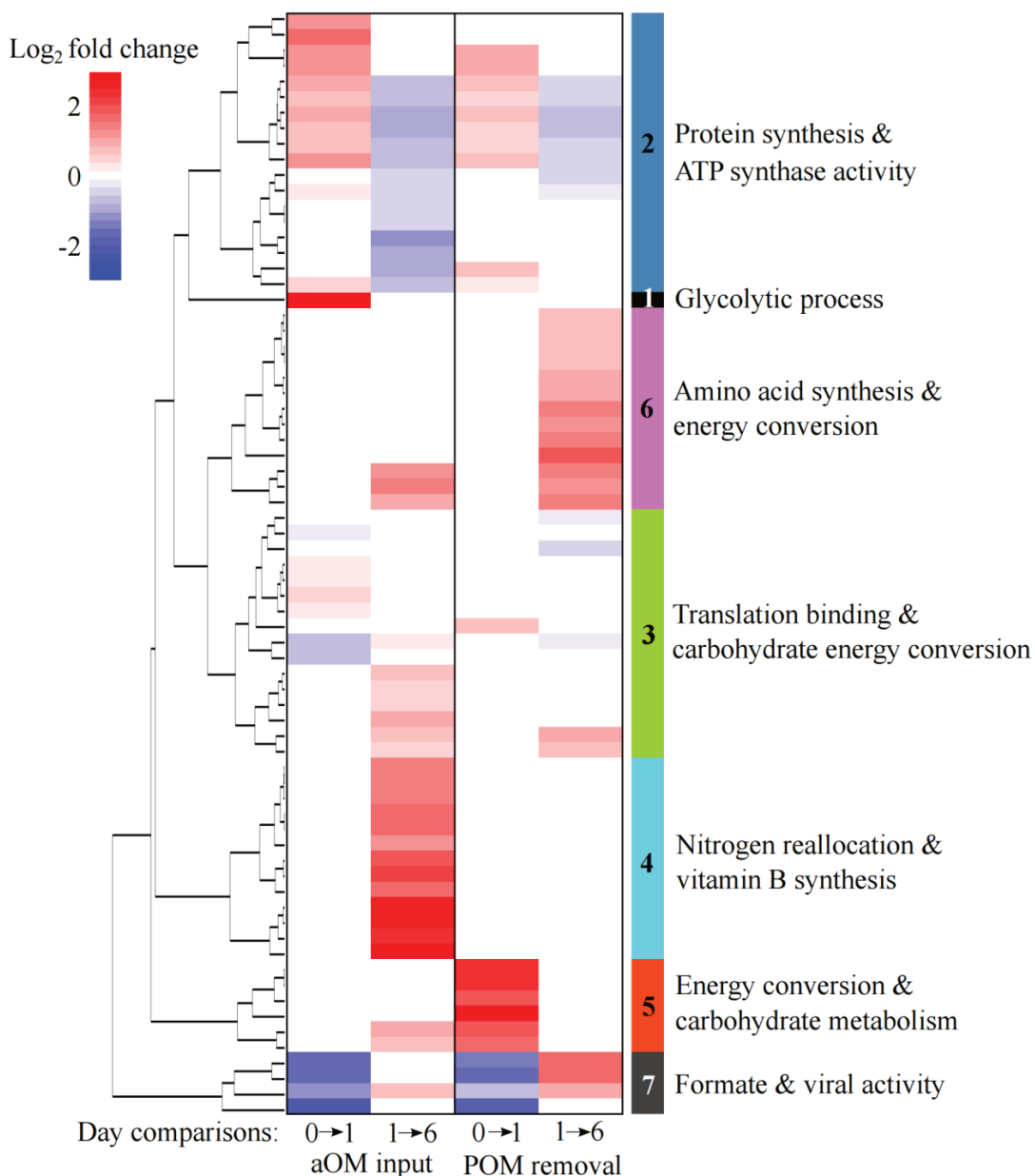


**Table 3 - Changing functions in Bering Strait microbiome.** Log<sub>2</sub> fold changes for Gene Ontology (GO) functions that changed significantly over time (Bonferroni-corrected p-value < 0.01 from a two-tailed test of proportions) within the Bering Strait (BSt) incubations. A negative value = a decrease over time. BSt represents the initial microbiome. d1 = day 1; d6 = day 6. aOM = algal organic matter inputs; POMr = particulate organic matter removal as control treatment.

Cluster #	Function code	GO function	GO category	BSt to d1 aOM	d1 to d6 aOM	BSt to d1 POMr	d1 to d6 POMr
2 - Protein synthesis & ATP synthase activity	1	large ribosomal subunit rRNA binding	mf	1.59			
	2	regulation of translation	bp	2.85			
	3	peptidyl-prolyl cis-trans isomerase activity	mf	1.46		1.27	
	4	protein peptidyl-prolyl isomerization	bp	1.47		1.28	
	5	small ribosomal subunit	cc	1.13	-0.94	0.86	-0.67
	6	translation	bp	0.99	-0.88	0.69	-0.65
	7	structural constituent of ribosome	mf	1.72	-1.74	0.79	-0.77
	8	ribosome	cc	0.96	-1.82	0.68	-0.79
	9	large ribosomal subunit	cc	0.87	-1.25	0.72	-0.57
	10	tRNA binding	mf	1.47	-0.97	0.96	-0.66
	11	unfolded protein binding	mf		-0.68		-0.57
	12	protein folding	bp	0.37	-0.61		-0.45
	13	proton-transporting ATP synthase activity, rotational mechanism	mf		-0.56		
	14	plasma membrane ATP synthesis coupled proton transport	bp		-0.50		
	15	proton-transporting ATP synthase complex, coupling factor F(o)	cc		-1.37		
	16	DNA-templated transcription, termination	bp		-1.99		
	17	rRNA binding	mf		-1.86	0.99	
	18	intracellular	cc	0.74	-0.89	0.45	
1	19	glycolytic process	bp	3.53			

Table 3 – continued.

Cluster #	Function code	GO function	GO category	BSt to d1 aOM	d1 to d6 aOM	BSt to d1 POMr	d1 to d6 POMr
6 - amino acid synthesis & energy conversion	20	transferase activity, transferring acyl groups	mf				1.44
	21	glutamine family amino acid biosynthetic process	bp				1.70
	22	coenzyme binding	mf				0.93
	23	ligase activity, forming carbon-nitrogen bonds	mf				0.92
	24	ligase activity, forming carbon-sulfur bonds	mf				1.34
	25	dicarboxylic acid metabolic process	bp				1.28
	26	valine biosynthetic process	bp				1.68
	27	isoleucine biosynthetic process	bp				1.59
	28	oxidoreductase activity, acting on the CH-NH <sub>2</sub> group of donors	mf				1.79
	29	serine family amino acid metabolic process	bp				2.48
	30	ketol-acid reductoisomerase activity	mf			1.66	1.72
	31	ATP-binding cassette (ABC) transporter complex	cc			1.88	1.55
	32	4 iron, 4 sulfur cluster binding	mf			1.30	1.68

Table 3 – continued.

Cluster #	Function code	GO function	GO category	BSt to d1 aOM	d1 to d6 aOM	BSt to d1 POMr	d1 to d6 POMr
3 - translation binding & carbohydrate energy conversion	33	membrane	cc				-0.16
	34	transport	bp	-0.36			
	35	RNA binding	mf				-0.58
	36	nucleoside-triphosphatase activity	mf	0.39			
	37	protein binding	mf	0.45			
	38	translation factor activity, RNA binding	mf	0.55			
	39	ATP binding	mf	0.27			
	40	alpha-amino acid metabolic process	bp			0.98	
	41	receptor activity	mf	-0.76	0.44		-0.23
	42	cell outer membrane	cc	-0.88			
	43	lyase activity	mf		0.84		
	44	monocarboxylic acid metabolic process	bp		0.72		
	45	metal ion binding	mf		0.57		
	46	oxidoreductase activity, acting on the aldehyde or oxo group of donors	mf		1.19		
	47	tricarboxylic acid cycle	bp		1.44		1.74
	48	oxidation-reduction process	bp		0.72		0.98

Table 3 – continued.

Cluster #	Function code	GO function	GO category	BSt to d1 aOM	d1 to d6 aOM	BSt to d1 POMr	d1 to d6 POMr
4 - nitrogen reallocation & vitamin B synthesis	49	glutamate-ammonia ligase activity	mf		1.83		
	50	pyridoxal phosphate binding	mf		1.82		
	51	glutamine biosynthetic process	bp		1.85		
	52	enzyme regulator activity	mf		1.99		
	53	nitrogen compound transport	bp		1.99		
	54	nitrogen fixation	bp		1.59		
	55	formate-tetrahydrofolate ligase activity	mf		2.53		
	56	folic acid-containing compound biosynthetic process	bp		2.57		
	57	tetrahydrofolate metabolic process	bp		2.26		
	58	glutamate synthase (NADPH) activity	mf		3.38		
	59	regulation of nitrogen utilization	bp		3.42		
	60	glutamate biosynthetic process	bp		3.17		
61	thiamine biosynthetic process	bp		3.75			

Table 3 – continued.

Cluster #	Function code	GO function	GO category	BSt to d1 aOM	d1 to d6 aOM	BSt to d1 POMr	d1 to d6 POMr
5 - energy conversion & carbohydrate metabolism	62	oxidoreductase activity, acting on NAD(P)H, quinone or similar compound as acceptor	mf			2.99	
	63	nicotinamide nucleotide metabolic process	bp			2.90	
	64	nucleoside diphosphate phosphorylation	bp			2.54	
	65	metal ion transport	bp			3.77	
	66	single-organism catabolic process	bp		1.22	2.36	
	67	single-organism carbohydrate metabolic process	bp		0.96	2.18	
7 - formate & viral activity	68	molybdenum ion binding	mf	-2.13		-1.73	2.17
	69	formate dehydrogenase (NAD <sup>+</sup> ) activity	mf	-2.99		-2.21	2.26
	70	outer membrane-bounded periplasmic space	cc	-1.45	0.89	-0.94	1.18
	71	viral capsid	cc	-2.64		-2.55	

perturbation directs community functionality without major alterations to the taxonomic distribution at the class level (Figure 5).

Despite the differences in bacterial abundance and POM carbon and nitrogen concentrations between the OM perturbation experiments (Table 1), ten GO functions associated with protein synthesis changed similarly in both OM environments through time (#3-12, cluster 2) (Figure 7; Table 3). The comprehensive and immediate increase in protein synthesis peptides across the Bering Strait incubations by day 1 suggests that the microbial community, under contrasting OM conditions, stimulated cellular growth prior to division. Although some caution is warranted since microbial community responses can be influenced by incubation conditions (e.g. removal of grazers or artifacts ('bottle effects') associated with container based incubations [72]), protein synthesis is frequently the first functional response of bacteria to environmental stimulus, such as carbon or nutrient addition [38, 69, 73, 74]. This includes ribosomal proteins that are important indicators of cellular activity and are shown to correlate with growth phases of some bacteria [71].

Coinciding with the high energy requirements of bacterial biomass production was the increase across a suite of functions related to carbohydrate metabolism (#19, #36-39, #62-67), with some of the largest  $\log_2$  fold changes at day 1 (vs. the initial Bering Strait sample) under both OM perturbation treatments (ranging from 2.2 – 3.8) (Figure 7). Carbohydrates are among the first substrates to be consumed from diatom-derived OM pools [75] as they are largely bioavailable to marine bacteria (e.g., [18, 76, 77]). The increase in glycolysis-related peptides (#19, cluster 1) and corresponding essential functions (#36-39, cluster 3) [78] after aOM input indicate that cellular adenosine triphosphate (ATP) was in high demand as the microbes incorporated substrates and started building new proteins [79]. Similarly, one day after POM removal, a cluster of functions involved in the electron transport chain for energy flow and storage (#62-65; cluster 5) during carbohydrate metabolism (#66-67) suggest that early energy acquisition from carbon sources and ATP generation from glucose was a cellular priority at this time. While glucose as an energy source increased at day 1, the utilization of small molecules decreased, as evidenced by decreases in two primary cofactors in one-carbon (C1) metabolism,  $\text{NAD}^+$ -formate dehydrogenase (FDH) and molybdenum (Mo) ion binding (FDH/Mo, #68-69, cluster 7). C1 metabolism is widespread among microorganisms and allows them to efficiently



transfer the otherwise volatile C1 molecules. Access to this metabolic pathway provides specialized microbes the ability to utilize a wide range of organic carbon molecules for energy production [80], in particular compounds that arise as by-products of the degradation process.

By day 6 of the Bering Strait experimental incubations, protein synthesis (cluster 2) declined within both OM environments, as metabolic functions related to energy production and resource utilization continued to increase (Figure 7). The increase of peptides associated with the TCA cycle (#43-48, cluster 3) and formate C1 metabolism (#55-57 in the aOM input treatment; #68-69 in the control) at day 6 indicates that small carbon-based metabolites were being mobilized and recycled. These C1 molecules appeared to be important carbon sources in the Bering Strait before the incubations started and again at day 6, suggesting this may be the secondary carbon-based response as carbohydrates become depleted. Similar responses between OM perturbation treatments also included increases in the expression of peptides from the ATP-binding cassette (ABC) transporter complex (#31, cluster 6), suggesting additional investments in nutrient uptake under differing OM environments. These important transmembrane complexes have high substrate-specificity and substrate-affinity, which increases cellular OM assimilation efficiency [81], and represents an important response under nutrient extremes across the global ocean [67, 82, 83].

### 2.3.3 Changes in community function under contrasting organic matter perturbations

An increase in intracellular nitrogen transport and regulation (#49, #51, #53-54, #58-60, cluster 4) between days 1 and 6 after aOM input to the Bering Strait microbiome aligned with the widespread decrease in peptide abundances associated with protein synthesis at day 6 (Figure 7). Included in this cluster was an increase in N-fixation peptide expression (#54), further suggesting a need for the bacteria from this community to acquire nitrogen at that time. These N-fixing genes recruit and coordinate other enzymes involved in the N-fixation pathway in addition to assimilating atmospheric N<sub>2</sub>. In rapidly responding cells, this intracellular coordination provides rapid access for reduced nitrogen to be incorporated into various critical system-complexes that support peptide synthesis (e.g., nitrogenase, transporters, RNA, amino acids, etc.). Additionally, there was substantial peptide evidence that the recently acquired N was being redistributed intracellularly with increases in glutamine synthetase (GS) (#49, #51) and glutamate synthase (glutamine:2-oxoglutarate aminotransferase, GOGAT) (#58, #60). The enzymes in the

GS/GOGAT pathway are central to intracellular ammonium assimilation and distribution [84], where the primary products can be used in the synthesis of new amino acids or other N-rich molecules [85]. The increase of these nitrogen-based biochemical processes were in response to post-bloom conditions since increases in these metabolic functions were absent in the control.

The Bering Strait microbiome continued to undergo tightly regulated metabolic transitions in response to aOM input days after receiving these substrates, as seen by the tight clustering of internal bacterial nitrogen cycling and vitamin B synthesis functions (#50, #55-57, #61, cluster 4). The synthesis of thiamine (vitamin B1), a crucial vitamin and coenzyme involved in diverse and essential metabolic processes including amino acid and carbon metabolism and the regulation of gene expression [86], increased nearly 4-fold (cluster 4; #61). It has been observed that the presence of algal exudates during blooms can signal vitamin synthesis in some heterotrophic bacteria, representing a symbiotic relationship between coexisting microfauna (e.g., [19, 87]). In addition, the increased abundance of pyridoxal phosphate (vitamin B6) binding (#50) and formate tetrahydrofolate (THF) pathway peptides (#55-57) (involving vitamin B9) indicate that bacteria from the Bering Strait were stimulated by the algal OM to transfer C1 derivatives from THF during the synthesis of purines or amino acids [67, 88-90].

The controlled experimental incubations where POM was removed without subsequent aOM input provided insights into primary functional dynamics in the Bering Strait microbiome under reduced resources. In general, the taxonomic composition (at the rank of genus) of the starting and ending Bering Strait community structure changed little (Figure 6) and there was less proteome remodeling under POM removal compared to aOM input. Even so, a functional shift measured exclusively 6 days after POM removal was evident by increases in peptides involved in the metabolism and mobilization of intracellular molecules, such as amino acids (#21, #26-27, #29-30) (Figure 7). The transport and metabolism of amino acids is a core function of marine microbes [87] and is a strictly regulated process to meet energy requirements [91]. Intracellular reallocation of amino acids and the deconstruction of proteins to generate individual amino acids, peptides, and signaling molecules provide an energetically low-cost mechanism to efficiently conserve and recycle carbon and nitrogen. This can conserve needed energy to drive critical cellular functions. Further, the increase in formate oxidation peptides (FDH/Mo #68-69, cluster 7) on day 6 (versus day 1) indicated that simple C1 molecules became an important

source for energy production under POM removal at that time [80, 92, 93] or that internal formate concentrations had increased and this enzyme complex was employed as a removal mechanism to promote growth [83].

#### 2.3.4 Bacterial classes of Bering Strait community functions

Many microbial species adapt to fill a particular environmental niche, yet across multiple taxa some functional redundancy may be required to maintain the stability of a complex ecosystem (e.g., [87]). Metaproteomics provide a snapshot of cellular functions within a diverse microbiome at the time of sampling as well as insight into taxonomy because each peptide that contributes to the GO functions also has a taxonomic designation (Datasets 1-4). Tracking the Bering Strait microbiome within both simulated bloom (aOM input) and oligotrophic (control where POM was removed) environments, I found that many temporally controlled community functions were conserved among the major taxonomic groups (Figure 8) irrespective of the fact that temporal taxonomic restructuring was evident at the class level when examining the complete metaproteomic and 16S rRNA datasets (Figure 5). To an extent, this broad redundancy in functional roles may reflect the level of taxonomic resolution (i.e., class level) used in the present analysis [5, 94], however Aylward et al. [38] showed that even at a detailed bacterial classification (i.e., OTUs), rapid responses to algal dynamics can be dominated by broad functional redundancies. However, tracking community functionality with an unbiased method in the current work also revealed that unique shifts in bacterial classes occurred across time and between the OM perturbations.

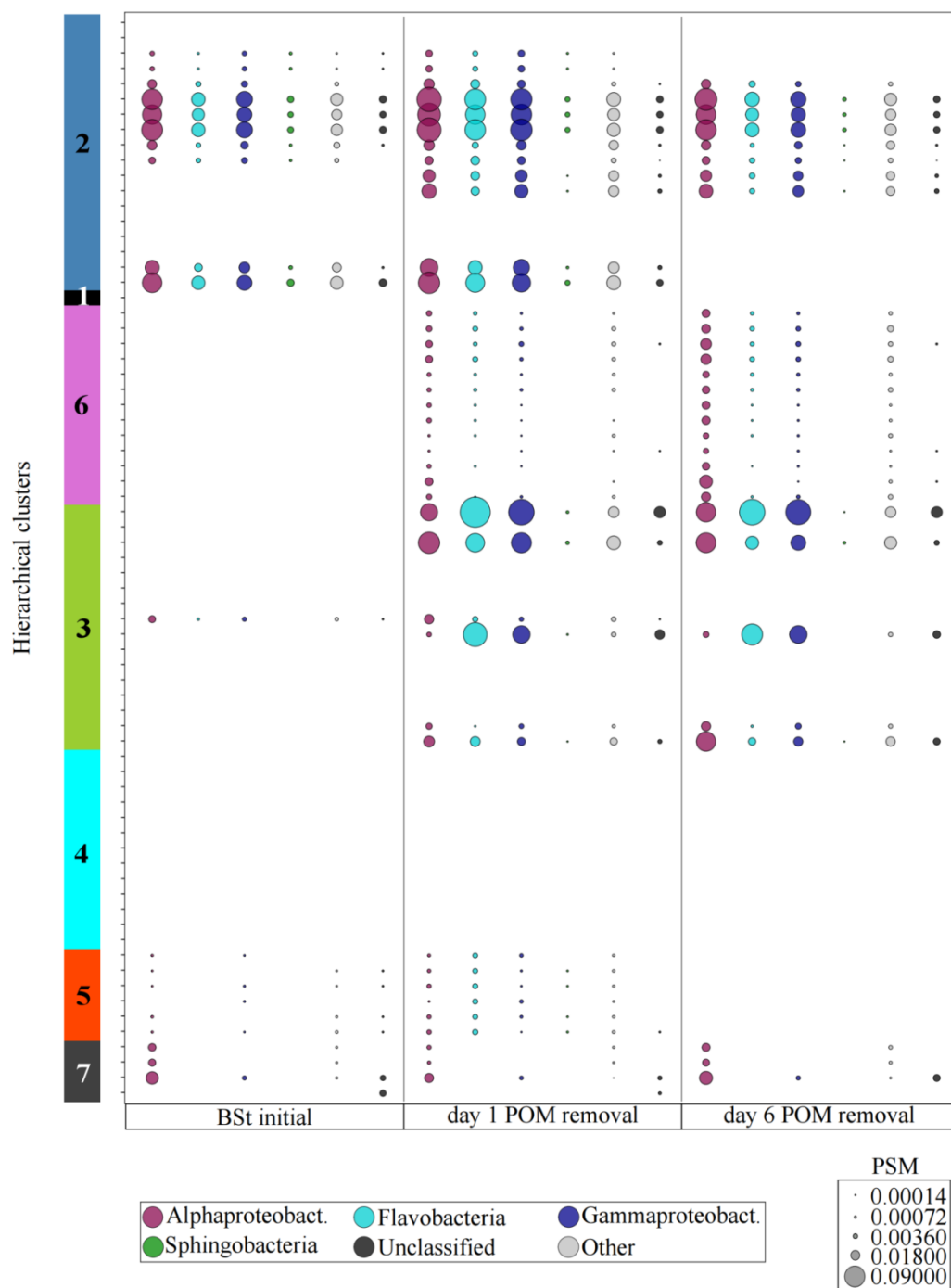
**Figure 8 - Bacterial classes associated with changing community functions.** Peptide spectrum match (PSM) values for the six major Bering Strait (BSt) microbiome taxonomic categories for incubations A) with algal particulate organic matter input (aOM) and B) the substrate limited control (POM removal). The sizes of bubbles are scaled to PSM counts by area. Alphaproteobact. = Alphaproteobacteria; Gammaproteobact. = Gammaproteobacteria. Clusters with function code identifiers are presented in Table 3.

A)



Figure 8 – Continued.

B)



Within the Bering Strait bacterial community, a taxonomic shift related to carbohydrate degradation (#19) was seen as peptides associated with the glycolytic process transitioned from a minor bacterial class within the *in situ* bacterial community to the dominant bacterial classes one day after aOM input (Figure 8A). This evidence of competition for labile resources within the bacterial community occurred as the core microbiome responded to a new supply of algal-derived carbohydrates at a more rapid pace than the minor bacterial class. It has been shown that different bacterial clades are physiologically poised to respond to a particular stimuli (e.g., [17, 18, 20, 95]), initiating metabolic-specific niches and divergent ecological strategies [96]. Examples of this in the dataset were seen by Alphaproteobacteria being important in all community-level changes in carbohydrate-related functions within Bering Sea incubations independent of OM environment (#19, #47-48, #66-67), while Flavobacterial activity for the TCA cycle (#47-48) was dependent on organic conditions within the incubations (Figure 8). Further, few Gammaproteobacteria-specific peptides were associated with glycolysis-related functions (#19), but several peptides specific to the TCA cycle were observed under both OM scenarios (#47-48). This dynamic response by the core microbiome corroborates previous findings by Teeling et al. [24] that broad microbial classes occupy different ecological niches during algal-derived carbohydrate oxidation. Unique to this study, however, was the use of an unbiased biological enrichment analysis to discover and reveal functional shifts representative of carbon and nitrogen acquisition, reallocation and degradation processes independent of taxonomic origin.

Although Alphaproteobacteria were important across a majority of functions related to carbohydrate metabolism and protein synthesis, Bering Strait Flavobacteria dominated increases of the peptides associated with these functions (Figure 8). This dominance is indicative of a competitive advantage by Flavobacteria to rapidly respond to fluctuating OM conditions, such as increased pulses in OM typically observed during phytoplankton blooms [22, 24, 97]. The data suggests that their advantage under these conditions might be connected to a metabolic capability to efficiently exploit algal-derived carbohydrate substrates in order to fuel biomass production prior to division. The timing of these metabolic increases at day 1 suggests that these functions provide Flavobacteria with a mechanistic advantage under heterogeneous substrate environments, enabling them to rapidly respond and effectively compete in a complex community.

Flavobacterial functional response to the aOM input was apparent within the community proteome: increasing from 15% to >23% (days 0-1), an increase sustained to the end of the experiments under aOM input only (Figure 5). In this high substrate environment, the community-level increase in expressed activity (proteome) by Flavobacteria at day 1 preceded their increased contribution to community structure at day 6, as measured by a change in relative 16S rRNA sequence abundance from 32% at day 1 to 46% at day 6. This suggests that the ability to rapidly convert energy from carbohydrates into protein synthesis contributed to a trend towards compositional dominance, however with a temporal delay on the order of days. A preferential benefit occurred for the genus *Polaribacter* spp., as their relative abundances increased steadily between days 0-2 to reach 30% of total community structure under aOM input (Figure 6). Consistent with the proteome response by Flavobacteria to aOM input conditions, *Polaribacter* spp. have been found to increase enzymes that hydrolyze bonds within poly- and monosaccharides following phytoplankton blooms [24], supporting the idea that the increase in *Polaribacter* spp. measured in these Arctic microbiome incubations resulted from a specialized nutritional strategy that allowed them to dominate the ecological niche of algal-derived organic substrate-based growth.

An important observation was that although the Alphaproteobacteria class was functionally active towards the end of the incubations (days 6-10) contributing 36-46% of total community peptides identified, their community abundance decreased to equal only 16-26% of 16S rRNA sequences at this time (Figure 5). Decreasing abundances of Alphaproteobacteria are a characteristic feature of this class following phytoplankton blooms [24]. The functions associated with this class from the current experiments highlight its metabolic flexibility under diverse OM environments. For example, Alphaproteobacteria increased formate-related metabolic pathways at day 6, but peptide evidence for the fate of this C1 substrate differed depending on the OM environment; high substrate additions initiated biomass production (i.e., amino acids and purines) while energy production resulted from conditions within the control. Both of these enzymatic functions (formate-THF ligase and FDH/Mo) have also been measured at variable depths and seasons in Alphaproteobacteria from the NW Atlantic [67] and Southern coastal ocean [41]. Specifically, FDH/Mo is widely distributed within the genome of the dominant Alphaproteobacterial clade (*Pelagibacter* spp.) and this specialization to access C1 compounds as a source of energy delineates a niche for this bacterium to utilize a diversity of

organic compounds across a range of marine environments [80]. The divergent nutritional strategy seen in this study as a response to OM environment reflects the ability of Alphaproteobacteria to preferentially divert the same substrate into different metabolic pathways dependent on resource availability, representative of the strong niche diversification within this bacterial class [98].

Alphaproteobacteria is a very diverse bacterial class, and includes abundant taxonomic groups that characteristically target low molecular weight, labile OM [19, 99]. Within the current dataset, Alphaproteobacteria dominated a majority of the ABC transport complex (#31, cluster 6) and contributed to >93% of the increase in abundance at day 6 under both OM perturbation environments (Figure 8). ABC transporters are well-represented within Alphaproteobacterial genomes [98, 100] and this class dominates community expression of these transporters across diverse marine environments (e.g., [24, 67, 83]). Different modes of substrate acquisition are another way in which bacterial groups form resource-dependent ecological niches. In particular, transporters can be sensitive indicators of cellular adaptation [101] and substrate availability [18, 24]. The scavenging of a range of ambient monomers provides certain taxa within the ubiquitous Alphaproteobacteria class with a competitive advantage under heterogeneous conditions throughout the world's oceans.

Six days after aOM input, Alphaproteobacteria-assigned peptides drove the observed shifts in nitrogen transport, regulation and reallocation, plus vitamin synthesis (cluster 4) (Figure 8). Specific genera within this class of bacteria can degrade a diverse suite of substrates, allowing them to rapidly utilize phytoplankton exuded metabolites [21, 67, 98]. The dominance of Alphaproteobacteria nitrogen regulatory proteins has been observed previously during a natural phytoplankton bloom [67] and after carbon additions [71]. Specifically, peptides associated with the GS/GOGAT pathway were expressed by Alphaproteobacteria, evident of their ability to rapidly redistribute ammonium intracellularly. Proteins associated with this metabolic pathway are reported to be among the most abundant proteins identified under both replete ammonia [102] and oligotrophic conditions [83]. Further, the vitamin thiamine was specifically expressed by Alphaproteobacteria. This is a class with few clades that have the ability to synthesize thiamine, some of which may rely on phytoplankton hosts as a source of this vitamin [103]. These results suggest that temporal increases in nitrogen transfer and intracellular



cycling, plus vitamin synthesis, defined an important niche of Bering Strait Alphaproteobacterial functionality when algal-derived substrates were abundant in the environment, even as total relative abundances of this class decreased (Figure 5).

Consistent with other nitrogen-related functions, a majority (65%) of the peptides related to nitrogen fixation at day 6 were assigned to the Alphaproteobacterial class (Figure 8). Although reporting genus-level resolution would have limited the taxonomic assignment to 50% of the total peptides (Figure 3), all taxonomic levels associated with a peptide are embedded in this unique data-structure taxonomic resolution (Datasets 1-4). Exploring the finer taxonomic resolution of nitrogen fixation peptide assignments revealed that 70% of the 50% of peptides could be assigned a specific genera were assigned to *Sulfitobacter* spp. Although the significance or reason for nitrogen fixation to increase in the late stages of aOM degradation in the Bering Strait is not understood, discovering that *Sulfitobacter* spp. dominates the detected signal when looking at genus-level resolution potentially reveals a distinguished niche within the nitrogen pathway that favors this successful bacterium of the Bering Strait community (Figure 6A).

### 2.3.5 Delayed functional response in the bottom water microbiome of the Chukchi Sea

The Chukchi Sea bottom water Arctic microbiome was incubated in parallel to the Bering Strait experiments to compare the universality of the functional and taxonomic patterns identified. Despite the depth of origin and geographic separation, aOM input stimulated bacterial growth (Table 1) with the same three taxonomic classes comprising the core microbiomes of the Bering Strait and Chukchi Sea, however in different proportions (i.e., Gammaproteobacteria contributed to >46% of the Chukchi Sea 16S rRNA temporal sequences while representing <35% in the Bering Strait) (Figure 5B). Similar between microbiomes, the genus *Polaribacter* spp. (Flavobacteria) benefited from the high substrate environment, however the increased growth of this clade in the Chukchi Sea was delayed by 2 days compared to Bering Strait incubation (day 2-4 instead of days 0-2 in the Bering Strait) (Figure 6). This suggests that within a matter of days, this dominant degrader of algal-derived organic matter effectively competes with other genera for growth substrates within the shallow shelf system of the western Arctic Ocean, independent of geographic origin or depth in the water column. Unique to the Chukchi Sea was a large increase in the *Colwellia* clade (Gammaproteobacteria) within the high substrate

environment, while the rise of genus *Balneatrix* spp. (Gammaproteobacteria) was a dominant feature by the end of the control incubation, where POM was removed.

The peptide enrichment analysis revealed that the three dominant bacterial classes seen in the Bering Strait aOM additions also dominated changes for the same functional expressions in the Chukchi Sea community (Figure 9; Dataset 3). These community-wide metabolic functions were primarily controlled by Chukchi Sea Gammaproteobacteria and Flavobacteria, with decreased Alphaproteobacterial influence compared to the Bering Strait. For example, in the later phase of the Chukchi Sea incubations (days 6-10), Alphaproteobacterial abundances were at a minimum, responsible for <8% of total community peptides (Figure 5B). Gammaproteobacteria dominated the observed changes in peptide-based metabolic activity within the Chukchi Sea microbiome, specifically on day 1 with a surge in protein synthesis peptides.

Using an identical method to measure temporal GO term enrichment in the Chukchi Sea microbiome, as was completed for the Bering Strait, resulted in similar broad functional responses to increases in algal-derived substrates (Figure 10; Table 4). Specifically, several functions that significantly changed through time in the Chukchi Sea under aOM input were parent or sibling terms to functions that changed in the Bering Strait microbiome, but importantly, were delayed in their expression (e.g., peptides associated with multiple translation and carbohydrate metabolism terms increased at day 6 in the Chukchi Sea opposed to day 1 in the Bering Strait). Using functional traits as the primary metric, it appears that the initial bacterial response to high concentrations of algal inputs are similar between microbiomes across locations and water masses in the Arctic Ocean, albeit with a temporal offset as seen by increases in protein synthesis and carbohydrate metabolism. Several key functional shifts identified during Bering Strait incubations (e.g., vitamin B and nitrogen regulation) did not significantly change in the Chukchi Sea microbiome, suggesting that microbiomes with similar core taxonomic profiles may not be functionally equivalent when organic substrates are high, such as immediately following the decline of a phytoplankton bloom. This has important implications for both the timing and magnitude of response to organic inputs and a potential constraint on taxonomy alone as a predictor of functional response.

**Figure 9 - Chukchi Sea bacterial classes for Bering Strait functions.** Chukchi Sea (CS) peptide spectrum match (PSM) values for the six major taxonomic categories showing greatest PSM counts associated with the 71 significantly changing GO functions from the Bering Strait after algal organic matter input (aPOM). Bubble sizes are scaled to PSM counts by area. Alphaproteobact. = Alphaproteobacteria; Gammaproteobact. = Gammaproteobacteria. Clusters with function code identifiers are presented in Table 3. All PSM data to accompany this figure are available in Dataset 3, including a detailed breakdown of the ‘Other’ category.



**Figure 10 - Chukchi Sea functional shifts under algal substrate inputs.** Heatmap of Chukchi Sea (CS) Gene Ontology (GO) functions with significant peptide spectrum matches (PSM)  $\log_2$  fold changes (Bonferroni-corrected p-value < 0.01 from a two-tailed test of proportions) between time points with algal organic matter input (aOM): column 1: initial CS microbiome (CS) sample compared to day 1, column 2: day 1 to day 6, column 3: day 6 to day 10. Color shading indicates the degree of  $\log_2$  fold change as seen in the Color Key. Functions with  $\log_2$  fold changes are outlined in Table 4.

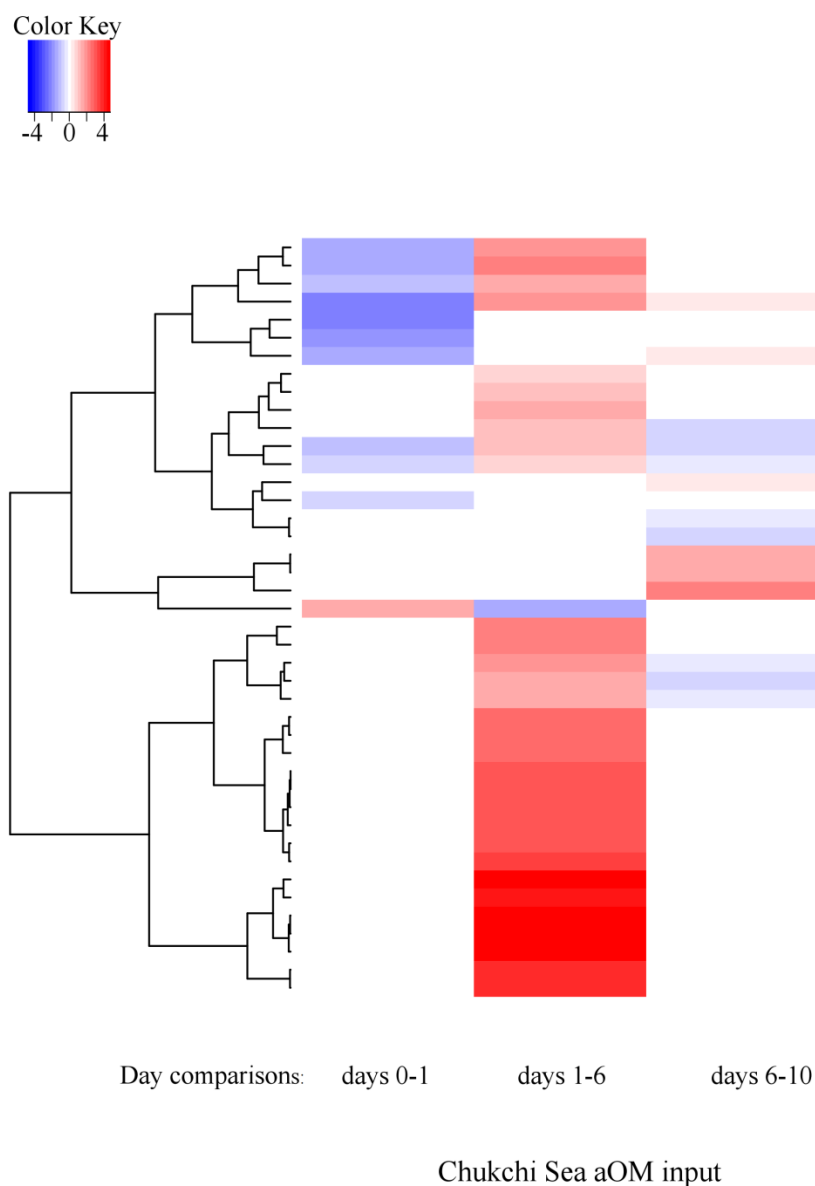


**Table 4 - Changing functions in Chukchi Sea microbiome with algal inputs.** Gene ontology (GO) functions from the Chukchi Sea (CS) incubations that changed significantly (Bonferroni-corrected p-value < 0.01 from a two-tailed test of proportions) over time and their log<sub>2</sub> fold changes under algal organic matter input (aOM input).

Cluster #	Function #	GO function	CS to day 1	day 1 to day 6	day 6 to day 10
4	1	oxidoreductase activity	-1.43	1.94	0.00
4	2	oxidation-reduction process	-1.52	2.09	0.00
4	3	DNA binding	-1.13	1.48	0.00
4	4	receptor activity	-2.16	1.91	0.39
4	5	regulation of transcription, DNA-templated	-2.25	0.00	0.00
4	6	protein refolding	-1.78	0.00	0.00
4	7	transport	-1.41	0.00	0.30
2	8	hydrolase activity	0.00	0.90	0.00
2	9	DNA-directed RNA polymerase activity	0.00	1.11	0.00
2	10	transcription, DNA-templated	0.00	1.39	0.00
2	11	protein folding	0.00	1.01	-0.60
2	12	unfolded protein binding	-1.20	1.02	-0.61
2	13	ATP binding	-0.67	0.84	-0.35
2	14	membrane	0.00	0.00	0.22
2	15	cellular macromolecule biosynthetic process	-0.60	0.00	0.00
2	16	ribosome	0.00	0.00	-0.56
2	17	ribosomal subunit	0.00	0.00	-0.60
5	18	transmembrane transporter complex	0.00	0.00	1.36
5	19	outer membrane-bounded periplasmic space	0.00	0.00	1.35
5	20	respiratory chain	0.00	0.00	2.18
5	21	proton-transporting ATP synthase complex, catalytic core F(1)	1.48	-1.40	0.00

Table 4 – Continued.

Cluster #	Function #	GO function	CS to day 1	day 1 to day 6	day 6 to day 10
3	22	regulation of cellular process	0.00	2.09	0.00
3	23	cellular component organization or biogenesis	0.00	2.40	0.00
3	24	structural constituent of ribosome	0.00	1.75	-0.56
3	25	rRNA binding	0.00	1.61	-0.57
3	26	translation	0.00	1.60	-0.39
3	27	organic substance catabolic process	0.00	2.79	0.00
3	28	cofactor metabolic process	0.00	2.83	0.00
3	29	proteolysis	0.00	2.65	0.00
3	30	magnesium ion binding	0.00	3.13	0.00
3	31	cellular catabolic process	0.00	3.13	0.00
3	32	ligase activity	0.00	3.11	0.00
3	33	protein transport	0.00	3.07	0.00
3	34	tricarboxylic acid cycle	0.00	3.20	0.00
3	35	coenzyme binding	0.00	3.24	0.00
1	36	pyruvate metabolic process	0.00	4.50	0.00
1	37	isomerase activity	0.00	4.34	0.00
1	38	single-organism catabolic process	0.00	4.74	0.00
1	39	phosphorylation	0.00	4.73	0.00
1	40	single-organism carbohydrate metabolic process	0.00	4.70	0.00
1	41	glutamine family amino acid metabolic process	0.00	3.78	0.00
1	42	alpha-amino acid biosynthetic process	0.00	3.77	0.00

## 2.4 Conclusions

Our understanding of how the primary functions of natural microbiomes change spatially and temporally in ocean systems is incomplete without information on functional responses across broad taxonomic groups. The recent demonstration by Coles et al. [104] that simulated microbiomes with limited functional genes can be modeled to recreate biogeochemical gradients should inspire a new era of multi-“omic” data delivery. Taking a discovery-based metaproteomics approach, I tracked environmentally relevant and statistically significant changes in primary metabolic functions of an oceanic microbiome. The operative functions identified in these complex systems showed coordinated timing across the bacterial classes in response to realistic algal OM input: 1) the uptake and degradation of carbon, 2) protein synthesis and ATP generation, 3) redox-driven activation of proton gradients, and 4) reallocation of cellular nitrogen and vitamin synthesis. These temporal responses, many of which were observed in both Bering Strait and Chukchi Sea microbiomes, predominantly occurred within the first 6 days after OM perturbations, providing important time constraints for future experiments and simulation-based organic carbon and nitrogen modeling. Additionally, this method yields complementary taxonomic distributions as 16S rRNA data at the class level, demonstrating that access to both taxonomy and expressed metabolism is possible with one proteomic analysis. In doing so, I was able to examine who was doing what across time.

The broader perspective of this enrichment method encourages researchers to consider a complete metaproteomics dataset rather than select favorite enzymes or element-specific pathways or transporters. The observation that many functional responses crossed major bacterial class levels suggests that functional composition, not taxonomy, may be the most relevant factor for the development of realistic stratified biogeochemical profiles in the coastal ocean, corroborating recent models [104]. This proteomic analysis significantly contributes to the important question: Does taxonomy matter when modeling oceanic biogeochemical cycling through time or depth? Can we focus our efforts on modeling expressed functional traits within a microbiome? I anticipate that the results and methods presented here can help guide the selection of key, site-specific microbial functions for the purpose of forecasting oceanic biogeochemical gradients.

## CHAPTER 3

3. ORGANIC MATTER PERTURBATIONS DRIVE COMPOSITIONAL AND  
FUNCTIONAL SHIFTS IN ARCTIC OCEAN MICROBIOMES

## 3.1 Introduction

The Bering Sea and much of the Chukchi Sea are highly productive systems, and due to their shallow shelves are important regions for both carbon cycling and sequestration [105, 106]. In shallow shelf systems of the Arctic regions, primary productivity (PP), zooplankton grazing and bacterial oxidation at the base of the food web can become uncoupled, contributing to elevated organic inputs reaching the shelf sediments, which in turn supports a productive benthic ecosystem and an abundance of higher trophic pelagic species [107-109]. These ecosystem-scale impacts driven by the dynamics of bacteria and PP [105] (e.g., regional carbon cycling and the richness of specific fisheries) are not limited to the Arctic Ocean region (e.g., [110]) and highlight the important ecological role that bacteria play within the global ocean [111].

The Arctic sea ice extent, age and thickness have steadily decreased within the time frame of a decade [112], which contributes to increasing anomalies in spatial and temporal heterogeneity of PP within the water column [113]. Because bacterial dynamics can be tightly linked to PP [114] and physiochemical conditions within the Arctic Ocean ecosystem [115, 116], they are also subject to changing sea ice conditions and water mass currents. Periods of reduced sea ice extent increase stratification of the water column, decreasing nutrient availability for phytoplankton in the subsurface chlorophyll maximum (SCM) and negatively influencing both PP and bacterial community numbers [117]. In addition, areas of increased PP as a result of earlier ice retreat and a longer ice-free season [113, 118] may intensify the already low ratios of bacterial production to primary production measured in the polar oceans compared to more temperate regions, but may also be moderated by higher bacterial degradative efficiencies with increasing water temperatures [119]. How potential changes in PP will impact the balance of OM availability for consumption or eventual sequestration in the sediments is dependent on the



intricate relationship between environmental controls over PP and its oxidation by bacteria and higher level consumers.

Even under cold water conditions in the high latitude oceans, native microbial communities effectively recycle organic matter [120, 121], which offshore, primarily originates from diatoms [122]. Bacterial taxonomic composition, metabolic strategies and enzymatic activities have been reported from cold water marine systems [5, 24, 123] all of which can be impacted by environmental conditions [124]. As tight biological connections often dominate the base of the food web of the Chukchi Sea and Bering Strait region, a central goal is to understand how rapid changes seen in OM inputs will influence community responses by the dominant degraders and recyclers in this system. The goals of this chapter were to investigate how rapid shifts in OM availability, as OM perturbations, influenced changes in Arctic bacterial community taxonomic composition of two native microbiomes and to quantify the metabolic responses under variable conditions.

To accomplish these goals, microbiomes were collected via size fractionation from the Bering Strait subsurface chlorophyll maximum (SCM) and from bottom waters of the northern Chukchi Sea for experimental shipboard incubations. At each site *in situ* particulate organic matter  $>1.0 \mu\text{m}$  in size (POM) was initially removed. Each remaining microbiome was then incubated in the dark at  $0^\circ\text{C}$  for ten days under conditions of either A) left unamended to act as an oligotrophic control under negligible POM concentrations, or B) supplemented with algal-derived organic matter  $>5 \mu\text{m}$  in size (aOM) collected from the Bering Strait SCM, concentrated and lysed prior to addition to mimic conditions during the decline of an algal bloom. Free-living bacterial community taxonomic compositions were tracked over time with 16S rRNA sequencing. Bacterial metabolism was tracked with metaproteomics (matched to a site-specific metagenomics library) and a peptide-based functional enrichment analysis was employed [36] to characterize and quantify functional differences between the two microbiomes and to identify the associated taxonomic classes.

Specific hypotheses guided the analysis: 1) the same rapid OM perturbation, aOM input or the control (POM removal), would lead to similar changes in taxonomic composition and function (i.e., convergence) of two distinct free-living Arctic communities over a time frame of

10 days, and 2) metaproteomic differences between the two microbiomes would reflect the mechanisms operative within each community that contribute to adaptation and niche differentiation under variable OM environments. The results indicate that changes induced to the OM environment influenced the relationship between microbial composition and function, with potential implications for local nutrient and carbon cycling.

## 3.2 Additional Methods

Methods which were consistent throughout the three research chapters are described in detail in Chapter 2. Additional methods specific to the results described in this chapter are provided here.

### 3.2.1 Hierarchical clustering

Dissimilarity between variables (gene ontology (GO) terms that differed significantly between stations) was performed with the *dist* function in R, and was measured with the Euclidean distance metric. Hierarchical clustering was performed using the *hclust* function in R with the complete linkage method, which maximizes the dissimilarity between merged variables and the rest of the variables, represented as node height. Cutting the dendrograms at a height of 4 ( $h=4$ ) resulted in 10 clusters differentiating GO functions between the two stations. A heatmap of the  $\log_2$  fold changes between microbiomes for the GO terms were created using the *heatmap.2* function in *gplot* package in R.

### 3.2.2 Beta-diversity statistics

All multivariate statistics were carried out on normalized 16S rRNA OTU abundance data with the *vegan* package in R and included all sampling time points (days 0, 1, 2, 4, 6, 10). The two sample sites were assumed to be independent of one another based on origin; the Bering Strait SCM sample was collected from warmer and less saline Bering Shelf Anadyr Water, which is a mixed water mass from the Anadyr Water and Bering Shelf Water [125] while the Chukchi Sea bottom water sample was collected from the colder and more saline Pacific winter water mass [115, 126] with high nutrient concentrations (Figure 2). Normalized 16S rRNA OTU abundance data was used to build a Bray-Curtis dissimilarity matrix (*vegdist* function) and a non-metric multidimensional scaling (nMDS) plot was created with the dissimilarity matrix using the

*metaMDS* function on two reduced dimensions to observe spatial patterns between samples based on the variables of station, treatment and time. Ordination stress was low (0.089) and scatter around the regression line was tight (Figure 11), both indicating good representation of the data.

A permutational analysis of variance (PERMANOVA) was run on the Bray-Curtis dissimilarity matrix (*adonis* function) to test for statistical differences in bacterial structure between variables (null hypothesis:  $H_0$  = “the centroids of the groups, as defined in the space of the chosen resemblance measure, are equivalent for all groups”) [127]. A PERMANOVA was chosen over an analysis of similarities (ANOSIM) test because the latter is limited to categorical variables and cannot handle continuous variables (i.e., time). In addition, PERMANOVA has been found to be a more robust and powerful measure of difference in taxonomic structure within ecological datasets [127]. An analysis of similarity percentages (SIMPER) (*simper* function) was run on the Bray-Curtis dissimilarity matrix to identify which OTUs drove compositional patterns between groups (beta-diversity between station or treatment) (Appendix 4). This function is biased for highly skewed data, where the more abundant and variable OTUs will have more sway.

### 3.2.3 Alpha-diversity statistics

A Shannon Diversity Index was completed in R (*diversity* function). The histogram displays a slight skew for the diversity measure (Figure 12), however a Shapiro-Wilk test of normality ( $H_0$ : population is normally distributed;  $\alpha = 0.01$ ) provided evidence that the diversity values had a normal distribution ( $p = 0.03$ ). Therefore, a mixed model analysis of variance (ANOVA) was performed (*aov* function) to measure if microbiome diversity was dependent on time, treatment or station ( $H_0$ : There is no difference in diversity between variables;  $\alpha = 0.01$ ). Time did not have significant influence on diversity ( $p = 0.38$ ), so this variable was excluded to simplify the model. Station and treatment both impacted microbial diversity ( $p < 0.01$ ), and because both of these variables are categorical, Shannon diversity could be compared with a post hoc Tukey honest significance differences (HSD) test (*TukeyHSD* function is a pairwise comparison between groups with corrections for multiple comparisons).

**Figure 11 - Shepherd plot.** Ordination stress in the non-metric multidimensional scaling (nMDS) plot was low (0.089) and scatter around the regression line was tight, both indicating good representation of the data.

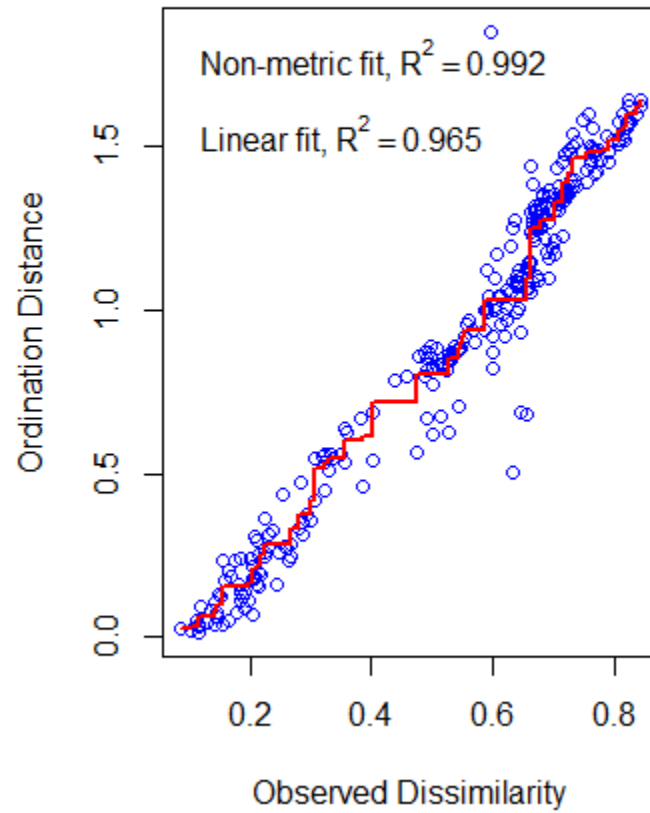
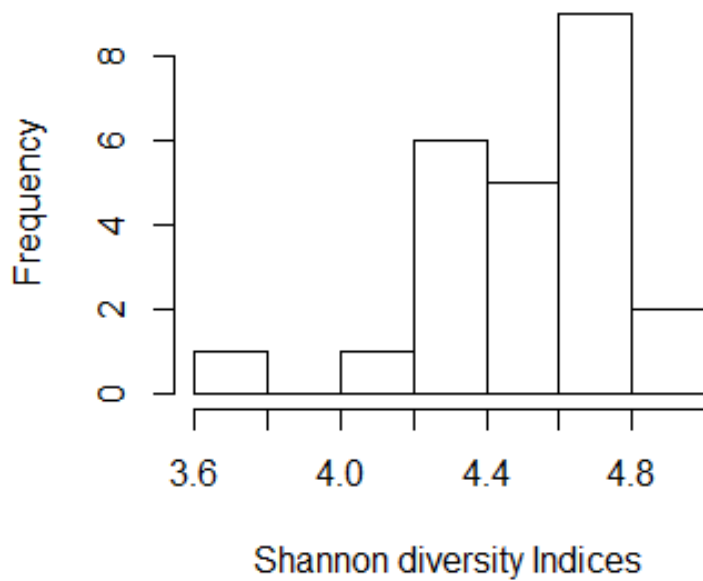


**Figure 12 - Histogram.** Histogram of Shannon diversity indices showing a normal distribution, based on a Shapiro-Wilk test of normality ( $\alpha > 0.1$ ).



### 3.2.4 Test of linearity

To determine if a linear relationship existed between bacterial structure and function, a test of significant correlation was run on dissimilarity values. The Bray-Curtis dissimilarity measures from the normalized 16S rRNA OTUs for each data point were used to compare bacterial community structure between the two microbiomes over time. To compare function between microbiomes, the sum of the number of GO terms with significant differences was used at each time point. A Pearson correlation test ( $H_0$ : true correlation is equal to 0) was completed in the vegan package of R (*cor.test* function). This test was also used to test for correlation between GO and OTU richness.

## 3.3 Results

### 3.3.1 Comparative taxonomic composition of the Bering Strait and Chukchi Sea

At the start of the incubations (day 0), 16s RNA analysis showed that bacterial taxonomic composition between the two sites were distinct as demonstrated by the separation along axis 1 of the non-metric multidimensional scaling (nMDS) plot (Figure 13). In addition, Bray-Curtis dissimilarity between these initial microbiomes was BC: 0.53-0.54 ( $n = 2$ ) (Figure 14A, Appendix 5), confirming a difference in composition was present in the original microbiome samples. Three bacterial classes, Alphaproteobacteria, Flavobacteria and Gammaproteobacteria, dominated the initial core microbiomes, contributing approximately 90% of OTU abundances at both locations (Figure 15A). Despite this dominance, the relative distribution among these core classes differed at each site. Within the Bering Strait microbiome, each core class represented nearly equivalent total relative abundances (28-34%). In contrast, Gammaproteobacteria dominated initial OTU abundances (50%) within the Chukchi Sea, which was significantly higher than in the Bering Strait (two-sample  $t$  test assuming unequal variances:  $t = -38.40$ ,  $p < 0.001$ ) and Flavobacterial abundance were significantly lower at 9% ( $t = 37.02$ ,  $\alpha = 0.05$ ,  $p = 0.018$ ). Alphaproteobacteria abundances were equivalent between stations ( $p > 0.05$ ).

**Figure 13 - NMDS.** A non-metric multidimensional scaling (nMDS) plot comparing Bray-Curtis dissimilarity of normalized bacterial operational taxonomic units (OTUs) from 16S rRNA sequencing from stations Bering Strait (BSt) and Chukchi Sea (CS) over the 10 day experiment and under the two organic perturbations (control treatment where particulate organic matter was removed (POM removal) and substrate treatment where algal organic matter was added (aOM input)). Ordination stress = 0.089. A permutational analysis of variance (PERMANOVA) confirmed that bacterial composition between the two stations were statistically different at  $\alpha = 0.01$  ( $p < 0.01$ ) and that treatment and time variables were significant at  $\alpha = 0.05$  (treatment,  $p = 0.012$  & time,  $p = 0.011$ ).

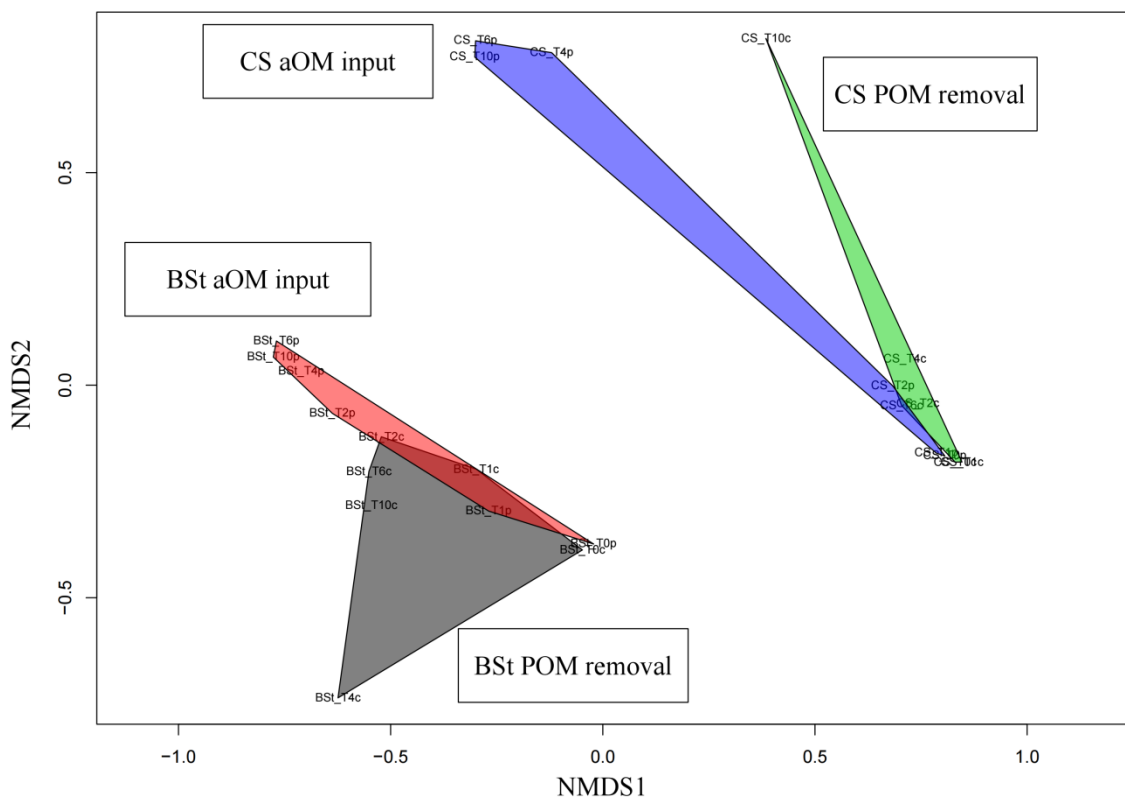


**Figure 14 - Bray-Curtis dissimilarity trends.** Bray-Curtis (BC) dissimilarity values over time comparing response of free-living bacterial composition between A) microbiomes Bering Strait (BSt) and Chukchi Sea (CS) as a function of organic perturbations (control treatment where particulate organic matter was removed (POM removal) and substrate treatment where algal organic matter was added (aOM input)), B) OM perturbation within each microbiome, and C) shifts in bacterial composition at each time point compared to the initial microbiome at day 0.

A)

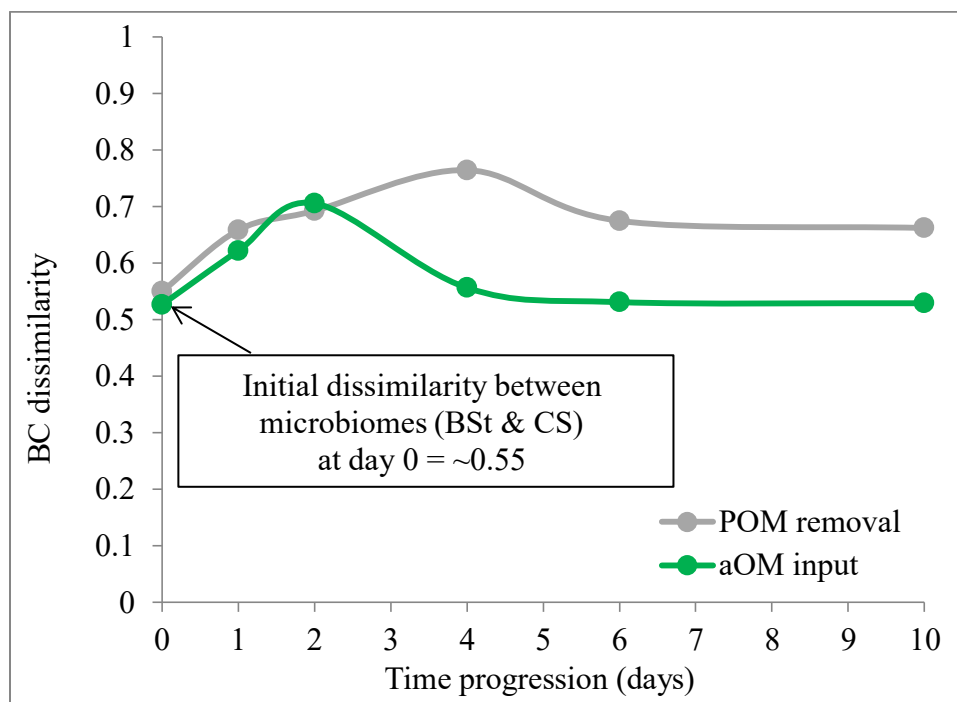
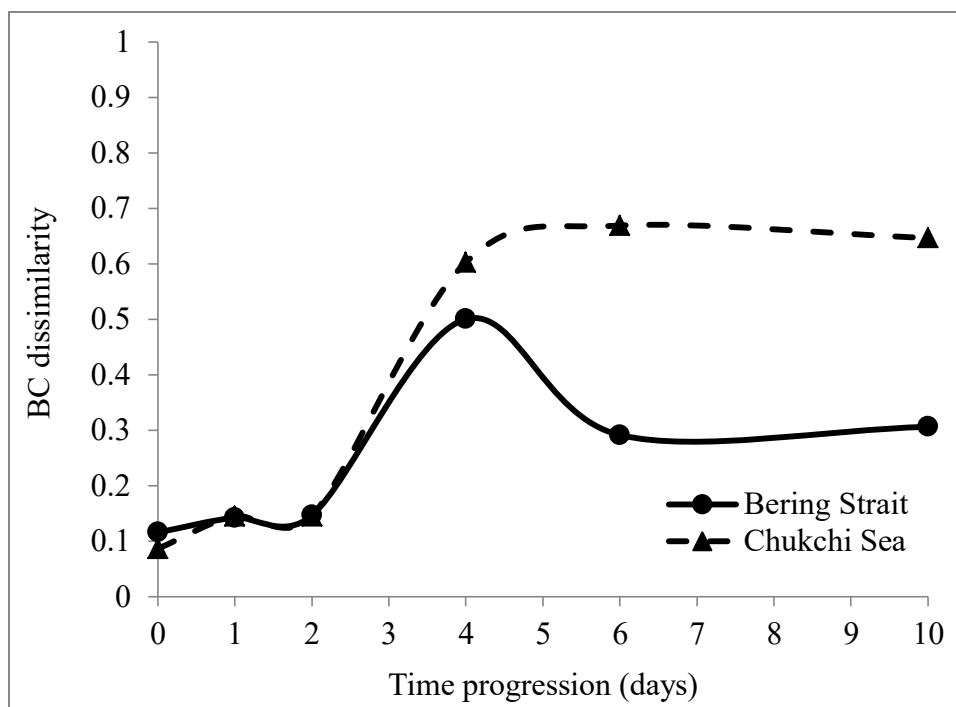


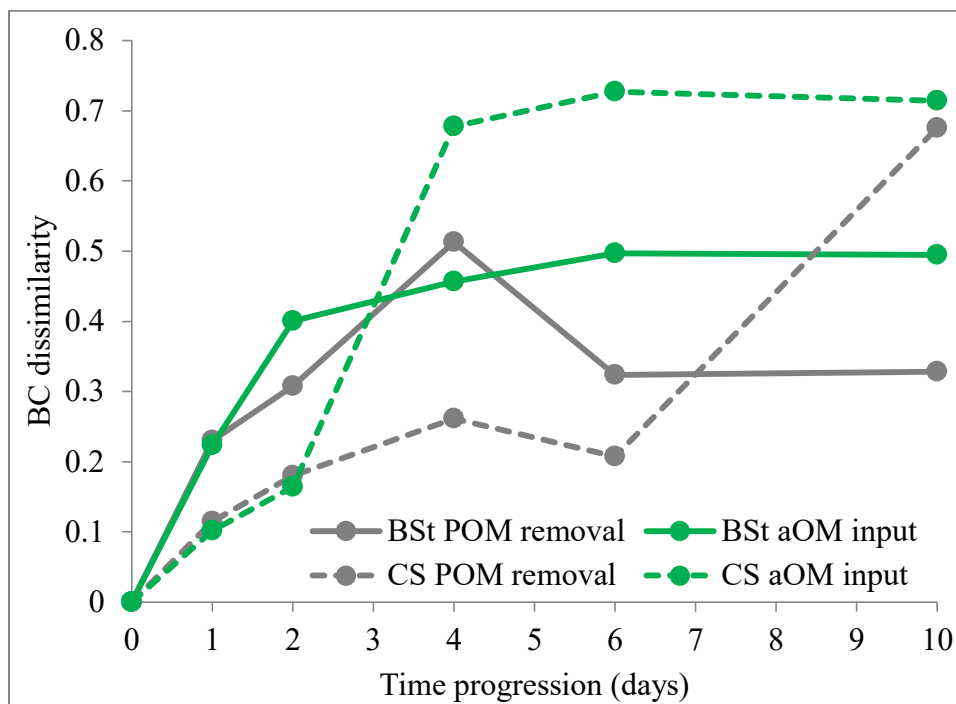


Figure 14 – Continued.

B)



C)



**Figure 15 - Initial compositions of bacterial communities.** The relative abundances of bacterial community composition at the start of the incubation experiments (day 0) in the Bering Strait (BSt) and Chukchi Sea (CS) based on normalized operational taxonomic units (OTUs) from 16S rRNA sequences for A) the 3 dominant bacterial classes, Alphaproteobacteria (Alpha), Flavobacteria (Flavo) and Gammaproteobacteria (Gamma), and the ‘Other’ category, which is a sum of the remaining classes. aOM input = algal organic matter input; POM removal = control treatment where POM >1.0  $\mu\text{m}$  was removed without aOM input. Significance tests (2-tail t-test assuming unequal variance) was used to determine difference of relative abundances of each class between the initial microbiomes (significantly different means ( $n=2$ ) denoted \* =  $\alpha$  of 0.01, \*\* =  $\alpha$  of 0.05). B) Alpha (order), Flavo (genus) and Gamma (order) taxonomic classifications at greater detail; taxonomic group was included if >5% in one sample and otherwise those groups that made up <5% abundances were summed into a residual category (e.g., ‘Alpha <5%’).

A)

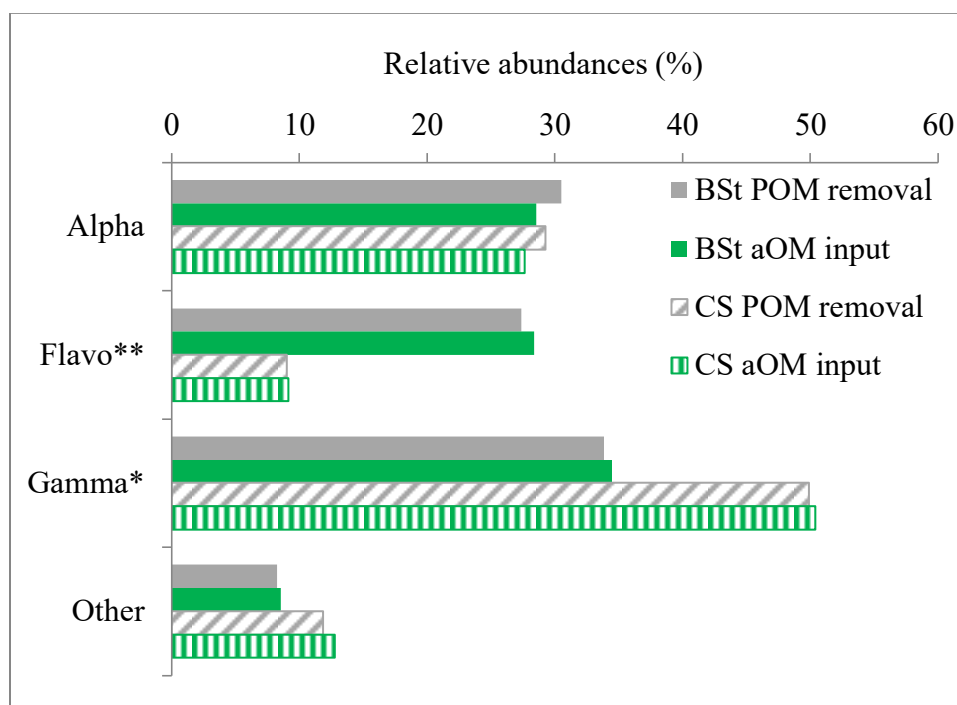
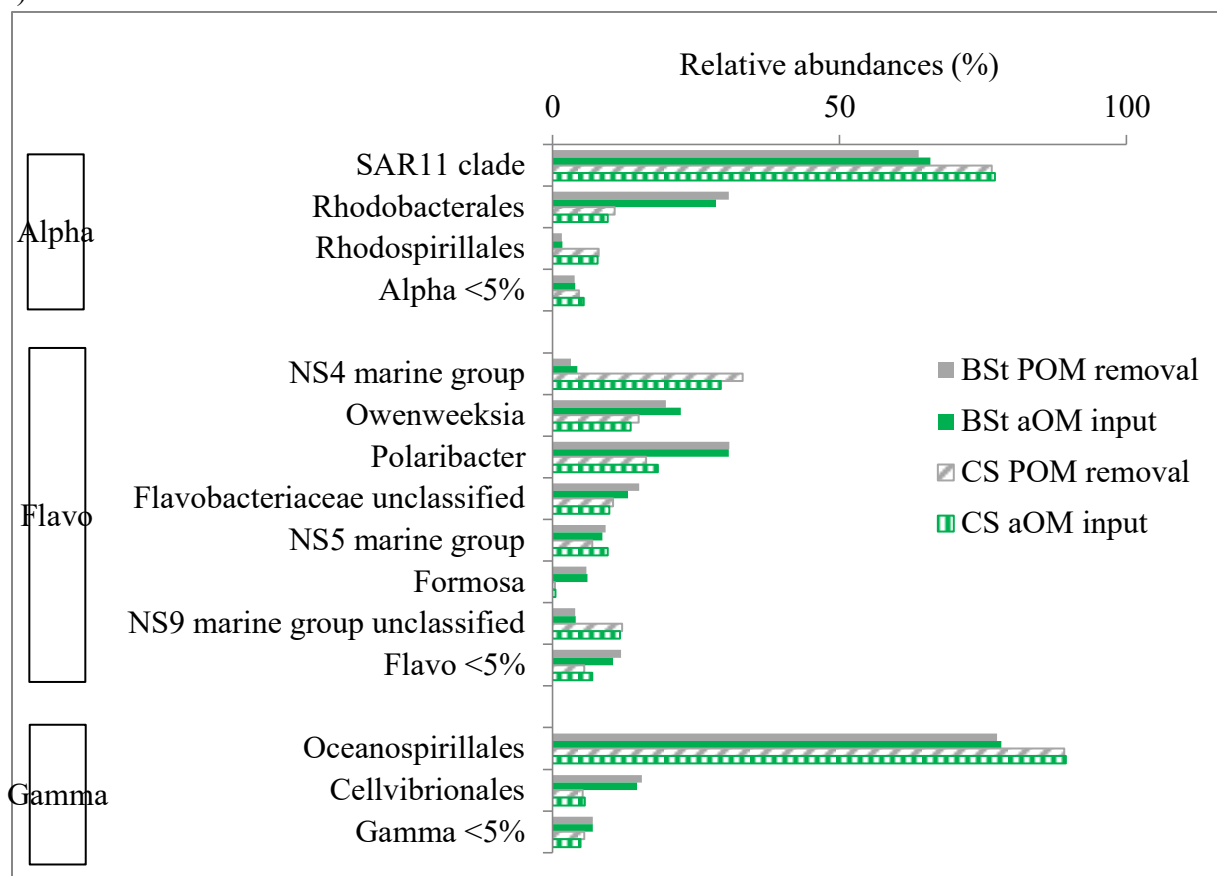


Figure 15 – Continued.

B)



An examination at a higher taxonomic resolution showed that the *Pelagibacter* spp. composed the highest relative abundances within Class Alphaproteobacteria at day 0, contributing roughly 65% within the Bering Strait and 75% within the Chukchi Sea (Figure 15B). The *Rhodobacterales* order composed 30% of Alphaproteobacteria within the Bering Strait while only contributing 10% to the Class within the bottom water sample, the latter microbiome which also had a high contribution by the *Rhodospirillales* order (~10%). Genus *Polaribacter* spp. of Class Flavobacteria had high relative abundances in the Bering Strait (30%) and Chukchi Sea (~20%), followed by *Owenweeksia* spp. (20% & 15%, respectively). Unique to the Chukchi Sea bottom waters were the high contributions of NS4 (30%) and NS9 (10%) marine groups, which composed <5% of Class Flavobacteria within the Bering Strait. Within the Class Gammaproteobacteria, the *Oceanospirillales* and *Cellvibrionales* orders had by far the greatest relative abundances within both the Bering Strait (80% & 15%, respectively) and Chukchi Sea (90% and 5%, respectively).

The difference seen between the Bering Strait and Chukchi Sea bacterial compositions measured at day 0 continued when all temporal samples were considered (Figure 13). A permutational analysis of variance (PERMANOVA) confirmed that bacterial composition between the two stations were statistically different at  $\alpha = 0.01$  ( $p < 0.01$ ) and that treatment and time variables were significant at  $\alpha = 0.05$  (treatment,  $p = 0.012$  & time,  $p = 0.011$ ). An analysis of similarity percentages (SIMPER) identified that 17 out of over 24,000 OTUs within the dataset contributed to 50% of the dissimilarity between the two Arctic microbiomes and 166 OTUs contributed to the top 80% of dissimilarity (Appendix 4). The OTUs associated with only 3 genera contributed to 34% of the dissimilarity measured between stations, each with a contribution of ~11% and included *Balneatrix* spp. and an unclassified *Oceanospirillales* spp., both within the *Oceanospirillales* order of Gammaproteobacteria, along with *Polaribacter* spp. of Flavobacteria. Genera *Pelagibacter* spp. (SAR11 clade) and *Sulfitobacter* spp. (*Rhodobacterales* order), both of Class Alphaproteobacteria, drove 6% and 5% dissimilarity, respectively. *Pelagibacter* spp. decreased abundances over the incubation period, which was consistent between both microbiomes. *Balneatrix* spp. was a dominant genus with no clear trend throughout, except for relatively large temporal fluctuations within the control (Figure 6); in the Chukchi Sea, the genus doubled in relative abundance over the 10 days while in the Bering Strait, it reached similar abundance by day 4 but then dropped again by day 10. Another

dominant feature was the large relative increases of *Polaribacter* spp. to reach ~30% total abundance after aOM input for both microbiomes, although the timing of these changes were dependent on microbiome origin. Further, high relative abundances of *Sulfitobacter* spp. in the Bering Strait and the unclassified *Oceanospirillales* spp. in the Chukchi Sea highlight some of the varied community compositions of the major bacterial genera.

### 3.3.2 Organic perturbations, community composition and bacterial abundance over time

Over the first 2 days of incubation, OM perturbation (i.e., treatment of aOM input or the control where POM was removed) had little influence on community composition (Bray-Curtis values, BC: <0.15) (Figure 14B). By day 4, however, a treatment-induced taxonomic shift occurred, as dissimilarity values increased to >0.5 (Figure 14B) and intra-community separation between OM treatments was seen along both nMDS axes (Figure 13). Changes in taxonomic abundances over time revealed that only a few genera drove a majority of the dissimilarities between OM treatments. For example, within both microbiomes, temporal increases in *Polaribacter* spp. under aOM input was not matched within the control incubations (Figure 6). OM perturbations appeared to have a greater influence over taxonomic composition within the Chukchi Sea microbiome, where BC values remained high between days 4-10 (Figure 14B). Compositional differences between Chukchi Sea OM perturbations included the relatively high abundances of *Balneatrix* spp. within the control and the aggregated increase of genera with relatively low abundances ('Other (<5%)') (Figure 6). Conversely, aOM input during this time stimulated increases in genera of the family *Colwelliaceae*, % increases that rivaled that of the *Polaribacter* spp.

Following aOM input into the incubations, there was a peak in taxonomic dissimilarity between the Bering Strait and Chukchi Sea microbiomes by day 2 (BC: 0.71) (Figure 14A), at a time when Flavobacterial relative abundances were high within the Bering Strait (45%) but still low within the Chukchi Sea (12%) (Figure 16). This high dissimilarity did not persist by day 4 (BC: 0.56) as Flavobacterial abundances increased to 30% within the Chukchi Sea microbiome, which likely contributed to the increased similarity in taxonomic composition at this time. At a finer taxonomic resolution, *Polaribacter* spp. reached >25% of total OTUs within both microbiomes, increases that occurred at day 2 within the Bering Strait compared to day 4 within the Chukchi Sea. This offset in *Polaribacter* spp. response between microbiomes likely explains

not only the peak in the BC values at day 2 under aOM input, but also the return to comparable dissimilarity values after this time (Figure 14A). Independent of microbiome, the large increases in *Polaribacter* spp. under aOM input were inversely related to changes in relative abundances of unclassified *Oceanospirillales* spp. ( $r = -0.89$ ,  $p < 0.01$ ) and *Pelagibacter* spp. ( $r = -0.98$ ,  $p < 0.01$ ).

Within the control incubation where POM was removed, the Chukchi Sea bacterial community displayed very little increase in bacterial abundances by day 6 whereas the Bering Strait community experienced a 6 fold increase through day 10 (Table 1). Greatest dissimilarity between the microbiomes under this treatment occurred at day 4 (BC: 0.76) and remained elevated until the end of the incubations at day 10 (BC: 0.66) (Figure 14A). Gammaproteobacteria had highest abundances within the Chukchi Sea under these conditions when Flavobacterial abundances remained low, whereas in the Bering Strait, bacterial contributions were more equivalent among these dominating classes (Figure 16) and appear to explain these dissimilarity trends within the control.

### 3.3.3 Alpha diversity

Biodiversity is an important factor of bacterial community functioning and stability during environmental change (e.g., [7]) and was followed using the Shannon index. Bacterial biodiversity was higher at the initiation of the incubation experiments (day 0) within the microbiome collected from the Bering Strait SCM layer (average = 4.75,  $n = 2$ , standard deviation =  $2.49E-03$ ) compared to the microbiome collected from Chukchi Sea bottom waters (average = 4.20,  $n = 2$ , standard deviation =  $1.64E-02$ ) (Appendix 6). A mixed model analysis of variance (ANOVA) assessed if significant differences in microbial diversity was dependent on categorical variables, station and treatment, or the continuous variable as time. The results indicated that microbial diversity was not dependent on time ( $p = 0.38$ ) nor treatment with all samples combined (ANOVA,  $p = 0.58$ ) or when separating each microbiome (Bering Strait,  $p = 0.38$ ; Chukchi Sea,  $p = 0.07$ ). However, the interaction between station and treatment had significant impacts on diversity ( $p < 0.01$ ). The higher diversity within the initial water sample from the Bering Strait was maintained throughout the 10 days under both treatments (Tukey Honest Significance Differences tests: aOM input,  $p < 0.01$ ; POM removal at  $\alpha = 0.05$ ,  $p = 0.016$ ) (Figure 17). The Chukchi Sea microbiome with aOM input resulted in the lowest overall

**Figure 16 - High temporal resolution of 16S rRNA bacterial classes.** Bacterial community taxonomic classes (relative abundances) from 16S rRNA sequences (days 0, 1, 2, 4, 6, 10). Classes with a minimum of 1% at one time point are shown, otherwise they are summed into the 'Other <1%' category. Organic perturbations consisted of the control, where particulate organic matter was removed (POM remova) or algal organic matter was added (aOM input).

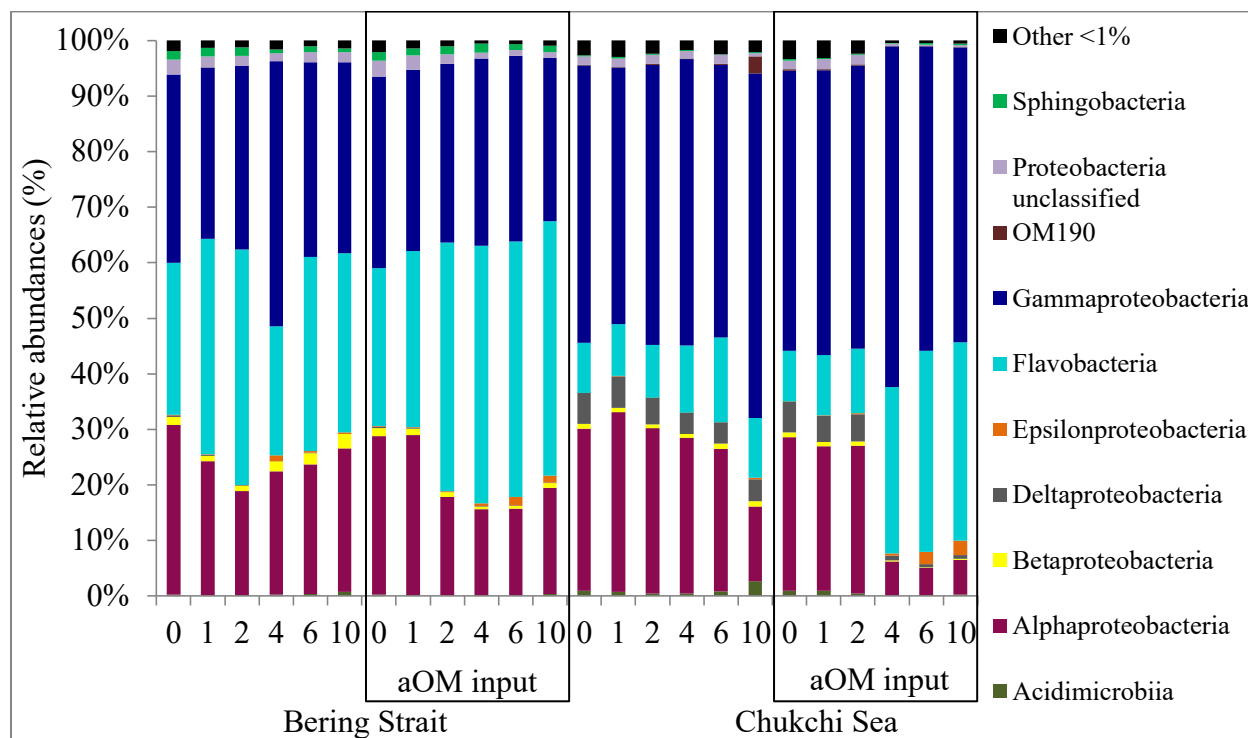
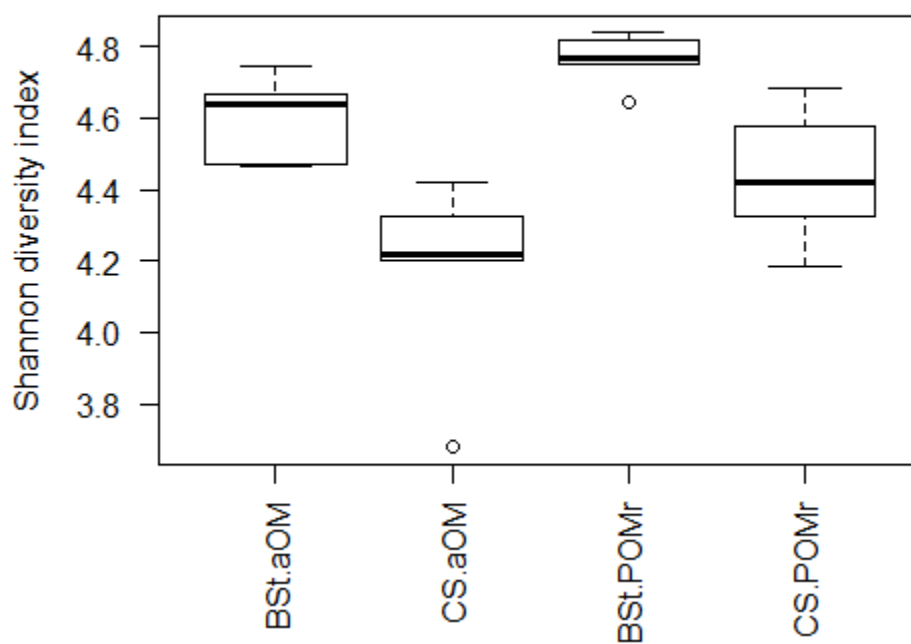


**Figure 17 - Boxplot of Shannon diversity indices.** Boxplot comparing Shannon diversity indices between microbiomes, Bering Strait (BSt) and Chukchi Sea (CS), with organic perturbations: the control where particulate organic matter was removed (POMr) or algal organic matter was added (aOM input). A mixed model analysis of variance (ANOVA) and Tukey honest significant difference test confirmed that Shannon diversities differed between microbiomes due to aOM input ( $p < 0.01$ ) and in the control (POMr) (at  $\alpha < 0.05$ ,  $p = 0.016$ ). Further, a significant difference in diversity occurred between microbiomes with opposite perturbations, BSt within the control versus CS after aOM input ( $p < 0.01$ ).





diversity, which was significantly lower than the Bering Strait bacterial diversity under both aOM input and the control where POM was removed (Tukey,  $p < 0.01$ ).

### 3.3.4 Peptide and Gene ontology (GO) identification

The Bering Strait microbiome contained a greater abundance of peptide spectrum matches (PSM) before and 10 days after OM perturbations, however, the increases measured over time were greater within the Chukchi Sea (100% vs 100-200%, respectively) (Table 2). Under aOM input, the increases in peptide expression were presumably linked to the relatively large increases in PSMs associated with Flavobacteria (Figure 5). Their increased activity was offset by a few days; Flavobacterial PSMs increased in the Bering Strait microbiome at day 1 (from 15% to 30%) but in the Chukchi Sea, this increase occurred between days 1-6 (from 9% to 46%). The 16S rRNA data (Figure 16) provided a different temporal resolution and indicated that Flavobacteria relative abundances of the Bering Strait increased at day 2 (from 32% to 45%) while in the Chukchi Sea, the increase occurred between days 2-4 (from 12% to 30%).

### 3.3.5 Comparative proteomic responses between microbiomes: Bering Strait community functions

An enrichment analysis on all gene ontology (GO) terms that matched to peptide sequences returned 81 functions with statistically different PSM counts ( $p$ -value  $< 0.01$ ) between the Chukchi Sea and the Bering Strait microbiomes over the 10 day incubation experiments. These GO terms grouped into 10 hierarchical clusters (Figure 18; Table 5). Within the initial Bering Strait community, 17 GO terms were more abundant than within the Chukchi Sea microbiome. Those with  $\log_2$  fold differences  $>1$  included magnesium ion binding (#37), organic substance catabolism (#38, #59) and outer membrane-bounded periplasmic space (#52). The remaining GO terms that were significantly greater in the initial samples from the Bering Strait ( $\log_2$  fold differences  $<1$ ) included functions in clusters 4 & 5 related to translation and transcription (#30-32, #57-58, #73-79) and transport (#17).

Within one day following aOM additions, the Bering Strait microbiome showed 26 functions more abundant than seen in the Chukchi Sea community. Cluster 9 contained those with the largest  $\log_2$  fold differences ( $>3$ ), which were related to peptidyl-propyl isomerization

(#55-56) and protein transport (#54). Cluster 4 represented Bering Strait functions that were higher at this time, and included a number of terms of translation ( $>2 \log_2$  fold differences, #57-64) as well as transcription, organic substance metabolism, energy production and conversion, and binding activity with proteins, ATP and metal ions (#65-79). By day 6 and 10 under aOM input, the Bering Strait microbiome was binding and transporting the monosaccharide xylose (#13-14) to a greater degree than the Chukchi Sea community ( $\log_2$  fold differences ranging from 3.78-5.26). Folic acid-containing compound biosynthesis (vitamin B9) (#9) also had a higher expression at day 6 ( $>3$ ) and the ABC transport complex was also significantly more abundant (#52-53,  $\sim 2 \log_2$  fold differences) at this time.  $\log_2$  fold differences between 1-2 also occurred in this time frame, including 4 iron, 4 sulfur binding (#5), molybdenum ion binding (#8) and nitrogen fixation (#34), plus few terms with  $<1$  greater abundance (i.e., the formation of C-N bonds (#35), protein folding (#72) and organonitrogen compound synthesis (#15-16)).

By day 6 after initiation of the control conditions where POM was removed without subsequent addition of aOM, Bering Strait microbiome functions with  $>1.5 \log_2$  fold differences compared to the Chukchi Sea microbiome occurred within clusters 2, 3 and 9 and were related to glutamine synthesis (#41-42), peptidyl-prolyl isomerization (#49, #56), synthesis of two branched chain amino acids with hydrophobic side chains (#47, #51), DNA metabolism (#43), ATP binding cassette (ABC) transport cellular components (#52-53) and a number of molecular functions of carboxylic acid conversion (#39, #44, #48, #50) and acid-thiol ligase activity (#46) (Figure 18, Table 5). At the end of the incubation (day 10), many of these functions continued to be more abundant within the Bering Strait microbiome, including the formation of C-N bonds (#35), polypeptide folding (#49, #56), ABC transporters (#52-53), energy conversion involving alcohol side chains (#50) and isoleucine synthesis (#51).

**Figure 18 - Heatmap of GO functions differentiating microbiomes.** Dendrogram and heatmap of Gene Ontology (GO) functions and significant  $\log_2$  fold differences (Bonferroni-corrected p-value  $< 0.01$  from a two-tailed test of proportions) of peptide spectrum matches (PSM) between microbiomes Bering Strait (BSt) and Chukchi Sea (CS) at each time point (Initial, 1, 6, 10) during the incubations; Organic perturbation included either the removal of particulate organic matter (POM) to act as the control, or algal organic matter (aOM) input. Blue shading indicates degree of  $\log_2$  fold difference with significantly greater functional abundances in the BSt metaproteome and red shading indicates degree of  $\log_2$  fold difference with significantly greater functional abundances in the CS metaproteome. Functions with  $\log_2$  fold change values are outlined in Table 5.

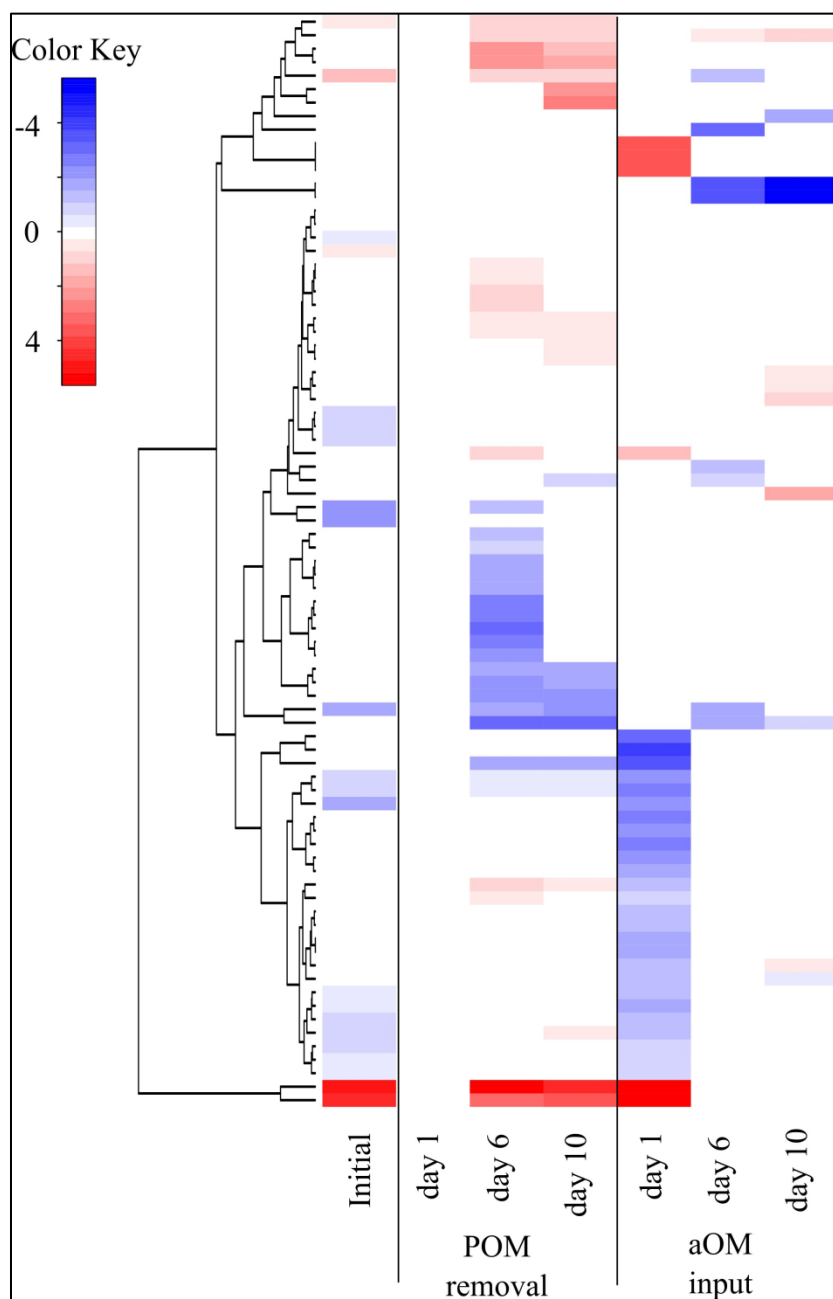


**Table 5 - Functional differences between microbiomes.** Gene Ontology (GO) functions and significant  $\log_2$  fold differences (Bonferroni-corrected p-value < 0.01 from a two-tailed test of proportions) of peptide spectrum matches (PSM) between microbiomes Bering Strait (BSt) and Chukchi Sea (CS) at each time point (Initial, d1, d6, d10). Organic perturbation included either the control where particulate organic matter was removed (POM removal) or algal organic matter (aOM) input. A negative  $\log_2$  fold difference indicates significantly higher PSM values within the BSt metaproteome and a positive value indicates significantly higher PSM values within the CS metaproteome. Function order matches the heatmap in Figure 18. Note: spectral data was missing for CS at day 1 within the control, therefore a comparison between microbiomes was not possible for the samples where POM was removed.

ID #	GO function	Cluster #	Initial	POM removal			aOM input		
				d1	d6	d10	d1	d6	d10
1	protein refolding	1	0.65	0	1.06	0.9	0	0	0
2	integral component of membrane	1	0	0	1.07	1.04	0	0.53	0.69
3	inorganic diphosphatase activity	1	0	0	2.09	1.55	0	0	0
4	hydrogen-translocating pyrophosphatase activity	1	0	0	2.26	1.67	0	0	0
5	4 iron, 4 sulfur cluster binding	1	1.3	0	0.9	0.89	0	-1.3	0
6	protein transport by the Sec complex	1	0	0	0	2.05	0	0	0
7	amino acid transport	1	0	0	0	2.75	0	0	0
8	molybdenum ion binding	1	0	0	0	0	0	0	-1.7
9	folic acid-containing compound biosynthetic process	8	0	0	0	0	0	-3.2	0
10	photosystem II	6	0	0	0	0	3.79	0	0
11	chloroplast thylakoid membrane	6	0	0	0	0	3.79	0	0
12	thylakoid	6	0	0	0	0	3.79	0	0
13	monosaccharide binding	7	0	0	0	0	0	-3.8	-5.3
14	D-xylose transport	7	0	0	0	0	0	-3.8	-5.3
15	organonitrogen compound biosynthetic process	5	0	0	0	0	0	0	-0.2
16	cellular biosynthetic process	5	0	0	0	0	0	0	-0.2
17	transport	5	-0.29	0	0	0	0	0	0
18	cytoplasm	5	0.45	0	0	0	0	0	0
19	monovalent inorganic cation transmembrane transporter activity	5	0	0	0.56	0	0	0	0
20	ion transmembrane transport	5	0	0	0.58	0	0	0	0
21	proton transport	5	0	0	0.68	0	0	0	0
22	electron carrier activity	5	0	0	0.81	0	0	0	0
23	plasma membrane	5	0	0	0.6	0.58	0	0	0
24	cell outer membrane	5	0	0	0.52	0.48	0	0	0
25	substrate-specific transporter activity	5	0	0	0	0.56	0	0	0

Table 5 – continued.

ID #	GO function	Cluster #	Initial	POM removal			aOM input		
				d1	d6	d10	d1	d6	d10
26	monovalent inorganic cation transport	5	0	0	0	0.61	0	0	0
27	transporter activity	5	0	0	0	0	0	0	0.34
28	membrane	5	0	0	0	0	0	0.22	0.4
29	generation of precursor metabolites and energy	5	0	0	0	0	0	0	0.72
30	single-organism cellular process	5	-0.7	0	0	0	0	0	0
31	RNA binding	5	-0.77	0	0	0	0	0	0
32	small molecule metabolic process	5	-0.92	0	0	0	0	0	0
33	proton-transporting ATP synthase complex, catalytic core F(1)	5	0	0	0.78	0	1.28	0	0
34	nitrogen fixation	5	0	0	0	0	0	-1.5	0
35	ligase activity, forming carbon-nitrogen bonds	5	0	0	0	-1	0	-0.8	0
36	respiratory chain	5	0	0	0	0	0	0	1.65
37	magnesium ion binding	5	-2.46	0	-1.5	0	0	0	0
38	cellular catabolic process	5	-2.21	0	0	0	0	0	0
39	monocarboxylic acid metabolic process	2	0	0	-1.5	0	0	0	0
40	cofactor binding	2	0	0	-1	0	0	0	0
41	glutamine biosynthetic process	2	0	0	-1.9	0	0	0	0
42	glutamate-ammonia ligase activity	2	0	0	-1.9	0	0	0	0
43	DNA metabolic process	2	0	0	-2	0	0	0	0
44	dicarboxylic acid biosynthetic process	2	0	0	-2.8	0	0	0	0
45	cell cycle	2	0	0	-2.7	0	0	0	0
46	acid-thiol ligase activity	2	0	0	-3	0	0	0	0
47	valine biosynthetic process	2	0	0	-2.5	0	0	0	0
48	transferase activity, transferring acyl groups	2	0	0	-2.4	0	0	0	0
49	peptidyl-prolyl cis-trans isomerase activity	2	0	0	-2	-1.9	0	0	0
50	oxidoreductase activity, acting on the CH-OH group of donors, NAD or NADP as acceptor	2	0	0	-2.2	-1.8	0	0	0
51	isoleucine biosynthetic process	2	0	0	-2.5	-2.3	0	0	0
52	outer membrane-bounded periplasmic space	3	-1.67	0	-1.9	-2.1	0	-2	0
53	ATP-binding cassette (ABC) transporter complex	3	0	0	-3	-3.3	0	-2	-1

Table 5 – continued.

ID #	GO function	Cluster #	Initial	POM removal			aOM input		
				d1	d6	d10	d1	d6	d10
54	protein transport	9	0	0	0	0	-3.2	0	0
55	isomerase activity	9	0	0	0	0	-4	0	0
56	protein peptidyl-prolyl isomerization	9	0	0	-2	-1.9	-3.6	0	0
57	translation	4	-0.93	0	-0.4	-0.5	-2.4	0	0
58	structural constituent of ribosome	4	-0.88	0	-0.3	-0.5	-2.7	0	0
59	organic substance catabolic process	4	-1.75	0	0	0	-2.2	0	0
60	rRNA binding	4	0	0	0	0	-2.5	0	0
61	cellular component organization or biogenesis	4	0	0	0	0	-2.4	0	0
62	carboxylic acid metabolic process	4	0	0	0	0	-2.8	0	0
63	tRNA binding	4	0	0	0	0	-2.2	0	0
64	regulation of cellular process	4	0	0	0	0	-2	0	0
65	unfolded protein binding	4	0	0	0.71	0.55	-1.3	0	0
66	ATP binding	4	0	0	0.3	0	-0.8	0	0
67	oxidation-reduction process	4	0	0	0	0	-1.4	0	0
68	metal ion binding	4	0	0	0	0	-1.5	0	0
69	regulation of primary metabolic process	4	0	0	0	0	-1.7	0	0
70	regulation of macromolecule metabolic process	4	0	0	0	0	-1.7	0	0
71	receptor activity	4	0	0	0	0	-1.5	0	0.31
72	protein folding	4	0	0	0	0	-1.4	0	-0.4
73	ribosome	4	-0.61	0	0	0	-1.3	0	0
74	DNA binding	4	-0.52	0	0	0	-1.6	0	0
75	transcription, DNA-templated	4	-0.82	0	0	0	-1.6	0	0
76	DNA-directed RNA polymerase activity	4	-0.86	0	0	0.48	-1.3	0	0
77	single-organism biosynthetic process	4	-0.82	0	0	0	-1	0	0
78	intracellular	4	-0.59	0	0	0	-1	0	0
79	nucleoside-triphosphatase activity	4	-0.67	0	0	0	-0.7	0	0
80	nitrate reductase activity	10	4.79	0	5.64	4.52	5.21	0	0
81	monooxygenase activity	10	4.56	0	3.02	3.63	5.47	0	0

### 3.3.6 Comparative proteomic responses between microbiomes: Chukchi Sea community

#### functions

Five GO terms were more abundant within the initial Chukchi Sea microbiome compared to the Bering Strait, including functions associated with nitrate reductase and monooxygenase activities (#80-81,  $\log_2$  fold changes of 4.79 and 4.56, respectively) and 4 iron, 4 sulfur ion binding (#5,  $\log_2$  fold change 1.3), protein refolding (#1,  $\log_2$  fold change 0.65) and a general cellular component term, cytoplasm (#18,  $\log_2$  fold change 0.45). After aOM input, 12 GO terms were detected at a greater abundance within the Chukchi Sea microbiome. At day 1, these functions included 3 cellular components of photosynthesis, all with  $\log_2$  fold changes of 3.79 (cluster 6, #10-12). Under aOM input, nitrate reductase and monooxygenase activities were only significant at day 1, although the differences were large ( $\log_2$  fold changes of 5.21 and 5.47, respectively) and ATP synthase complex was also greater at this time. After day 1 of aOM input, only one GO term was identified in the Chukchi Sea with a  $\log_2$  fold change  $>1$ , respiratory chain (#36). The other GO functions at day 6 and 10 included all general terms; receptor activity (#71), component of membrane (#2), transporter activity (#27), membrane (#28) and generation of precursor metabolites and energy (#29) with  $\log_2$  fold differences  $<1$ .

From day six to ten after initiation of the control (POM removal), 21 GO terms with significantly higher abundances within the Chukchi Sea microbiome were included in clusters 1 (#1-7), 5 (#19-26, #33), 4 (#65-66, #76) and 10 (#80-81). Similar to the initial microbiomes, nitrate reductase and monooxygenase activities (#80-81) had largest differences between the two microbiomes. Functions in cluster 1 with  $\log_2$  fold differences  $>2$  included molecular functions related to energy production by pyrophosphate hydrolysis (#3-4) and the transport of proteins and amino acids (#6-7). As in the initial microbiomes, protein refolding (#1) and 4 iron, 4 sulfur ion binding (#5) functions continued to be elevated within the Chukchi Sea microbiome 6-10 days after POM removal. The functions with greater abundance in the Chukchi Sea microbiome from cluster 5 involved ion transport (#19-26, #33), including the ATP synthase complex (#33). Lastly, functions from cluster 4 included a transcription term (#76) and binding of protein and ATP (#65-66).

### 3.4 Discussion

At the community level, water mass, OM perturbations and time all appear to contribute to the structuring of bacterial taxonomy and functionality in these shallow shelf Arctic Ocean ecosystems. It has previously been suggested that depth is a principle driver in determining bacterial taxonomic composition in the northern Chukchi Sea, where different water masses act as boundaries to dispersal [115]. The Bering Strait SCM sample was collected from warmer and less saline Bering Shelf Anadyr Water, which is a mixed water mass composed of Anadyr Water and Bering Shelf Water [125] while the Chukchi Sea bottom water represents the colder and more saline Pacific winter water mass [115, 126] with higher nutrient concentrations (Figure 2). The different water masses likely contributed to the compositional distinction measured in the initial microbiomes, despite the close proximity of the two stations in oceanographic terms.

The addition of labile algal organic matter to the Bering Strait and Chukchi Sea microbiomes stimulated large increases in bacterial abundance within the 10 day incubations, demonstrating that at a community level the two microbiomes were similarly equipped to access labile material for growth and replication. This response was expected, as increases in bacterial abundance after algal blooms is a dominant feature within the global ocean [19], including the Arctic Ocean [128]. Within the control incubation, where POM was absent, however, changes in bacterial abundance over the 10 days within each microbiome were considerably different, indicating that the Bering Strait microbiome was more adapted to rapid perturbations in OM concentrations while the Chukchi Sea microbiome displayed greater sensitivity. This difference was unexpected, given that incubation temperatures were 2°C cooler compared to Bering Strait *in situ* conditions (from 2.06°C to 0°C under incubation) while the Chukchi Sea underwent a nearly 2°C increase in temperature (from -1.72°C to 0°C) and the assumption that in the cold ocean, bacterial abundance and production is not only dependent on OM concentrations, but also on temperature [110, 129]. The divergent response in bacterial abundance under POM removal may be a consequence of the significant differences in bacterial diversities between the microbiomes, where the more diverse Bering Strait community maintained a greater stability and capacity to adapt to disturbed environmental conditions [7, 130]. It appears that differences in diversity may lead to distinct changes in abundance for a specific Arctic microbiome and may be a factor in predicting ecosystem responses to OM perturbations.



Both communities underwent some successional shift in bacterial composition from their original compositions dependent upon both time and treatment (Figure 14), consistent with the theory that bacterial community taxonomic composition is selected by the environment (e.g., [124, 131]). The consistency in the early compositional shifts (days 0-2) between stations and treatments indicates that changes to bacterial composition measured were likely a response to isolation ('bottle effects') [132]. Structural rearrangement as a consequence of initial microbiome taxonomic composition or OM perturbation was therefore resistant until 2+ days after incubation, when it became evident that the Chukchi Sea microbiome was more sensitive than the Bering Strait microbiome to OM disturbances, corroborating abundance data. However, following definitions outlined by Allison and Martiny [3], neither microbiome was completely resilient or resistant to the OM disturbances over a ten day period, with shifts in composition occurring as early as day 1. Although structural rearrangement also occurred within the Bering Strait, it was less extensive, especially within the control where there was a return of bacterial composition towards more similar initial community composition than the other scenarios, demonstrating a resiliency to this specific OM perturbation within the more diverse microbiome [133]. A longer incubation time would be needed to determine if the surface microbiome would return to its initial bacterial composition.

Based upon the results obtained from these shipboard incubations, I addressed one of the hypotheses that the taxonomic composition of two distinct free-living Arctic communities would become more similar as a response to rapid aOM exposure. The structural rearrangement that occurred after aOM input within each microbiome over a ten day period (Figure 14) occurred in similar ways to one another by days 4-10, as evidence by the return of Bray-Curtis values comparing the two stations to those from the initiation of the experiments. This suggests that high aOM concentrations supplied from diatom phytodetritus did not drive the two microbiomes to taxonomically converge or diverge by day 10, but that availability of labile substrates drove the same bacterioplankton taxonomic groups to benefit. Indeed, the increase by *Polaribacter* spp. to nearly 30% of total bacterial composition after aOM input was a dominant response within both microbiomes, lending support to the characterization of this genus and the Flavobacterial class as highly responsive to substrates originating from phytoplankton blooms [24, 134]. This class is capable of close association with phytoplankton by moving into their phycosphere [135, 136] and have been found to be positively correlated with silicate [135], an important element in

the cell wall of diatoms. These results suggest that origin within cold waters may impact the response time of Flavobacteria to convert bioavailable substrates from phytoplankton into energy for growth, as the timing for increases in abundance was delayed by 2 days within the bottom water microbiome.

The large relative increases by *Polaribacter* spp. under aOM input over the ten days indicates that the adaptability by this genus comes at the expense of community resilience, at least over a short time frame, as seen by the lack of a return by the two microbiomes to pre-perturbation conditions. This response to aOM input may in part be a consequence of the diverse set of enzymes belonging to Flavobacteria that degrade algal-derived carbohydrates and allow the rapid transport of large molecules across their cell membrane [20, 24, 134], enabling this taxonomic group to effectively compete with other bacterioplankton for early access to substrates from phytoplankton blooms. Missing from the current observations were a succession of Flavobacterial genera (i.e., *Ulvibacter* spp. and *Formosa* spp.) to shift dominance within the class [24], which may be a reflection of the short incubation time of 10 days.

Under aOM input, the increase in *Polaribacter* spp. was balanced by the temporal decline of the ubiquitous oligotrophic bacteria *Pelagibacter* spp. (SAR11 clade), a pattern that also occurs in Antarctic waters [134]. Some members of *Pelagibacter* spp. do not respond to shifts in nutrient availability and instead rely on background OM pools under both high and low nutrient concentrations, one characteristic that makes them highly efficient competitors in the global ocean [100, 137]. In these incubations, however, the decline in *Pelagibacter* spp. was a dominant feature independent of station or OM perturbation (Figure 6), suggesting a negative response by this genus to incubation conditions beyond the OM environment. *Pelagibacter* spp. has been measured to decline in abundance with depth *in situ* [115], which was attributed to a decrease in the efficiency of the proteorhodopsin family of proteins under increased darkness. As the experiments were carried out in the dark, this may be one explanation for their decreasing temporal abundances.

Directly comparing the two Arctic microbiomes, it was evident that OM conditions within the control incubations led to more unique taxonomic compositions over the 10 day time frame (i.e., partial divergence), rather than the hypothesis that both OM perturbations would

drive the two microbiomes towards compositional convergence. This trend within the control was primarily influenced by taxonomic rearrangement within the Chukchi Sea microbiome, further indicating that there was less compositional resiliency by the bottom water microbiome after the POM disturbance, resulting in a replacement effect [5]. Increases in Gammaproteobacteria to reach 62% of total class abundance by day 10 drove this community restructuring, with *Balneatrix* spp. contributing much to the increase. The results show that a majority of the taxonomic restructuring that increased dissimilarity between the microbiomes was due to a rearrangement of the most abundant bacterial taxonomic groups. This is in agreement with other work that dominant taxa are responsible for environmentally-dependent bacterial compositional changes within the Arctic Ocean [138] and suggests that measurements of the most abundant taxa are of primary importance when detecting compositional restructuring within this ecosystem with potential impacts to carbon cycling.

In addition to identifying significant differences in ecosystem measures of bacterial biodiversity and composition between the two Arctic communities, this research highlighted community-scale mechanisms related to substrate transport, energy production and growth that differentiated how two naturally occurring microbiomes functionally responded to the same OM perturbations. Trait-based methods are imperative to delineate microbial functionality which can be important indicators of ecosystem functioning [68]. This approach allowed us to address the 2<sup>nd</sup> hypothesis that functional differences between the microbiomes would inform on mechanisms at play within each community that contribute to adaptation and niche differentiation to certain OM conditions. This idea is supported by observations that biological characteristics of bacteria with differing trophic strategies provide some indication for how niche diversification within an ecosystem may develop [139].

A peak in functional dissimilarity between the two Arctic microbiomes occurred one day after aOM input and was primarily a consequence of the widespread increase in transcription, translation, protein transport and carboxylic acid metabolism by Bering Strait Alphaproteobacteria, Flavobacteria and Gammaproteobacteria (Dataset 1). Functional convergence between Arctic microbiomes occurring within 6 days after aOM input tracked results for taxonomic convergence, reflecting a temporal offset by Chukchi Sea Flavobacteria to synthesize new proteins as a response to carbon and nutrient inputs [69]. This trend indicates that

although two Arctic microbiomes may have different alpha diversities, and therefore may not be equivalent in their resiliency or productivity under environmental fluctuations [7, 133], certain dominant bacterial classes within each may be equipped to adapt in functionally and structurally similar ways as a response to high inputs of algal derived OM, such as during phytoplankton blooms. The trait-based observations for Flavobacteria in the Chukchi Sea microbiome suggests that this bacterium efficiently competes with other dominant bacterial groups within the community for access to phytoplankton-derived substrates that it allocates for growth [134], which presumably contributed to their large increase in abundance at a community scale. In areas of the Arctic Ocean where PP is anticipated to increase, these findings suggest that Flavobacteria will play an important role in the early remineralization of aOM irrespective of its location in the water column or initial abundances.

The aOM input treatment was designed to mimic the degradation phase of a phytoplankton bloom and the results one day after perturbation suggest that a priming effect on degradation [6] influenced the Bering Strait microbiome to more rapidly hydrolyze substrates (i.e., carboxylic acids) for energy production to support growth compared to the Chukchi Sea community. This may reflect the environment in which the microbiomes originated. For example, collected from the subsurface chlorophyll maximum of the water column, Bering Strait bacteria may be adapted to episodic fluxes in aOM concentrations *in situ* as phytoplankton populations bloom and sink, therefore impacting the differences measured in response rates [5]. In addition, the aOM substrates were collected from the same water as the Bering Strait microbiome, possibly explaining the rapid response of this community to the reintroduction of this organic material. The greater biodiversity measured within the Bering Strait microbiome could have contributed to this rapid response at day 1 as the controlling organisms would have a higher likelihood of being present to impact community functioning [7, 130, 140]. Although these specific metabolic responses to aOM input occurred more rapidly within the Bering Strait, the community-scale increase in total metabolic activity within the Chukchi Sea was comparably larger (PSMs +100% compared to +200%, respectively) and may indicate a particularly high plasticity within the Chukchi Sea community to the added substrates [5, 141].

Even as the microbiomes converged at 6 days after aOM input, Bering Strait Alphaproteobacteria acquired and metabolized small substrates (e.g., sugars through ABC

transporters) in higher quantities than within the Chukchi Sea (Dataset 1), which suggests that this bacterium of the SCM microbiome was adapted to access these labile substrates more efficiently compared to the deeper microbiome. In particular, the high levels of binding and transport of the monosaccharide xylose within the Bering Strait microbiome corroborates recent results from the central Arctic Ocean that surface bacterial populations in ice-free water have greater xylan hydrolysis activities than communities from deeper in the water column [142]. Although Balmonte et al. [142] reported no compositional affiliation with the hydrolysis of these substrates, the trait-based approach used in the current study indicates that the binding and transport of the carbohydrate xylose through ABC transporters was solely associated with Alphaproteobacteria at this time, an indication of heterotrophic mechanisms that define a niche for this bacterium in the SCM to compete for labile substrates.

An increase in the number of GO terms differentiating the Bering Strait from the Chukchi Sea 6 days after POM removal compared to the start of the incubation indicated functional divergence occurred as time progressed within the control. In particular, substrate limitation accentuated how energy conversion and production characterized metabolic strategies of the bacterioplankton depending on the originating community. For example, the dominance of Bering Strait Alphaproteobacteria (47-95% of PSMs) related to transport and energy conversion fueling amino acid synthesis (clusters 2 & 3) (Dataset 2) reflects the importance of these biomolecules for Alphaproteobacterial metabolism when substrates are scarce in the surface Arctic Ocean [143]. In the Chukchi Sea, however, ion transport and energy production were largely associated with Gammaproteobacteria (#19-26, >50%) while functions related to energy production for polypeptide transport (#3-4, 6-7) were directed by an ambiguous bacterial class (Inconclusive) (42-55%) (Dataset 4).

Chukchi Sea bottom water Class Planctomycetia utilized nitrate as an energy source (#80, 81) at a significantly higher abundance than in the Bering Strait, with the highest  $\log_2$  fold differences of the experiments (4.5 – 5.6) (Datasets 3 and 4). Nitrate concentrations are typically low in the surface waters of the Chukchi Sea and Bering Strait regions in late summer [144], however relatively high nitrate concentrations were measured within the bottom waters of the Chukchi Sea at the time of water sampling (Figure 2) and the elevated nitrate reductase activity is suggestive of intense denitrification. In addition, deviation ( $N^*$ ) from the N:P of the Redfield

Ratio using the equation  $[\text{NO}_3^-] - 16[\text{PO}_4^{3-}] + 2.9$  [145], further supports the enrichment analysis that denitrification was occurring (value for 55 m in the Chukchi Sea was around -11).

Planctomycetia appears to be ubiquitous within the Chukchi Sea at various depths [138, 146] and this type of nitrogen metabolism by Planctomycetia has been measured in deep sea sediments near hydrothermal vents [147]. Although I could not identify which of the three prokaryotic nitrate reductases were expressed here [148], the enrichments over time provided evidence that nitrate was more important as an electron acceptor during organic matter remineralization within the bottom water community. A number of other GO functions enriched within the Chukchi Sea and also associated with Planctomycetia may be related to the nitrate reductase activity, such as 4 iron - 4 sulfur cluster binding, oxidation-reduction process and metal ion binding.

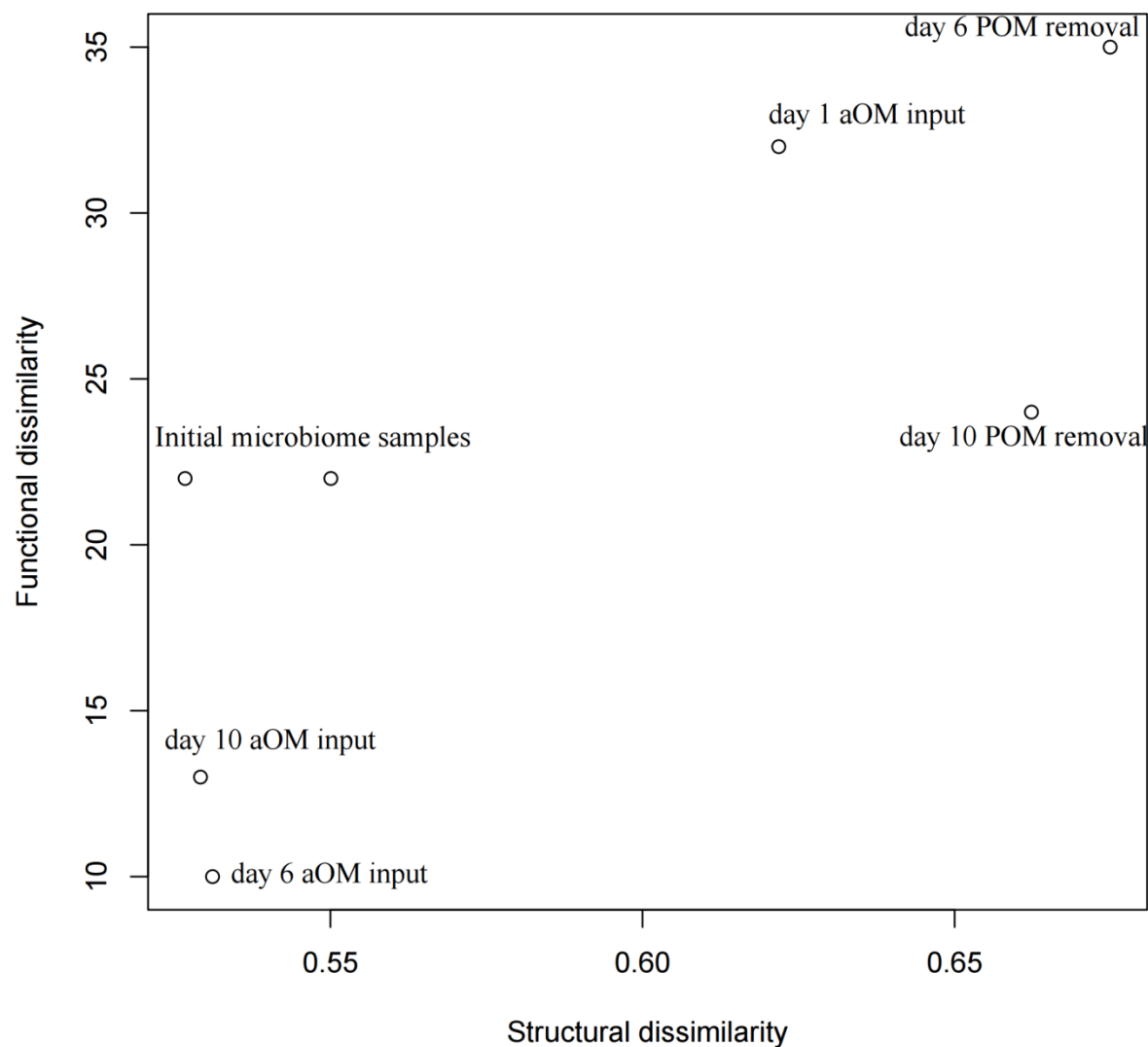
The shipboard incubations captured functional differences between two Arctic microbiomes to OM perturbations over a ten day period. As the results did not include an analysis of how biodiversity influenced long-term functional changes, I cannot directly address the ‘insurance hypothesis’ [7]. From this work, however, it is apparent that early metabolic responses (<10 days) by these free-living bacterial communities to increased labile substrates occurred more rapidly within a more diverse microbiome, and that a majority of these functions were related to protein synthesis one day after the perturbation occurred. The advantage of a higher biodiversity, however, did not persist, as functional differences by day 10 after aOM input were nearly equivalent between the two microbiomes. Further, this did not translate when POM concentrations were decreased, when the less diverse bacterial community had slightly higher functional responses over this short time frame. It is likely that, in addition to biodiversity influencing the differences in timing and functionality between microbiomes, differences in initial bacterial composition may also impact function [149].

The relationship between taxonomy and functional traits within microbial communities is of primary importance to better predict and understand impacts to biogeochemical cycling, but as discussed by Violle et al. [1] and others [150, 151], this connection between these important bacterial factors is not well defined and limits our ability to effectively represent the suite of microbial diversity in biogeochemical models. Galand et al. [4, 68], however, showed that significant relationships between bacterial production and phylogenetic similarity can occur, and that environmental stimulus potentially contributes to shifts in community structure, which are in

turn drivers of functional changes within microbial communities. In the current work, a comparison of bacterial compositional dissimilarity and the number of significant differences of GO functions between two microbiomes after OM perturbation showed a significant positive correlation at  $\alpha = 0.05$  ( $r = 0.79$ ,  $n = 6$ ,  $p = 0.034$ ) between the two important metrics of microbial ecology, taxonomic structure and community function (Figure 19). The results that structure and function are related corroborate with other work, including from cold marine waters [5, 123] and contests the idea of strict functional redundancy [4, 94].

Unique to this study, I also showed how these metrics varied temporally as a consequence of the OM perturbation and the functions that distinguished the two Arctic microbiomes. In particular, the later portion of the experiments (days 6-10) drove the correlation between taxonomic structure and function and were dependent on the OM perturbation (Figure 19). The functions responsible for the high dissimilarity within the control did not only include degradative enzyme activity [123] (i.e., nitrate reductase) but encompassed a collection of GO terms related to energy production and conversion matched with ion transport and amino acid synthesis. In contrast, this work highlights that Arctic phytoplankton blooms may induce an early (i.e., day 1) temporal offset in the early structural and functional rearrangement within microbiomes, but that over a longer time frame of 10 days, a high degree of functional convergence occurs between them. Previous reports suggest that major bacterial groups acquire labile substrates under high organic concentrations in a generalist behavior [137]. The results presented here agrees that a rapid increase in algal substrates leads to enhanced functional redundancy in two communities that regularly experience high input of algal-derived OM. In addition, these findings also demonstrate that time was an important factor to reach functional similarity between microbiomes.

**Figure 19 - Structure-function relationship.** Relationship between structural dissimilarity (based on Bray-Curtis dissimilarity of normalized 16S rRNA OTUs) and functional dissimilarity (based on number of GO terms with significant differences) between the two Arctic microbiomes. Based on a Pearson correlation test, the relationship was significant at  $\alpha = 0.05$  ( $r = 0.79$ ,  $n = 6$ ,  $p = 0.034$ ). Organic perturbation included either particulate organic matter (POM) removal (the control) or algal organic matter (aOM) input.





Given the relationship measured between taxonomic structural and functional trait dissimilarities over time, it is remarkable that among the thousands of GO functions identified between the Bering Strait and Chukchi Sea metaproteomes (Table 2), no more than 35 terminal GO functions differentiated the two microbiome proteomic landscapes at any one time. Therefore it is difficult to dispute that some degree of partial redundancy must occur in compositionally distinct natural microbial communities, as this functional overlap would provide resiliency to intact populations [87]. An estimate of water transit time between the two locations is on the order of months [126], which is longer than the response times measured here. Therefore, water column transport and mixing between sites is an unlikely explanation for the partial functional redundancy measured between microbiomes.

The increasing popularity of applying functional traits instead of solely using traditional taxonomic methods (biodiversity or species richness) to analyze and predict spatial and temporal ecosystem functioning and response (e.g., [1, 104]) builds from the concept that functional diversity is a more powerful indicator of community productivity than traditional taxonomic measures (e.g., [140, 152]). A simple comparison of all Gene Ontology data as a proxy for richness of community function and all OTUs as an indicator of community compositional richness returned no linear correlation between the two ( $p > 0.05$ ). As a first step this suggests that within these two Arctic Ocean microbiomes, an increase in compositional richness did not increase functional richness, which is not consistent with bacterioplankton ecology from the Mediterranean Sea [4] but corroborates this idea that taxonomic measures are not equivalent to functional measures. If available, a recommendation would be to incorporate a range of methods to increase the scope of descriptive data when investigating the functioning of complex communities in relation to ecosystem dynamics.

### 3.5 Conclusions

The Chukchi Sea region is characterized by tight benthic-pelagic coupling, dynamic cycles of phytoplankton blooms and recent climatic changes, including projected impacts to the timing, quantity and quality of phytoplankton blooms. Much of the primary production is recycled by the microbial loop and this dissertation revealed that the timing of bacterial response to inputs of phytoplankton-derived substrates may be dependent on initial community taxonomic

composition. Although a number of ecosystem measures (bacterial biodiversity, composition and metabolic functions) significantly differentiated them, similar community-wide responses to aOM input were apparent, measured as comparable shifts in bacterial abundance, taxonomic composition and metabolic functions. However, even as the microbiomes converged under the high substrate environment, certain bacterial classes and their functions differentiated the microbiomes based on origin (e.g., Bering Strait Alphaproteobacteria binds and transports small sugars through ABC transporters).

The increase in community metabolism within both microbiomes within the control incubation conditions was not matched by equivalent increases in bacterial abundances between stations, and drove the microbiomes apart structurally and functionally. These results suggest that during periods where POM concentrations are reduced, the taxonomic composition of Arctic microbiomes will likely diverge, along with community functionality related to energy conversion and production. Overall, this trait-based method revealed that different bacterial groups drove functional differences between microbiomes (i.e., Chukchi Sea Planctomycetia controlled nitrate reductase), which implies that conditions which select for certain bacterial groups may have impacts on local biogeochemical cycling.

These findings also contribute to the ongoing discussion regarding functional redundancy versus niche separation in natural microbiomes (e.g., [3]), with particular relevance for the incorporation of microbial taxonomic data into oceanic-scale biogeochemical models. An important issue for such models are what type of bacterial community details will impact the accuracy of representing rates of ecologically-important biogeochemical cycles [3]. The results presented here suggest that, for the Chukchi Sea region, distinguishing microbial origin and community taxonomic composition for predicting mechanistic responses is especially important under environmental conditions when labile substrates are comparatively scarce. Alternatively, under scenarios where aOM substrate concentrations are high, such as during phytoplankton blooms, these results suggest that the incorporation of data describing community function and composition may provide minimal benefit for predictive models after initial restructuring of the microbiomes has occurred (>6 days). These conclusions can assist modeling efforts by identifying 1) which physiological traits to focus on, 2) temporal resolution appropriate for variable functions and 3) taxonomic associations. Lastly, it is clear that scale matters; although

redundancy exists when analyzing a large quantity of functions (i.e., the complete metaproteome of natural bacterial communities), pinpointing those functions that differentiate microbiomes show that relatively few functions may impact the biogeochemical environment (e.g., nitrogen cycling). Such processes accentuate the niche separation occurring within the communities, even at a broad taxonomic classification of class.

## CHAPTER 4

4. SELECTIVE LOSS OF ALGAL BIOMARKERS BY DISTINCT ARCTIC OCEAN  
MICROBIOMES AND EVIDENCE OF ENZYME ACTIVITY THROUGH  
METAPROTEOMICS

## 4.1 Introduction

The availability of labile organic matter (OM) and nutrients regulate microbial community composition and functionality in a variety of marine environments (e.g., [19, 37, 38]). In cold regions of the ocean, OM source and abundance also appears to be an important factor for the growth rate and structuring of prokaryotic communities [153, 154]. Despite the lower temperatures, complex communities of cold water marine bacteria show degradation kinetics comparable to other systems and preferentially degrade labile fractions of OM over the timescale of days to change the composition and concentration of OM (e.g., [14, 77]). Previous Arctic research has suggested that composition of marine bacterial communities may regulate enzymatic activity for degradation [123], however it remains uncertain how compositionally distinct microbiomes impact changes to OM composition during degradation, and if functional enzymatic expression is selective or broadly seen across a community. Analysis completed in the 2nd chapter showed that the input of algal substrates led to functional converging of the two microbial communities over a 10 day period, although they remained compositionally unique throughout the incubations. Here, I characterized temporal changes in organic composition of the particulate organic matter (POM) and followed lipids and amino acids as specific biochemical components within each microbiome to determine if the two communities had similar degradation potentials for this fraction of the POM. A hypothesis was that selective loss of lipid classes and amino acid concentrations of the added particles would be comparable between microbiomes and would have similar temporal patterns irrespective of differences in initial community composition.

While there is a broad history within the literature on tracking removal of specific biochemical constituents by microbiomes (e.g., [75, 155, 156]), there is little research linking

bacterial function using –omic methodology to geochemical data. The coupling of such information within models can lead to a greater understanding of how microbial processes control and respond to environmental biogeochemical gradients [25, 157, 158], with implications for carbon and nutrient cycling. In the current work, I took a multidisciplinary approach to collectively determine if community taxonomic structure (16S rRNA sequencing) of two natural Arctic Ocean microbiomes and their enzymatic functionality measured through metaproteomic assessment were linked to changes in the lipid composition of algal-derived particles. In the first two chapters, I discovered that enzyme expressions distinguishing the microbiomes and time progression were limited to a handful of functions related to internal nitrogen cycling and energy conversion. Therefore, I did not expect to identify additional enzymes with significant temporal changes or differences between microbiomes, however I hypothesized that similar patterns between the two methodologies, bacterial enzyme profiles and shifts in POM lipid composition, could be identified. Further, because some labile compounds appear readily accessible to most major bacterial groups (e.g., [18]) without necessarily impacting bacterial community composition (e.g., [154]), I expected the same bacterial classes within each Arctic microbiome to be responsible for the enzyme profiles associated with lipid degradation. The specific hypothesis being tested was that bacterial classes associated with degradative lipid enzymes would be the same within each microbiome over the short time-frame of 10 days.

## 4.2 Additional Methods

Methods which were consistent throughout the three research chapters are described in detail in Chapter 2. Additional methods specific to the results described in this chapter are provided here.

### 4.2.1 Particulate organic carbon and nitrogen

For particulate organic carbon and nitrogen (POC & PON) analysis, 400 ml of water from the algal organic matter addition incubations (aOM input) were filtered through combusted 25mm glass fiber filters (Whatman GF/F) and frozen at -80°C. Filters were thawed, acidified drop-wise with HCl (aq) for an hour in a clean desiccator, and transferred to a 60°C oven to dry. Samples were repackaged in combusted foil packets for analysis by standard methods [159].

#### 4.2.2 Lipid extraction and analysis

Particle samples (1 L) collected onto combusted GF/F filters were extracted wet via microwave-assisted solvent extraction (MASE; MARS-5 system) with 2:1 dichloromethane : methanol (DCM:MeOH) (see Harvey et al. [159] and references therein). Total lipid extract (TLE) was evaporated to dryness. Base hydrolysis of total lipid used 0.1N KOH with 5 $\alpha$ -cholestane and C19:0n fatty acid serving as the internal standards for the neutral and polar fractions, respectively. The entirety of the particle extract was hydrolyzed and used to measure individual markers.

Following base hydrolysis of total lipid, neutral lipids were partitioned with 9:1 hexane : diethylether. Following acidification with concentrated hydrochloric acid (aq), polar fatty acids were similarly partitioned. Neutral components were derivatized using BSTFA to form their trimethylsilyl (TMS) products, and fatty acids were converted into their corresponding methyl esters using boron trifluoride (10% in methanol). Both fractions were quantified with an Agilent 6890N gas chromatograph with flame ionization detector (GC-FID) and identified with an Agilent 6890 gas chromatograph coupled to an Agilent 5973N mass spectrometer (GC-MS). Both instruments utilized a 60m DB5-MS column. Chromatographic details are described in Belicka et al. [160] but with an inlet temperature of 250°C. Neutral lipids were analyzed in detail and individual components were also categorized and summed as total alcohols, sterols, tocopherols, or glycerol monoethers. For identification of double bond positions of fatty acids, a portion of fatty acids were converted to picolinyl esters [161] to provide confirmatory fragmentation information. Polyunsaturated fatty acids and fatty acids in low concentration were also validated by comparison of retention time and mass spectra of a 52-component fatty acid methyl ester standard (Nu-Chek Prep, Inc.).

#### 4.2.3 Particulate amino acids

Samples for amino acid analysis (1 L) were collected onto 47 mm combusted GF/F filters and frozen until analysis. Filters were sliced into 1/4 (for Chukchi Sea) or 1/8 (for Bering Strait) pieces and technical duplicates or triplicates per sample were prepared in parallel. A blank filter was also prepared to correct for lab contamination. Particulate total hydrolysable amino acid (THAA) analysis by gas chromatography-mass spectrometry (GC-MS) followed methods

outlined in Moore et al. [162]. Briefly, 75-100  $\mu\text{l}$  of Norvaline were added to each sample to act as an internal standard prior to a 4 hour acid hydrolysis with 6 M HCl at 100-110°C [163], followed by a pH-adjustment with sodium carbonate to obtain a pH range 1.5-5. Solid phase extraction and derivatization (with propyl chloroformate and propanol) was completed with an EZ:Faast method (Phenomenex). Samples were then evaporated under  $\text{N}_2$  gas and redissolved in an 80:20 Isooctane:Chloroform solvent. Amino acids were separated using gas chromatography (Agilent 7890A, Santa Clara, CA) with a DB-5 MS capillary column (0.25 mm ID, 30 m); oven temperature increased from 110°C to 280°C at a rate of 10°C per minute and held for 5 minutes, followed by ionization and structural identification via mass spectrometry (Agilent 5975C, Santa Clara, CA) with helium as the carrier gas. Selective Ion Monitoring was used to isolate and measure individual THAAs by identifier ions (masses provided by Phenomenex). Final quantification was made by peak integration, comparison to the internal standard and a blank-subtracted correction.

#### 4.2.4 Enzyme profiles and taxonomic assignments

Gene ontology (GO) terms and peptide spectrum matches (PSMs) from the complete Bering Strait and Chukchi Sea datasets were mapped to enzyme commission numbers (EC#). The conversion data file was downloaded from the Gene Ontology website (<http://www.geneontology.org/page/download-mappings>) [65, 66, 164] on December 19, 2018. Nomenclature of the EC#s were downloaded from the ENZYME database (<https://enzyme.expasy.org/cgi-bin/enzyme/enzyme-search-cl?3>) [165, 166] on December 19, 2018. Taxonomic assignments at the class level for select EC#s were identified from the Bering Strait and Chukchi Sea GO databases (Datasets 1-4) and PSMs were assigned to each class to quantify taxonomic contribution to each enzyme function.

### 4.3 Results

#### 4.3.1 Changes in fatty acid composition

Total fatty acid concentrations of added particles and aggregates at day 1 were higher within the Bering Strait (43.4  $\mu\text{g}/\text{mg}$  POC) compared to the Chukchi Sea (25.4  $\mu\text{g}/\text{mg}$  POC), however fatty acid distributions were comparable (Figure 20; Table 6). Monounsaturated

(MUFA) and saturated (SFA) fatty acids dominated the total fatty acid composition, ranging from 38.1-39.4% and 41.4-42.6%, respectively. Polyunsaturated fatty acid (PUFA) and odd + branched chain fatty acid (Odd + br FA) distributions were lower, ranging from 14.5-15.8% and 3.5-4.7%, respectively. Total fatty acid concentrations either remained stable or increased between days 1-6, then sharply decreased by day 10 (Figure 20). Over the ten days, total fatty acid concentrations declined by 41.2% in the Bering Strait incubation and by 22.3% in the Chukchi Sea incubation (Table 7). Variable changes in fatty acid classes occurred between day 1 to day 6 when SFA concentrations increased within the Chukchi Sea microbiome experiment and MUFA concentrations increased within the Bering Strait (Figure 20) before both decreasing by day 10. Over the 10 days, a greater loss of SFA concentrations occurred in each microbiome (47.5% and 33.9% over ten days, respectively) compared to total fatty acids and relative loss of PUFAs were highest (60.0-66.4%) among all classes (Table 7). In both microbiomes there was a substantial increase in Odd + br FAs concentrations during the incubations, increasing by 70.5% in the Bering Strait and 137% in the Chukchi Sea (Table 7), with these fatty acid classes accounting for >11% of fatty acid class distributions by day 10 (Table 6). Small increases in the relative abundance of MUFAs also occurred within each microbiome (Table 6), however, appeared to be a consequence of their slower degradation since absolute concentrations over the 10 day incubations declined by 38.6% in the Bering strait and 12.1% in the Chukchi Sea treatment (Table 7).



**Figure 20 - Fatty acid concentrations over time.** Fatty acid class concentrations ( $\mu\text{g}/\text{mg}$  POC) of the particles from the Bering Strait (BSt) and Chukchi Sea CS microbiomes over days 1 (d1), 6 (d6) and 10 (d10).

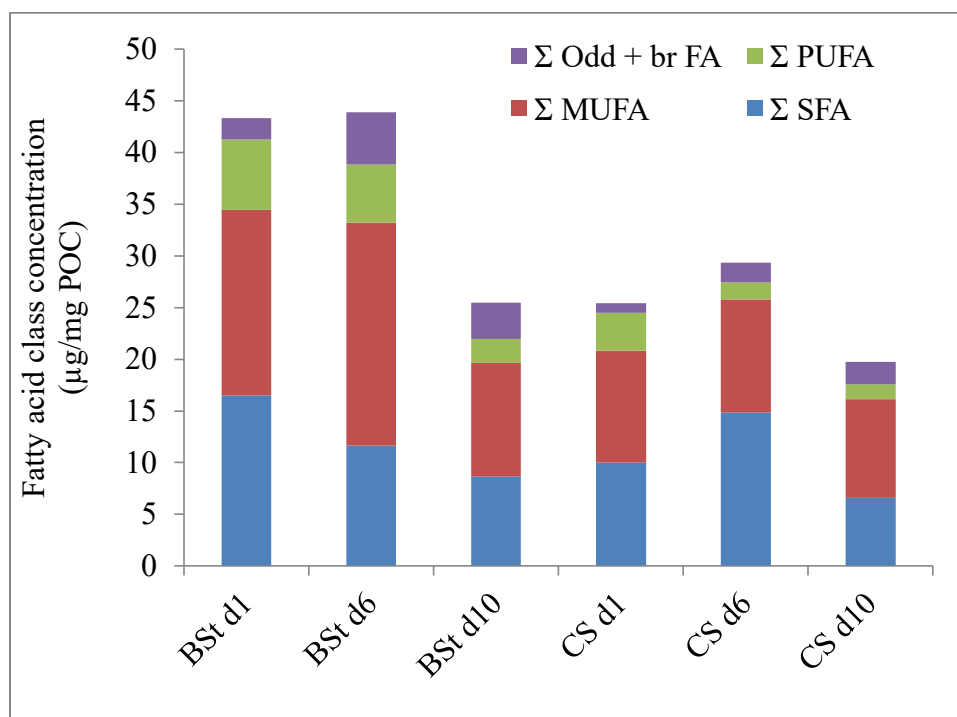


**Table 6 - Fatty acid distributions.** Fatty acid compound class distributions (% of total) for the A) Bering Strait and B) Chukchi Sea.

A)

Fatty acid class	Compound	day 1	day 6	day 10
SFA	C12:0n	0.2	0.5	0.2
	C14:0n	8.9	7.4	6.8
	C16:0n	20.5	13.2	16.6
	C18:0n	7.3	4.6	9.8
	C20:0n	0.0	0.2	0.0
	C22:0n	0.9	0.5	0.4
	C24:0n	0.1	0.1	0.1
	C26:0n	0.1	0.1	0.1
MUFA	C14:1**	0.2	1.5	1.5
	C16:1**	36.9	1.9	1.6
	C16:1 (n-7)	0.3	34.5	28.8
	C18:1*	0.0	0.1	0.1
	C18:1 (n-9)	3.1	1.9	2.0
	C18:1 (n-11)	0.1	7.8	8.8
	C20:1**	0.9	1.5	0.5
PUFA	C16:2	0.5	0.7	0.7
	C16:2	0.0	0.0	0.0
	C16:3	0.0	0.3	0.3
	C16:3	0.0	0.7	0.8
	C16:4	0.9	0.9	0.6
	C18:2	2.0	0.6	0.6
	C18:2**	0.2	0.4	0.4
	C18:3	0.1	0.1	0.1
	C20 PUFA	0.4	0.2	0.1
	C20:4 (n-6)	0.1	0.1	0.1
	C20:5 (n-3)	10.4	7.9	4.6
	C22:6 (n-3)	1.0	0.8	0.8

Table 6A – Continued.

Fatty acid class	Compound	day 1	day 6	day 10
Odd + br	C13:0i	0.0	0.7	0.5
	C13:0a	0.0	0.2	0.2
	C13:0n	0.0	0.1	0.1
	C14:0i	0.1	0.4	0.5
	C15:0i	0.8	1.8	2.3
	C15:0a	0.4	0.7	1.2
	C15:0n	0.7	0.7	0.8
	C15:1**	1.5	5.8	6.5
	C16:0i	0.0	0.0	0.0
	C17:0a	0.0	0.0	0.1
	C17:0n	0.4	0.3	0.8
	C17:1*	0.2	0.4	0.3
	Methylphytanate	0.0	0.0	0.0
	C21:0n	0.2	0.1	0.2
	C21:1*	0.1	0.1	0.1
	C23:0n	0.1	0.1	0.1
	C25:0n	0.1	0.1	0.1
Summary	<b>% SFA</b>	38.1	26.5	34.0
	<b>% MUFA</b>	41.4	49.1	43.3
	<b>% PUFA</b>	15.8	12.8	9.0
	<b>% Odd + br</b>	4.7	11.5	13.8

Table 6 – Continued.

B)

Fatty acid class	Compound	day 1	day 6	day 10
SFA	C12:0n	0.0	0.0	0.0
	C14:0n	9.2	2.4	6.4
	C16:0n	24.0	28.3	19.4
	C18:0n	4.4	17.6	7.1
	C20:0n	0.5	0.6	0.4
	C22:0n	1.0	1.3	0.3
	C24:0n	0.1	0.1	0.0
	C26:0n	0.2	0.2	0.0
MUFA	C14:1**	0.0	0.2	1.8
	C16:1**	36.5	29.5	37.4
	C16:1 (n-7)	0.0	0.5	0.0
	C18:1*	0.1	0.1	0.1
	C18:1 (n-9)	1.8	1.5	2.2
	C18:1 (n-11)	1.4	3.7	5.1
	C20:1**	2.8	1.8	1.7
PUFA	C16:2	0.0	0.3	0.4
	C16:2	0.0	0.0	0.0
	C16:3	0.0	0.0	0.2
	C16:3	0.0	0.3	0.8
	C16:4	0.8	0.1	0.2
	C18:2	0.7	0.2	0.3
	C18:2**	2.6	2.0	2.2
	C18:3	0.1	0.0	0.1
	C20 PUFA	0.3	0.0	0.3
	C20:4 (n-6)	0.3	0.0	0.0
	C20:5 (n-3)	9.1	2.4	2.6
	C22:6 (n-3)	0.6	0.3	0.4

**Table 6B – Continued.**

Fatty acid class	Compound	day 1	day 6	day 10
Odd + br	C13:0i	0.0	0.3	0.2
	C13:0a	0.0	0.0	0.1
	C13:0n	0.0	0.0	0.0
	C14:0i	0.0	0.0	0.3
	C15:0i	0.1	0.2	2.1
	C15:0a	0.0	1.0	0.9
	C15:0n	0.8	0.8	0.1
	C15:1**	0.1	1.5	4.9
	C16:0i	0.7	0.0	0.0
	C17:0a	0.1	0.1	0.1
	C17:0n	0.7	1.5	0.9
	C17:1*	0.2	0.1	0.4
	Methylphytanate	0.0	0.0	0.0
	C21:0n	0.1	0.0	0.1
	C21:1*	0.6	1.1	0.6
	C23:0n	0.1	0.2	0.0
	C25:0n	0.0	0.1	0.0
Summary	<b>% SFA</b>	39.4	50.5	33.5
	<b>% MUFA</b>	42.6	37.2	48.2
	<b>% PUFA</b>	14.5	5.7	7.4
	<b>% Odd + br</b>	3.5	6.6	10.8

Key: Monounsaturated fatty acids (MUFA), saturated fatty acids (SFA), polyunsaturated fatty acids (PUFA), odd + branched chain fatty acids (Odd + br FA). \*: several isomers combined, \*\*: multiple isomers summed because bond positions could not be verified. i = iso branched, a = anteiso branched, n = normal chain length.

**Table 7 – Changes in fatty acid concentrations.** Changes in particulate organic matter (POM) fatty acid concentrations ( $\mu\text{g}/\text{mg}$  POC) between day 1 and day 10 of the incubation experiments.

Microbiome	Fatty acid class	% change
Bering Strait	SFA	-47.5
	MUFA	-38.6
	PUFA	-66.4
	Odd+br FA	+70.5
	Total ( $\mu\text{g}/\text{mg}$ POC)	-41.2
Chukchi Sea	SFA	-33.9
	MUFA	-12.1
	PUFA	-60.0
	Odd+br FA	+136.8
	Total ( $\mu\text{g}/\text{mg}$ POC)	-22.3

Key: Monounsaturated fatty acids (MUFA), saturated fatty acids (SFA), polyunsaturated fatty acids (PUFA), odd + branched chain fatty acids (Odd + br FA).

### 4.3.2 Particulate neutral lipids

Total neutral lipid concentrations of the particles at day 1 were higher in the Bering Strait (13.4  $\mu\text{g}/\text{mg}$  POC) than in the Chukchi Sea (7.2  $\mu\text{g}/\text{mg}$  POC) (Figure 21). However, distribution patterns of the major neutral lipid classes at this time were comparable between incubations; alcohols (25.9-31.5%), phytol (46.6-52.8%), sterols (13.5-15.9%) and alkanes (5.3-7.6%) made up the largest % contributions to the total neutral lipid fraction (Figure 21; Table 8). In both microbiome incubations, concentration losses of phytol, the isoprenoid side chain of chlorophyll a, were highest (32.9% in the Bering Strait and 46.8% in the Chukchi Sea) (Table 9). Total loss in alcohols (<15.5%) and sterol (<18%) concentrations were low over the ten days, however concentrations losses of one dominant sterol class, 27 $\Delta$ 5,24 + 28 $\Delta$ 5,22 (abbreviations for sterol compounds are available in the key below Table 8), surpassed total sterols with a 30% loss in each microbiome. Differentiating the two microbiomes was a 105.0% increase in alkane concentrations within the Chukchi Sea over the 10 day timeframe and a 48.3% loss of glycerol monoether concentrations within the Bering Strait (Table 9).

### 4.3.3 Biomarkers

Individual and groups of fatty acid and neutral lipid biomarkers were categorized to track changes in those structures that could be assigned to biota-specific classes (Table 10). As the diatom-specific fatty acid distributions decreased from >78.5% to <67.3% over the 10 days, fatty acids with a bacterial origin (Odd + br FAs) increased from <4.7% to >10.8% at day 10 (Table 11A). Vascular plant biomarkers of terrestrial origin were low (<0.5%) for all time points within each microbial incubation. Neutral lipid biomarkers primarily included those with an algal (specifically diatom) origin, which were highly dominated by phytol (Table 11B). Trends for the neutral lipids tracked those for the fatty acid biomarkers, further indicating loss of diatom-specific lipid classes over time (>50.2% to <44.1%), irrespective of the bacterioplankton community present.

**Figure 21 - Neutral lipid concentrations over time.** Neutral lipid class concentrations ( $\mu\text{g}/\text{mg}$  POC) of the particles from Strait (BSt) and Chukchi Sea (CS) microbiome incubations over days 1 (d1), 6 (d6) and 10 (d10).

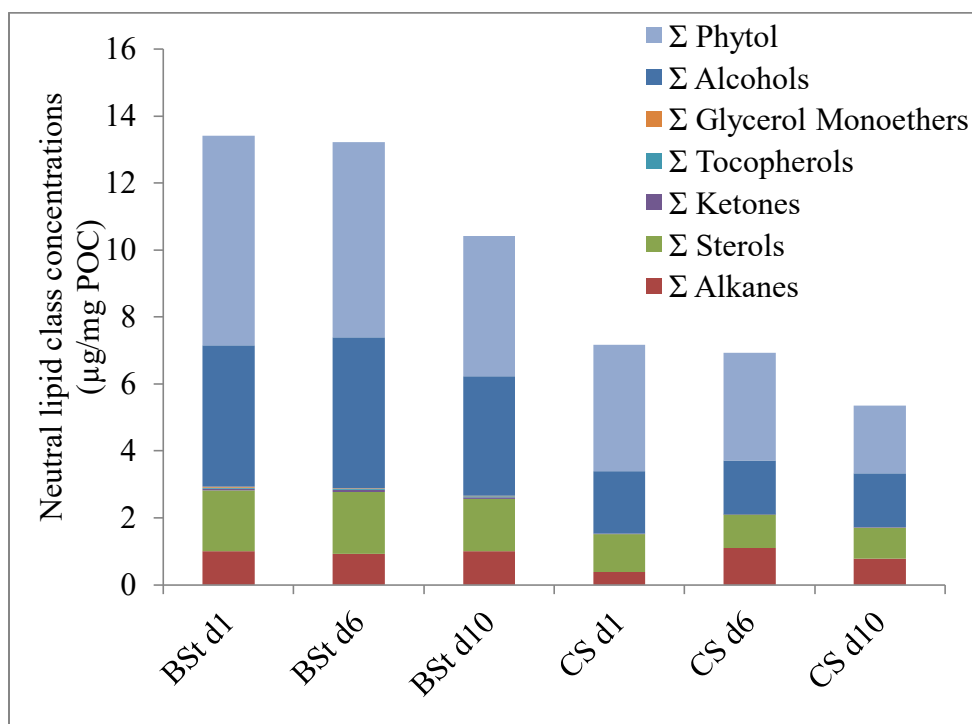




**Table 8 - Neutral lipid distributions.** Neutral lipid compound class distributions (% of total) for the A) Bering Strait and B) Chukchi Sea.

A)

Neutral lipid class	Compound	day 1	day 6	day 10
Alcohols	C12:0 Alc (straight chain unless *)	0.0	0.2	0.0
	C13:0 Alc	0.0	0.0	0.0
	C14:0 Alc	1.3	1.5	0.6
	C15:0 Alc	0.3	0.6	0.5
	C16:0 Alc	3.2	3.0	2.4
	C16:1 Alc	1.6	1.6	1.7
	C18:0 Alc	11.9	15.5	20.8
	C18:0 Alc (*isoprenoid)	0.2	0.2	0.1
	C20:0 Alc	0.5	0.5	0.6
	C20:1 Alc	4.2	3.7	2.9
	C20:1 Alc (*isoprenoid)	0.7	0.8	0.7
	C22:0 Alc	0.3	0.3	0.6
	C22:1 Alc	6.9	5.8	3.0
	C23:0 Alc	0.0	0.0	0.0
	C24:0 Alc	0.2	0.2	0.2
Phytol	46.6	44.2	40.3	
Alkanes	C19:0 Alk	0.1	0.1	0.1
	C20:0 Alk	0.4	0.3	0.4
	C21:0 Alk	0.7	0.7	0.9
	C22:0 Alk	0.6	0.5	0.9
	C23:0 Alk	0.8	0.6	1.1
	C24:0 Alk	0.9	0.6	1.0
	C25:0 Alk	0.9	0.8	1.2
	C26:0 Alk	0.7	0.6	0.9
	C27:0 Alk	0.6	0.6	0.7
	C28:0 Alk	0.4	0.5	0.5
	C29:0 Alk	0.3	0.4	0.4
	C30:0 Alk	0.5	0.6	0.6
	C31:0 Alk	0.2	0.3	0.4
	Squalene	0.6	0.4	0.5

**Table 8A – Continued.**

Neutral lipid class	Compound	day 1	day 6	day 10
Sterols	24-norcholesta-5,22-dien-3 $\beta$ -ol	0.7	0.7	0.9
	27-nor-24-methylcholesta-5,22-dien-3 $\beta$ -ol -OR- cholesta-5,22-dien-3 $\beta$ -ol	0.4	0.5	0.6
	cholest-5-en-3 $\beta$ -ol	1.9	2.0	2.1
	cholesta-5,24-dien-3 $\beta$ -ol (desmosterol) & 24-methylcholesta-5,22-dien-3 $\beta$ -ol (brassicasterol)	6.1	5.6	5.6
	24-methylcholest-5,24(28)-dien-3 $\beta$ -ol (24-methylenecholesterol)	3.4	3.4	4.1
	24-methylcholest-5-en-3 $\beta$ -ol	0.2	0.3	0.4
	24-ethylcholest-5-en-3 $\beta$ -ol & contam	0.2	0.2	0.4
	24-ethylcholest-5,24(28)-dien-3 $\beta$ -ol (24-ethylenecholesterol)	0.3	0.6	0.7
	24-ethylcholest-7-en-3 $\beta$ -ol	0.3	0.5	0.4
Ketones	6,10,14-trimethylpentadecanone	0.1	0.2	0.3
	C18:0 ketone	0.2	0.2	0.2
	$\alpha$ -tocopherol	0.3	0.3	0.3
	C20:1 glycerol monoether	0.2	0.2	0.1
Summary	<b>% Alcohols</b>	31.5	34.0	34.2
	<b>% Phytol</b>	46.6	44.2	40.3
	<b>% Alkanes</b>	7.6	7.1	9.6
	<b>% Sterols</b>	13.5	13.9	15.1
	<b>% Ketones</b>	0.4	0.4	0.4
	<b>% Tocopherols</b>	0.3	0.3	0.3
	<b>% Glycerol Monoethers</b>	0.2	0.2	0.1

**Table 8 – Continued.**

B)

Neutral lipid class	Compound	day 1	day 6	day 10
Alcohols	C12:0 Alc (straight chain unless *)	0.0	0.2	0.1
	C13:0 Alc	0.0	0.0	0.0
	C14:0 Alc	0.5	0.9	1.7
	C15:0 Alc	0.3	0.4	0.7
	C16:0 Alc	2.5	2.3	6.6
	C16:1 Alc	1.3	1.6	2.8
	C18:0 Alc	9.6	7.2	8.3
	C18:0 Alc (*isoprenoid)	0.0	0.0	0.0
	C20:0 Alc	0.0	0.0	0.0
	C20:1 Alc	4.5	4.7	3.8
	C20:1 Alc (*isoprenoid)	0.6	0.6	0.6
	C22:0 Alc	0.0	0.0	0.0
	C22:1 Alc	5.7	4.2	3.8
	C23:0 Alc	0.9	1.2	1.7
	C24:0 Alc	0.0	0.0	0.0
Phytol	52.8	46.3	37.7	
Alkanes	C19:0 Alk	0.1	0.1	0.1
	C20:0 Alk	0.4	0.4	1.3
	C21:0 Alk	0.8	1.1	2.2
	C22:0 Alk	0.4	1.6	1.5
	C23:0 Alk	0.6	1.2	2.1
	C24:0 Alk	0.6	1.2	1.9
	C25:0 Alk	0.6	1.4	1.6
	C26:0 Alk	0.8	3.6	2.0
	C27:0 Alk	0.3	1.4	0.7
	C28:0 Alk	0.1	0.9	0.2
	C29:0 Alk	0.0	0.6	0.0
	C30:0 Alk	0.1	0.6	0.1
	C31:0 Alk	0.1	1.6	0.3
	Squalene	0.4	0.4	0.3

**Table 8B – Continued.**

Neutral lipid class	Compound	day 1	day 6	day 10
Sterols	24-norcholesta-5,22-dien-3 $\beta$ -ol	0.7	1.9	0.8
	27-nor-24-methylcholesta-5,22-dien-3 $\beta$ -ol -OR- cholesta-5,22-dien-3 $\beta$ -ol	0.0	0.0	0.0
	cholest-5-en-3 $\beta$ -ol	2.3	1.7	2.9
	cholesta-5,24-dien-3 $\beta$ -ol (desmosterol) & 24-methylcholesta-5,22-dien-3 $\beta$ -ol (brassicasterol)	6.9	4.9	6.3
	24-methylcholest-5,24(28)-dien-3 $\beta$ -ol (24-methylenecholesterol)	4.5	4.2	5.8
	24-methylcholest-5-en-3 $\beta$ -ol	0.4	0.5	0.5
	24-ethylcholest-5-en-3 $\beta$ -ol & contam	0.5	0.7	0.6
	24-ethylcholest-5,24(28)-dien-3 $\beta$ -ol (24-ethylenecholesterol)	0.4	0.3	0.4
	24-ethylcholest-7-en-3 $\beta$ -ol	0.2	0.2	0.2
Ketones	6,10,14-trimethylpentadecanone	0.0	0.0	0.0
	C18:0 ketone	0.2	0.2	0.3
	$\alpha$ -tocopherol	0.0	0.0	0.0
	C20:1 glycerol monoether	0.0	0.0	0.0
Summary	<b>% Alcohols</b>	25.9	23.2	30.1
	<b>% Phytol</b>	52.8	46.3	37.7
	<b>% Alkanes</b>	5.3	16.0	14.5
	<b>% Sterols</b>	15.9	14.4	17.4
	<b>% Ketones</b>	0.2	0.2	0.3
	<b>% Tocopherols</b>	0.0	0.0	0.0
	<b>% Glycerol Monoethers</b>	0.0	0.0	0.0

Key: full compound description (abbreviation) for sterols mentioned in text or Table 3. 24-norcholesta-5,22-dien-3 $\beta$ -ol (26 $\Delta$ 5,22); cholesta-5,24-dien-3 $\beta$ -ol (desmosterol) & 24-methylcholesta-5,22-dien-3 $\beta$ -ol (brassicasterol) ((27 $\Delta$ 5,24) + (28 $\Delta$ 5,22)); 24-methylcholest-5,24(28)-dien-3 $\beta$ -ol (24-methylenecholesterol) ((28 $\Delta$ 5,24(28))); 24-ethylcholest-5-en-3 $\beta$ -ol & contam ((29 $\Delta$ 5)).

**Table 9 - Changes in neutral lipid concentrations.** Changes in particulate neutral lipid concentrations ( $\mu\text{g}/\text{mg}$  POC) between day 1 and day 10 of the microbial incubation experiments.

Microbiome	Neutral lipid class	% Change
Bering Strait	Alcohols	-15.5
	Phytol	-32.9
	Alkanes	-1.4
	Sterols	-13.1
	Ketones	-6.5
	Tocopherols	-15.6
	Glycerol Monoethers	-48.3
	Total ( $\mu\text{g}/\text{mg}$ OC)	-22.3
Chukchi Sea	Alcohols	-13.3
	Phytol	-46.8
	Alkanes	105.0
	Sterols	-18.0
	Ketones	-2.6
	Tocopherols	NA
	Glycerol Monoethers	NA
	Total ( $\mu\text{g}/\text{mg}$ OC)	-25.5

**Table 10 - Lipid biomarkers.** Fatty acid and neutral lipid biomarkers indicative of origin and reactivity (with citations). Abbreviations for neutral lipid sterol compounds are available in the key below Table 8.

Total fatty acids	
<b>bacterial</b>	all odd & branched (but specifically C15 & C17) are bacterial in origin (Kaneda [167])
<b>algal</b>	high 16:1w7 (MUFA); 16:0 (SFA); 20:5w3 (PUFA); 14:0 (SFA) (Volkman et al. [168]) low 22:6w3 (PUFA) (Belicka et al. [169]) dominance of C16 over C18 PUFAS (Belicka et al. [169])
<b>vascular plants</b>	even-carbon SFA, >C24 (Belicka et al. [169] + references therein)
<b>specifically recalcitrant</b>	SFAs (Fagervold et al. [37])
<b>specifically labile</b>	Unsaturated FAs (Harvey and Macko [156]) PUFAs (Hu et al. [170])
Neutral lipids	
<b>algal</b>	phytol (Harvey and Macko [156]) 28 $\Delta$ 5,24(28) (Belicka et al. [169] + references therein) 29 $\Delta$ 5
<b>mixed sources (including diatoms, other algae &amp; zooplankton)</b>	cholesterol (Belicka et al. [169] + references therein) 26 $\Delta$ 5,22 27 $\Delta$ 5,24 + 28 $\Delta$ 5,22 (Rontani et al. [171])
<b>specifically labile</b>	phytol (Harvey and Macko [156])

**Table 11 – Distributions of lipid biomarkers.** Lipid biomarker relative distributions (%) over time for A) Fatty acids and B) neutral lipids. Biomarkers used for quantitative analysis are identified in Table 10.

A)

origin	Bering Strait			Chukchi Sea		
	day 1	day 6	day 10	day 1	day 6	day 10
bacterial	4.7	11.5	13.8	3.5	6.6	10.8
bacterial (only C15+C17)	4.1	9.7	11.9	2.0	5.0	9.4
algal	78.5	67.5	60.8	79.6	63.8	67.3
terrestrial	0.3	0.2	0.2	0.2	0.4	0.0

B)

origin	Bering Strait			Chukchi Sea		
	day 1	day 6	day 10	day 1	day 6	day 10
diatom	50.2	47.7	44.7	57.7	51.2	44.1
diatom (only phytol)	46.6	44.2	40.3	52.8	46.3	37.7
mixed source (incl. algal)	8.7	8.4	8.6	9.9	8.5	10.0

#### 4.3.4 Particulate amino acids

Total hydrolyzable amino acid concentrations of the added POM substrate (POM-THAA/POC) at day 1 were comparable between the Bering Strait (282.15  $\mu\text{g}$  THAA/mg POC) and Chukchi Sea (277.42  $\mu\text{g}$  THAA/mg POC), with concentrations almost doubling by day 10 (Table 12). Of the 11 amino acid groups quantified by GC/MS, leucine was the most prominent amino acid within the POM added to the Bering Strait at day 1 (mole% of 52.2%  $\pm$  17.6%), and was most abundant in both microbiomes by day 10 (39.0%  $\pm$  21.0% & 29.9%  $\pm$  3.5%) (Figure 22). Proline was one of the dominant THAAs in Chukchi Sea particles at day 1 (25.0%  $\pm$  7.0%), with decreasing distribution by day 10 (14.3%  $\pm$  5.1%) while it was relatively unchanged within the Bering Strait POM over time (9.1%  $\pm$  4.8% to 9.8%  $\pm$  3.4%). Glycine was another THAA with a decreasing temporal trend within Chukchi Sea particles, with changes measured from 18.9% ( $\pm$  4.5%) to 8.7% ( $\pm$  0.9%), a decrease that was also missing in the Bering Strait POM composition.

#### 4.3.5 Bacterial enzyme profiles

To examine the bacterial enzymatic response of the microbial communities to the introduction of algal organic matter, enzyme commission (EC) numbers were assigned to gene ontology (GO) functions and the peptide spectrum matches (PSMs) for each EC category were summed to classify and quantify enzymatic changes over time. The number of EC identifications increased over time within both microbiomes, from <203 at the initial sample to >388 at day 10 (Table 13). In addition, the percent coverage of EC categories assigned PSMs also increased over time (<31.2% to >40.7%) (Table 13). Initial microbial enzyme profiles at this broad categorization were variable between the Bering Strait and Chukchi Sea microbiomes at the time of collection from the water column (i.e., initial time point), with hydrolases and transferases together composing 76.6% of total enzyme distributions within the Bering Strait and 67.4% within the Chukchi Sea (Figure 23). The distribution of initial Bering Strait bacterial oxidoreductases (14.0%) were about half of what they were in the Chukchi Sea (26.5%), while isomerases and ligases had greater distributions in the Bering Strait (both  $\sim$ 4% versus  $\sim$ 1% in the Chukchi Sea). By day 10, temporal shifts in enzyme distributions occurred within each microbiome that resulted in more comparable broad enzymatic profiles between the Arctic bacterioplankton communities, with hydrolase and transferase combined contributions



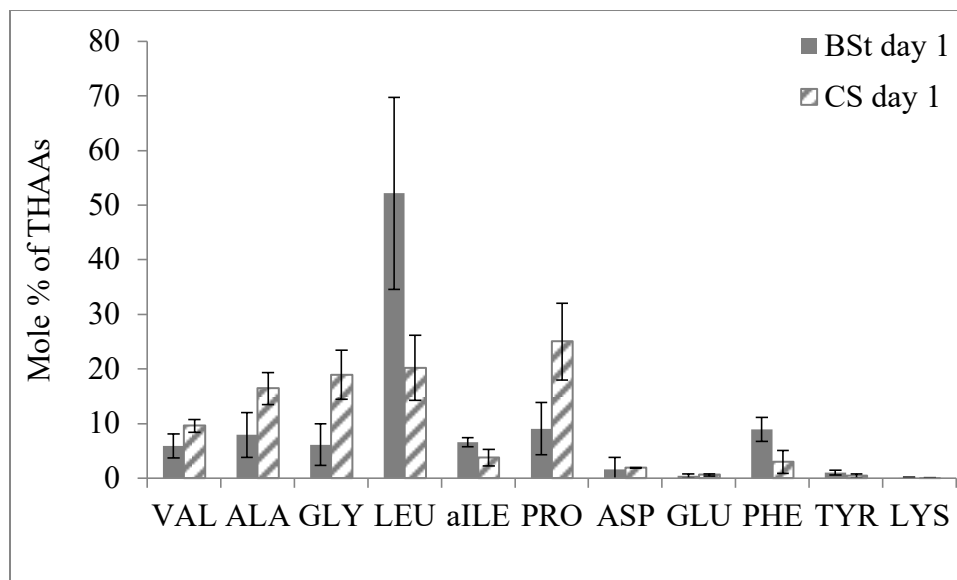
**Table 12 - Amino acid concentrations.** Total hydrolyzable amino acid concentrations of the added particles normalized to particulate organic carbon (POC) concentrations ( $\mu\text{g THAA}/\text{mg POC}$ ) for each microbiome, Bering Strait and Chukchi Sea, on days 1 and 10 of the incubation experiments.

Time Microbiome	Day 1		Day 10	
	Bering Strait	Chukchi Sea	Bering Strait	Chukchi Sea
VAL	16.54	28.59	24.12	33.18
ALA	16.76	36.87	34.93	83.83
GLY	11.14	36.34	22.64	31.40
LEU	146.21	66.33	200.26	187.95
aILE	19.33	12.28	28.14	34.07
PRO	25.59	73.72	49.93	79.73
ASP	5.57	6.39	81.02	43.50
GLU	1.61	2.28	3.06	4.23
PHE	34.59	12.11	68.41	63.40
TYR	4.40	1.95	20.89	6.50
LYS	0.42	0.57	2.24	0.30
<b>Totals</b>	<b>282.15</b>	<b>277.42</b>	<b>535.65</b>	<b>568.08</b>

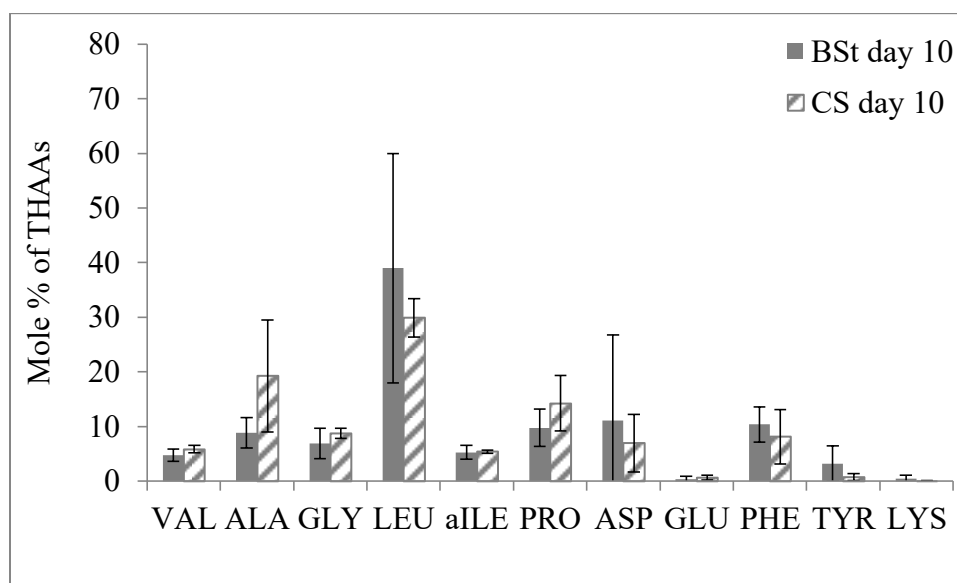
Key: VAL = valine, ALA = alanine, GLY = glycine, LEU = leucine, aILE =  $\alpha$ -isoleucine, PRO = proline, ASP = aspartic acid + asparagine, GLU = glutamic acid + glutamine, PHE = phenylalanine, TYR = tyrosine, LYS = lysine.

**Figure 22 - Amino acid distributions.** Mole % of total hydrolyzable amino acids (THAAs) on A) day 1 and B) day 10 of the incubation experiments. Error bars represent standard deviations for each amino acid (BSt = Bering Strait, n=3; CS = Chukchi Sea, n=2).

A)



B)



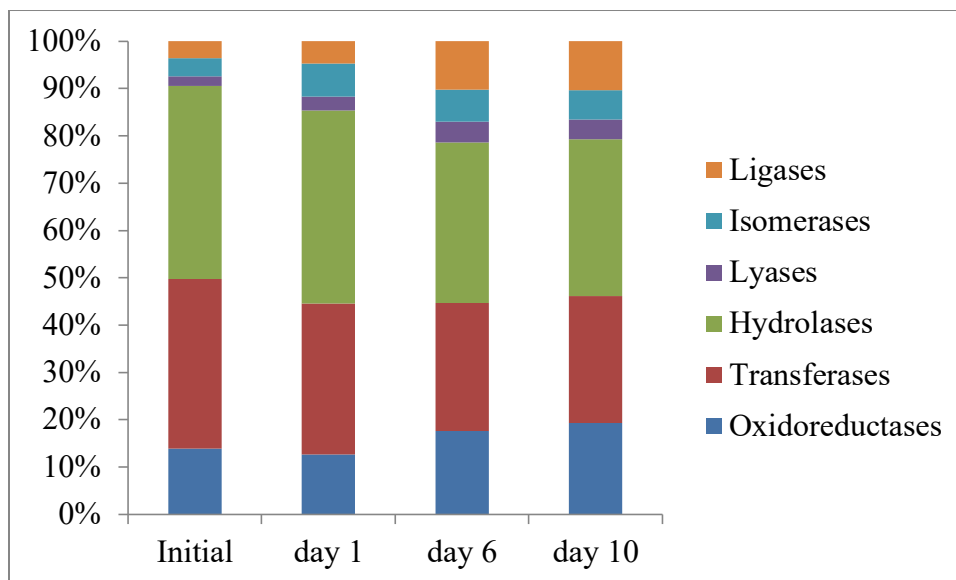
Key: VAL = valine, ALA = alanine, GLY = glycine, LEU = leucine, aILE =  $\alpha$ -isoleucine, PRO = proline, ASP = aspartic acid + asparagine, GLU = glutamic acid + glutamine, PHE = phenylalanine, TYR = tyrosine, LYS = lysine.

**Table 13 – Enzyme Commission number data.** Count of bacterial enzyme commission numbers (EC#) assigned to gene ontology (GO) functions and the summed percent of total peptide spectrum matches (%PSM) at each time point that match to an EC number for the 6 broadest EC categories over the 10 day incubation experiments of Bering Strait and Chukchi Sea microbes. Broad EC categories: 1: oxidoreductases, 2: transferases, 3: hydrolases, 4: lyases, 5: isomerases, 6: ligases.

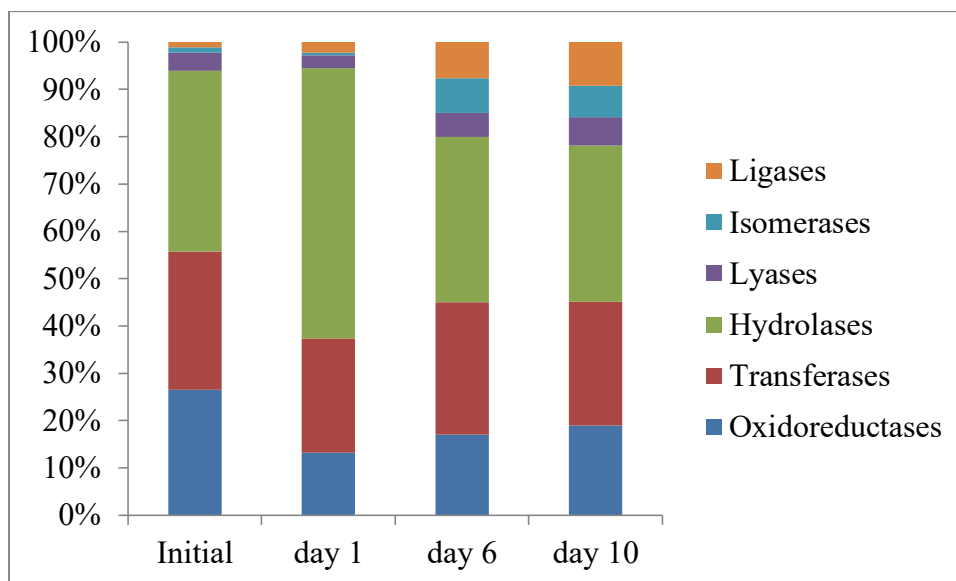
Time	Bering Strait		Chukchi Sea	
	EC#	%PSM	EC#	%PSM
Initial	203	31.21	120	26.64
day 1	291	36.19	68	45.96
day 6	451	42.25	386	44.51
day 10	446	40.67	388	43.25

**Figure 23 – Enzyme commission category distributions.** Broad enzyme commission (EC) category distributions (% of total) of the bacteria from the A) Bering Strait and B) Chukchi Sea samples over ten days incubation time.

A)



B)



decreasing to ~60% while lyases (4.1-6.0%), isomerases (6.2-6.6%) and ligases became more abundant (9.2-10.3% of total enzyme distributions) (Figure 23).

Hydrolases specifically acting on acid anhydrides (>69%) and peptide and ester bonds (4-15% each) were the most abundant hydrolase classes within both microbiomes, while glycosylase activities remained relatively minor (<3%) (Table 14). No lipase enzymes, which are specific to lipid degradation, were detected after translating GO functions into EC categories. Yet, a majority of lipase enzymes fall under the more broad EC category of hydrolases acting on ester bonds (EC:3.1) [165, 166] and made up between 5.3-7.2% of total hydrolases initially, with distributions generally doubling by day 10 in each microbiome (Table 14). More specifically, lipase enzymes are categorized as carboxylic ester hydrolases (EC:3.1.1) and phosphoric diester hydrolases (EC:3.1.4) [165, 166], both of which were identified within the dataset. Regardless of their importance in lipid degradation, both of these ester hydrolase classes made up a small fraction (<1%) of total hydrolases and were not consistently present across all time points (i.e., neither enzyme group was detected at day 1 in the Chukchi Sea). Relative abundances of these enzymes (per GO PSMs) appeared to peak at day 6 and then decrease at day 10, except for Chukchi Sea phosphoric diester hydrolases, which had a slight increase between these days (Figure 24). Taxonomic assignments of bacterial classes for these enzymes indicated that Flavobacteria and Alphaproteobacteria were largely responsible for their expression in both microbiomes, however the distributions were variable. In general, Alphaproteobacteria appeared important for activity of both enzyme groups within the Bering Strait microbiome compared to the Chukchi Sea, where Flavobacteria had a more prominent association with these enzymes.

**Table 14 - Hydrolase distributions.** Bacterial enzyme commission (EC) categorical distributions (%) of hydrolases (EC:3.-) for the A) Bering Strait and B) Chukchi Sea.

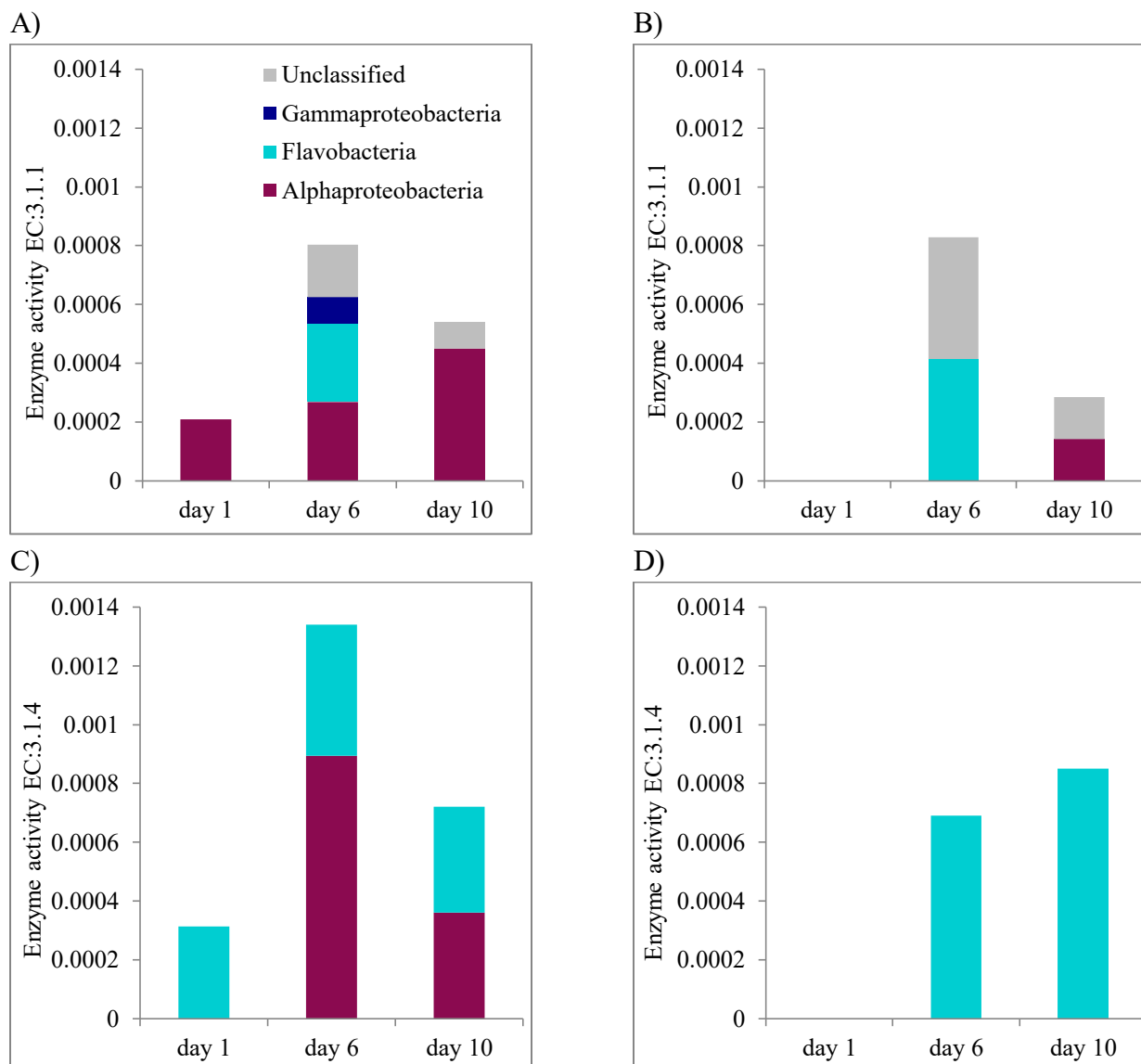
A)

GO Accession	EC number	Hydrolase EC name	Bering Strait			
			initial	day 1	day 6	day 10
GO:0016788	EC:3.1	Acting on ester bonds	7.21	11.32	15.34	14.14
GO:0016798	EC:3.2	Glycosylases	2.19	1.41	1.75	1.87
GO:0016801	EC:3.3	Acting on ether bonds	0.00	1.49	1.50	1.20
GO:0008233	EC:3.4	Acting on peptide bonds (peptidases)	13.79	9.41	10.41	10.27
GO:0016810	EC:3.5	Acting on carbon-nitrogen bonds, other than peptide bonds	0.47	0.35	2.18	3.20
GO:0016817	EC:3.6	Acting on acid anhydrides	77.43	78.15	70.07	69.91
GO:0016822	EC:3.7	Acting on carbon-carbon bonds	0.00	0.07	0.06	0.00

B)

GO Accession	EC number	Hydrolase EC name	Chukchi Sea			
			initial	day 1	day 6	day 10
GO:0016788	EC:3.1	Acting on ester bonds	5.34	3.85	11.37	11.82
GO:0016798	EC:3.2	Glycosylases	2.91	2.88	1.78	2.48
GO:0016801	EC:3.3	Acting on ether bonds	1.46	0.96	0.71	0.89
GO:0008233	EC:3.4	Acting on peptide bonds (peptidases)	11.17	3.85	14.39	14.70
GO:0016810	EC:3.5	Acting on carbon-nitrogen bonds, other than peptide bonds	0.00	0.00	1.42	1.59
GO:0016817	EC:3.6	Acting on acid anhydrides	79.61	85.58	72.91	68.92
GO:0016822	EC:3.7	Acting on carbon-carbon bonds	0.00	0.00	0.00	0.00

**Figure 24 - Bacterial ester hydrolases.** Bacterial taxonomic class distributions among enzyme ester hydrolases over time (as percentage of enzyme commission peptide spectral matches) for carboxylic acid hydrolases (EC3.1.1) from the A) Bering Strait and B) Chukchi Sea metaproteomes, as well as for phosphoric diester hydrolases (EC:3.1.4) from the C) Bering Strait and D) Chukchi Sea.



#### 4.4 Discussion

In the shallow shelf system of the Chukchi Sea, POM quality in bottom water differs from the surface ocean during early autumn, suggesting that the bacterial community residing at a greater depth receives a more degraded source of organic matter compared to the surface [172]. This may lead to a metabolic adaptation of the community at depth to access refractory material as an energy source [123]. Indeed, in Chapter 2, while tracking community functions that shifted over time within the microbiomes collected from the surface water of the Bering Strait and bottom water of the Chukchi Sea, I identified some ecologically significant distinctions in response to algal organic additions. Therefore, I questioned how lipid degradation patterns of added particles would compare between the two microbiomes, and if I could identify differences in enzyme profiles that might explain lipid diagenesis over a short time frame. This analysis also included an assessment of which taxonomic bacterial classes expressed these degradative enzymes in each community.

The POM collected from the Bering Strait chlorophyll subsurface maximum was presumed to have a primarily autochthonous origin [173]. Although fatty acid and neutral lipid concentrations in the particles at day 1 were lower than what has previously been reported from POM collected near the surface of the Chukchi Sea water column, many of the lipid class distributions were comparable to these previous distributions, such as particularly high contributions by MUFAs, SFAs and phytol, an algal-derived alcohol [169]. Specific lipid classes are particularly useful geochemical biomarkers of organic matter origin (e.g., [75, 156, 169]) and confirmed a primarily algal origin with a particularly strong diatom signal. For example, the high contribution of PUFAs associated with diatoms and low contribution of long chain fatty acids derived from vascular higher plants verified the marine origin of the particulate additions. Initial POC:PON ratios  $\sim 5$  (Table 1) agreed with the biomarker data that the added POM substrate originated primarily from an algal source, although it was enriched in nitrogen compared to POM previously collected from Chukchi Sea surface waters [169]. Inconsistent with the lipid composition and POC:PON, the POM-THAA/POC concentrations at day 1 of the incubation experiments were low for typical concentrations indicative of a phytoplankton or bacterial source [174]. Considering the preceding evidence that the POM was composed of algal organic matter, the possibility that the POM-THAA/POC values originated from a methodological constraint to



only quantify 11 amino acids seems more likely than a macrophytic origin [174] or previous degradation of labile components [175].

Temporal increases in bulk POC & PON concentrations were likely a result of particulate aggregation, as has been previously reported for diatom cultures [176]. Initiation of bulk POM decay at this low temperatures (0°C) may take longer than the 10 day time frame employed, while at warmer temperatures decomposition can occur more rapidly (e.g., [75, 110]). Although bulk POC and PON concentrations did not show a net decline over the 10 days, changes in the POM compositional indicators, such as decreasing POC:PON ratios between days 1-10 and increases in POM-THAA/POC indicate compositional changes were underway, such as ammonia adsorption, carbon removal during degradation or an increase in bacterial biomass on the particles [177, 178]. The latter two explanations are especially probable since cell numbers increased >1000%, matched with evidence of the loss of selective lipid classes.

As bacterial enzymatic coverage (%) increased within both microbiomes, particulate diagenesis was evident over the 10 day incubation period. The 20-40% decline in total fatty acid concentrations over 10 days in the current work is comparable to other studies from a variety of environments, including for diatom degradation under oxic conditions at ambient temperatures [156]. However, the loss of fatty acid and neutral lipid concentrations over the 10 days while POC, PON and THAA concentrations increased was surprising as bulk POC and protein decay rates tend to be higher than lipid decay rates [75]. Temporal losses of selective lipid classes as bulk POM parameters increased demonstrates that portions of the added substrate were vulnerable to enzymatic attack by bacterioplankton from both the Bering Strait and Chukchi Sea, although degrees of decomposition were somewhat variable.

Differences between the two Arctic microbiomes in the decay of lipid classes and amino acids opposes the 1<sup>st</sup> hypothesis and indicates that community composition within this ecosystem may have an impact on the degree of degradation for these specific POM structures. For example, greater decreases in total fatty acid concentrations within the Bering Strait incubation suggests that there is a higher remineralization rate for POM fatty acids in the microbial community originating from the subsurface chlorophyll maximum. This pattern may be explained by a community-wide adaptation to rapid influxes of labile, algal-derived POM

compared to the bottom water microbiome of the Chukchi Sea. Unlike total fatty acids, the decrease of total neutral lipid concentrations over 10 days were comparable between microbiomes, indicating that both bacterial assemblages had nearly equivalent capacities for the degradation of this type of lipid. Different distributions of neutral class losses, however, distinguished the two microbiomes. For example, the Chukchi Sea microbiome demonstrated a greater ability to access phytol than the Bering Strait over a 10 day timescale. This is a surprising find, considering that the other major algal biomarker, PUFAs, decreased at similar concentrations between the two microbiomes. These inconsistencies suggest that compositionally distinct microbial communities contain some metabolic dissimilarity in the degradation potential of specific labile POM lipid compounds.

Despite the variations in degree of degradation for some lipid classes, a predictive order of decomposition between microbiomes emerged within each lipid category (Fatty acids: 1. PUFAs, 2. SFAs, 3. total fatty acids, 4. MUFAs; neutral lipids: 1. phytol, 2. total neutrals, 3. alcohols & sterols), independent of significant differences in bacterial composition, which supports the 1<sup>st</sup> hypothesis. Harvey and Macko [156] showed that the saturation of fatty acids impacts lability, particularly from a diatom source; unsaturated fatty acids degrade at a more rapid rate than saturated fatty acids. Although this trend was observed for the PUFAs, it was not true for the monounsaturated class (MUFA) concentrations, which had a relatively lesser degree of loss than the saturated class (SFA) over the ten days in each microbiome. In addition, sterols are generally classified as less labile than other lipid classes, however they can degrade by abiotic and biotic processes at a similar rate to total POC [171]. Evidence of sterol decay was lower than many fatty acid and neutral lipids, however their concentrations decreased to a greater degree than MUFA in the Chukchi Sea. Some selective loss of sterol classes (27 $\Delta$ 5,24 + 28 $\Delta$ 5,22) over this short time frame of 10 days occurred and was unexpected, as previous decay of sterols was shown to be nonselective and only detectable after 40+ days in a comparable bacterial incubation experiment of diatoms, but at a warmer temperature [156].

In addition to indicating substrate origin, certain lipid classes are useful as biomarkers to define paths and rates of degradation (e.g., [75, 156, 179]). An inverse relationship between bacterial biomarkers and algal biomarkers was noted (algal fatty acid significance at  $\alpha = 0.05$  (Pearson  $r = -0.82$ ,  $n = 6$ ,  $p = 0.046$ ); algal neutral lipid significance at  $\alpha = 0.05$  (Pearson  $r = -$

0.87,  $n = 6$ ,  $p = 0.024$ )). This negative correlation suggests that as bacteria presumably colonized the particles, they remineralized algal-specific fatty acids and neutral lipids primarily composed of PUFAs and phytol, respectively. Corroborating this analysis was the 1000% increase in bacterial cell numbers, alongside increases in the particulate bacterial biomarkers, odd + branched chain fatty acids. The decline of PUFA concentrations was especially noteworthy and evident of their high degree of lability [170]. Although previous work has shown that bacterial assemblages are able to preferentially extract labile matter from a range of substrates without a change in bacterial composition [17, 154], the results presented here indicate that shifts in bacterial composition occurred as a response to the algal substrate input (Figure 6; Figure 14). In particular, PUFA concentrations have been shown to influence bacterial assemblages in cold water sediments [37] and suggests that their accessibility to both microbiomes may have contributed to the taxonomic converging of these two microbial communities over a time frame of a few days.

As opposed to the degradative information obtained from individual lipid class data, only a modest amount of information on substrate lability was identified based on changes in distributions among the eleven amino acids measured; with few trends emerging to differentiate the two communities. In contrast with the selective preservation of amino acids associated with the cell wall of diatoms [175], mole percentage of glycine within the particles decreased over time within the Chukchi Sea microbiome experiment. This indicates that the reactivity of this amino acid to this microbial community was not solely controlled by its integration into a relatively refractory component of the diatom cell. Glycine is also considered of low nutritional value to heterotrophic bacteria and it is easily synthesized [14], further distinguishing the nutritional strategy by the bottom water community from the surface community. In contrast to the Chukchi Sea microbiome, mole percentage of leucine decreased within the Bering Strait incubations, however the high lability of this amino acid [14] was obscured by high standard deviations between technical replicates. Other amino acids that are good indicators of substrate lability such as glutamic acid, tyrosine, phenylalanine and isoleucine [14, 174] did not prove to be useful biomarkers of degradation for these Arctic microbiomes over this short time frame, as many of the mole percentages of these THAAs actually increased over the 10 day incubation period. Future work would benefit from employing a method with greater precision and one that

is capable of measuring a wide range of amino acids, such as in recent work by McMahon et al. [180].

The high abundance of acid anhydride hydrolases in both bacterial communities was expected as these bonds within substrates are readily hydrolyzed for easy energy acquisition (i.e., ATP contains two anhydride bonds). In the current dataset, although total bacterial hydrolases decreased over the ten days, the near doubling of ester-specific hydrolases over the same time frame is consistent with the evidence of particulate lipid degradation within both microbiomes. In particular, hydrolytic enzymes specifically related to organic matter degradation tend to increase within bacteria during phytoplankton blooms [181, 182] and can indicate which types of substrates are seen as ‘bioavailable’ for different bacterial taxa [24]. The delayed increase in the ester-specific hydrolases within the Chukchi Sea microbiome at day 6 compared to increases in the Bering Strait at day 1 has potential implications for degradation response rates for ester-linked compounds of algal substrates in the bottom water of the western Arctic Ocean, corroborating earlier evidence of similar delays in the metabolic response (Chapter 2) and taxonomic restructuring of the Chukchi Sea microbiome (Chapter 3). The greater cumulative enzymatic diversity (# of EC classes) in the bacterioplankton collected from the SCM of the Bering Strait may indicate a wider range of functions are required to thrive in the highly episodic environment of the surface Arctic Ocean. This greater enzymatic diversity may translate into a more rapid response rate to increase enzymes specific to substrate availability, such as ester hydrolases to target labile fatty acids in diatom cells when they become abundant. Despite an initial response delay in one microbiome over another, a slightly longer period of time (6 days versus 1 day) showed that two Arctic microbiomes can recalibrate to become more enzymatically equivalent when labile substrates are in abundance.

Although a search was conducted for bacterial lipases, as the class of enzyme that hydrolyze lipids, none were identified within the metaproteomic dataset. One reason that lipases may not have been identified is that they are primarily an extracellular enzyme [183] and therefore, if synthesized, might have been present as an exuded metabolite which would have been outside of the 0.2  $\mu\text{m}$  filtration size cutoff for free-living bacteria. Second, these enzymes are produced primarily during fermentation [183] and although some of the degradation

processes occurring within the particles were likely anaerobic, the collection of free-living bacteria might have limited the detection potential.

While no lipase-specific enzymes were identified within the EC dataset, the quantitative information available on carboxylic ester hydrolases (EC:3.1.1) and phosphoric diester hydrolases (EC:3.1.4), which encompass a majority of the lipase enzymes [165, 166], show that relative abundances of these bacterial enzymes peaked on day 6 before decreasing by day 10. The changes in carboxylic ester hydrolases are most appropriate to compare to decreasing concentrations of fatty acids, which are highly composed of ester-linkages. In addition, specific enzyme classes (i.e., carboxylesterases (EC:3.1.1.1)) are particularly important in hydrolyzing carbon for bacterial utilization [184]. It is conceivable that the increase in Bering Strait bacterial carboxylic ester hydrolases at day 6 had a temporally delayed impact on the decreases in the fatty acid class concentrations by day 10. Alternatively, this inconsistency with the timing of the peak in carboxylic ester hydrolases and decreases in labile fatty acids (i.e., PUFAs) may suggest that bacteria don't necessarily need to increase lipases to access highly reactive lipid classes. This latter idea is supported by research showing that although lipase activity can correlate with some lipid classes (i.e., monounsaturated, short-chain saturated and branched-chain FAs indicating bacterial lipid synthesis), this relationship can be lacking for the highly labile PUFAs [185]. Relative increases in these hydrolases at day 6 may have had additional impacts, such as increasing relative abundances of certain lipid classes (i.e., Bering Strait MUFAs), possibly indicating intermediate degradation products.

Preliminary connections between changes in particulate lipid classes and changes in the broad categories of bacterial hydrolases can be made using the current methodologies, partially supporting the 2<sup>nd</sup> hypothesis. The identification of broad enzymatic categorization, however, requires a conservative interpretation and the limitations lead to methodological suggestions for future research. Without directly measuring shifts of specific enzymes, it is difficult to link bacterial activity to changes in particulate lipid class composition. Follow-up research projects that attempt to make these ecological connections would benefit from employing lipase enzyme assays (e.g., [185]) to complement the metaproteomic-based identification of enzyme categories. In addition, the large increase (2x) of bacterial phosphoric diester hydrolases within the Bering Strait compared to the Chukchi Sea at day 6 is hard to explain without detailed particulate lipid

data on phospholipids. However, a greater expression of this enzyme category from bacteria collected from the chlorophyll maximum may suggest that this surface water microbiome had a particularly high adaptation to attacking and accessing phospholipids as an energy source from diatom cell structures (i.e., cell walls). Lastly, the peptide-based enrichment analysis (Chapter 2) provided evidence of the rapid processing of carbohydrates that occurred within both microbiomes. Therefore, I believe that changes in the composition of particulate carbohydrates would have been an excellent candidate for matching with bacterial enzyme profiles within this dataset, however this analytical method was not included in the current study. Future research could benefit from such analysis.

A limited number of bacterial lipase-relevant enzymatic groups, taxonomic associations and time points made it difficult to extrapolate the hydrolase group taxonomic data to an ecosystem level. The results, however, provide some preliminary evidence that taxonomic classifications for carboxylic ester hydrolases and phosphoric diester hydrolases reflected total taxonomic distributions within the metaproteomic dataset (Figure 5). Take, for example, the higher relative activity (i.e., % of metaproteome) of Bering Strait Alphaproteobacteria versus Chukchi Sea Flavobacteria, which may translate into greater specific hydrolase classes on particulate lipids. Bering Strait Alphaproteobacteria appeared to be more efficient at the degradation of carboxylic acids, as seen in the greater decrease in particulate fatty acid concentrations within this microbiome. Alternatively, the large increase in Flavobacterial activity and abundance between days 1-6 in both microbiomes was not seen in the carboxylic ester hydrolases, but seems to have played a role in the increase of phosphoric diester hydrolases. This complements previous investigations into the genome of this bacterial class, suggesting that they are capable of degrading algal biopolymers with a diverse resource of compound-specific enzymes common in algal cell walls [95]. Although not included in the current analytical methods, future research would benefit from including measurements of phospholipid composition of particles in combination with enzyme activities.

#### 4.5 Conclusions

The coupling of microbial –omics with geochemical measures in the same study are infrequent [25]. The current chapter combined measures of bacterial enzymatic profiles

identified within the metaproteomic dataset with changes to particulate organic compositional indicators of lability. Integrating these results with results earlier chapters, I aimed to discern how the former influenced the latter. Although bulk POC, PON and POM-THAA/POC concentrations increased over the 10 day incubation period, the inverse relationship between loss of diatom-specific particulate lipid biomarkers and increase of particulate bacterial lipid biomarkers indicated that carbon was selectively degraded as bacteria colonized the particles. Further, this work shows that bacterioplankton collected from different water masses within the western Arctic Ocean have a predictable order of particulate lipid degradation, independent of differences in bacterial taxonomic composition. Earlier work (Chapter 3) showed that the rapid inputs of algal-derived organic matter drove functional convergence between the two microbiomes. Even under this homogenizing scenario, access to specific algal-derived particulate lipid classes (total fatty acids and phytol) differentiated the microbiomes, possibly a reflection of differences in bacterioplankton community taxonomy and capacities to adapt enzymatically to new substrates. Although less conclusive than the particulate compositional data, enzymatic profiles showed that bottom water bacterioplankton from the Chukchi Sea were enzymatically less diverse than the surface ocean community from the Bering Strait. Even so, the slightly greater collective expression of the Chukchi Sea enzymes provided the functionality to degrade lipid substrates to nearly equivalent degrees as the more enzymatically diverse Bering Strait community. The findings in this study corroborate earlier results (Chapters 2 and 3) that a high degree of functional consistency persisted between the two microbiomes over a ten day period, as seen in the similar profiles of metabolic response to and lipid degradation of algal-derived substrates.

## CHAPTER 5

### 5. CONCLUSIONS

The complexity of natural bacterial communities and the environmental matrices in which they exist contribute to the difficulty of identifying how distinct taxonomic groups respond metabolically to changes, or perturbations, in their surroundings. In this dissertation, I aimed to address this problem and contribute to a major research goal in microbial ecology to connect bacterial activity to ecosystem functioning by applying a novel metaproteomics approach in combination with more traditional methods of taxonomic classification and organic matter compositional analyses.

A major finding from this work was that functional redundancy was characteristic of the natural bacterial communities collected within the shallow shelf ecosystem of the western Arctic Ocean. Even as these redundancies were evident, the results from this dissertation demonstrated that methodological scale is important; redundancy dominated when viewing the complete metaproteomic dataset, however the temporal functions that differentiated the microbiomes may have implications for how compositionally distinct communities interact with and subsequently influence their local biochemical environments. The finding that few functional traits may be important to define the functioning of a whole ecosystem is not new and in fact, is making its way into mainstream science view [2]. Results gained from this dissertation also showed that organic perturbations influenced the compositional and functional restructuring within the microbiomes, leading to the identification of response processes that drove functional shifts under realistic environmental perturbations of high inputs of algal-derived organic substrates versus periods when substrates were at a minimum. The taxonomic associations of such functions, even at a broad classification, provided insight into traits of substrate acquisition, nutrient cycling and energy production that may contribute to adaptation and niche separation within microbiomes during periods of environmental stimulus. In the context of a warming Arctic Ocean where the timing, scale and characterization of biological response to organic perturbations are difficult to predict, results from these trait-based methods suggest that



environmental conditions which select for certain bacterial groups may impact local biogeochemical cycling.

The first two research chapters (Chapters 2 & 3) showed that under environmental conditions where substrates become limited, initial bacterioplankton communities adapted by restructuring community composition and initiating divergent metabolic processes to access ambient organic substrates. Over the short incubation times of 10 days, this led to greater niche differentiation related to mechanisms of energy conversion and production. Under the high substrate environments seen as high inputs of marine phytoplankton, early temporal metabolic responses differentiated the two microbiomes, however within a matter of days semi-functional convergence was observed as the bacterial groups adapted in similar ways to access the substrates for growth and energy production. Regardless of the redundancies measured, it was evident that nitrogen metabolism was a key process differentiating the bacterial communities, likely a reflection of distinctive environmental forcing from the original oceanic environments at the time of collection and the specific metabolic capabilities of the initial bacterial classes. The third research chapter (Chapter 4) confirmed the high functional redundancy of these microbiomes over a ten day incubation period, primarily by the opportunistic bacterium of the Class Flavobacteria and members of Alphaproteobacteria to activate enzymes related to lipid substrate decomposition. This suggests that periods of intense primary productivity should result in nearly comparable degrees of remineralization independent of depth or initial bacterial composition in this shallow shelf ecosystem.

The incorporation of microbial –omic methodologies together with geochemical analyses can prove to be a powerful tool to identify metabolic activities important in the structuring of biogeochemical profiles within the ocean [25]. The multidisciplinary approach employed within this dissertation was essential to unravel the intricacies in the timing and processing of substrates within different organic matter environments. The current work demonstrated how the coupling of methodologies can describe specific processes in a complex system because of the unique insights provided by each method: 1. identification of key community functions through a metaproteomic enrichment analysis, 2. assignment of taxonomic classes to these functions, 3. incorporation of traditional methods to assess changes in taxonomic composition (16S rRNA

sequencing), and 4. measurements of community functionality through particulate lipid class decomposition.

Trait-based functionality of organisms and communities is becoming a more widely acknowledged and applied concept in systems ecology (e.g., [2, 140, 152]) and is trending to replace the sole use of traditional indicators such as biodiversity measures or the presence of specific species to analyze the productivity of a complex community and health of an ecosystem. For example, the use of functional diversity instead of taxonomic diversity alone is proving to be an accurate tool for the modeling of spatial distributions of ecosystem services and biogeochemical profiles [1, 104]. Still in its infancy, “functional-trait ecology” requires a standardized methodology to be designed in order to organize and characterize the vast quantity of molecular data available to researchers. The methods developed and employed during this dissertation, and their applications to complex, natural microbiomes during the early stages of organic matter decomposition contributes to this discussion. In particular, the trait-based methods were used to characterize and quantify microbial metabolic response to environmental conditions in a way that may benefit future experimental work and development of biogeochemical models for polar regions by identifying 1) which physiological traits to focus on, 2) temporal resolution of metabolic responses and 3) taxonomic-trait associations.

The datasets that were constructed throughout this research provide a rich resource of peptide data with high mass-accuracy, functional-taxonomic associations through gene ontology mapping and robust bioinformatics standards, as well as high taxonomic resolution through traditional 16S rRNA sequencing. All of this data will become publicly available for other researchers to probe in order to address future research questions relevant to complex polar bacterial communities and their functionality. The analysis completed thus far focused mainly on community-scale functions, followed by identification of which taxonomic groups dominated such expressions. Another powerful approach to access this dataset would be to complete characteristic profiles on different taxonomic groups (i.e., Flavobacteria) and track statistically changing functions solely identified within that group to further understand how each bacterium responded to the organic perturbations over time. This approach could lend support to definitions of niche formation in natural assemblages of bacteria. The results that came out of this dissertation also revealed areas of improvement for future research projects aiming to link

geochemical cycling of substrates with trait-based measures of microbial activity. This goal would benefit by widening the analytical window for particulate diagenesis. For example, the measurement of particulate carbohydrates would be useful, as environmental stimulus inducing metabolic responses related to carbohydrate recycling was apparent early in the incubations. In addition, inclusion of bacterial enzymatic activity assays of specific particulate biochemical classes (i.e., lipids, carbohydrates and amino acids) would also be recommended as a direct measure of enzymatic activity to compliment the enzyme commission classifications, and in general, to compliment the multidisciplinary scope outlined in this dissertation.

## REFERENCES

1. Violle C, Reich PB, Pacala SW, Enquist BJ, Kattge J. The emergence and promise of functional biogeography. *Proc Natl Acad Sci USA*. 2014;111(38):13690-6.
2. Cernansky R. The Biodiversity revolution. *Nature*. 2017:22-4.
3. Allison SD, Martiny JBH. Resistance, resilience, and redundancy in microbial communities. *Proc Natl Acad Sci USA*. 2008;105:11512-9.
4. Galand PE, Pereira O, Hochart C, Auguet JC, Debroas D. A strong link between marine microbial community composition and function challenges the idea of functional redundancy. *ISME J*. 2018.
5. Lindh MV, Figueroa D, Sjöstedt J, Baltar F, Lundin D, Andersson A, et al. Transplant experiments uncover Baltic Sea basin-specific responses in bacterioplankton community composition and metabolic activities. *Front Microbiol*. 2015;6.
6. Bird JA, Herman DJ, Firestone MK. Rhizosphere priming of soil organic matter by bacterial groups in a grassland soil. *Soil Biol Biochem*. 2011;43(4):718-25.
7. Yachi S, Loreau M. Biodiversity and ecosystem productivity in a fluctuating environment: The insurance hypothesis. *Proc Natl Acad Sci USA*. 1999;96(4):1463-8.
8. Falkowski PG, Barber RT, Smetacek V. Biogeochemical Controls and Feedbacks on Ocean Primary Production. *Science*. 1998;281(5374):200-6.
9. Falkowski PG, Fenchel T, DeLong EF. The Microbial Engines That Drive Earth's Biogeochemical Cycles. *Science*. 2008;320(5879):1034-9.
10. Hedges JJ. Global biogeochemical cycles - Progress and problems. *Mar Chem*. 1992;39(1-3):67-93.
11. Fuhrman JA, Steele JA. Community structure of marine bacterioplankton: patterns, networks, and relationships to function. *Aquat Microb Ecol*. 2008;53(1):69-81.
12. Kirchman D, K'nees E, Hodson R. Leucine incorporation and its potential as a measure of protein synthesis by bacteria in natural aquatic systems. *Appl Environ Microbiol*. 1985;49(3):599-607.
13. Arnosti C, Finke N, Larsen O, Ghobrial S. Anoxic carbon degradation in Arctic sediments: Microbial transformations of complex substrates. *Geochim Cosmochim Acta*. 2005;69(9):2309-20.
14. Dauwe B, Middelburg JJ. Amino acids and hexosamines as indicators of organic matter degradation state in North Sea sediments. *Limnol Oceanogr*. 1998;43(5):782-98.
15. Fuhrman JA, Azam F. Thymidine incorporation as a measure of heterotrophic bacterioplankton production in marine surface waters - Evaluation and field results. *Mar Biol*. 1982;66(2):109-20.
16. Malmstrom RR, Cottrell MT, Elifantz H, Kirchman DL. Biomass production and assimilation of dissolved organic matter by SAR11 bacteria in the Northwest Atlantic Ocean. *Appl Environ Microbiol*. 2005;71(6):2979-86.
17. Haynes K, Hofmann TA, Smith CJ, Ball AS, Underwood GJ, Osborn AM. Diatom-derived carbohydrates as factors affecting bacterial community composition in estuarine sediments. *Appl Environ Microbiol*. 2007;73(19):6112-24.
18. Poretsky RS, Sun SL, Mou XZ, Moran MA. Transporter genes expressed by coastal bacterioplankton in response to dissolved organic carbon. *Environ Microbiol*. 2010;12(3):616-27.

19. Buchan A, LeClerc GR, Gulvik CA, Gonzalez JM. Master recyclers: features and functions of bacteria associated with phytoplankton blooms. *Nat Rev Microbiol.* 2014;12(10):686-98.
20. Reintjes G, Arnosti C, Fuchs BM, Amann R. An alternative polysaccharide uptake mechanism of marine bacteria. *ISME J.* 2017;11(7):1640-50.
21. Riemann L, Steward GF, Azam F. Dynamics of bacterial community composition and activity during a mesocosm diatom bloom. *Appl Environ Microbiol.* 2000;66(2):578-87.
22. Pinhassi J, Azam F, Hemphala J, Long RA, Martinez J, Zweifel UL, et al. Coupling between bacterioplankton species composition, population dynamics, and organic matter degradation. *Aquat Microb Ecol.* 1999;17(1):13-26.
23. Morris RM, Nunn BL, Frazar C, Goodlett DR, Ting YS, Rocap G. Comparative metaproteomics reveals ocean-scale shifts in microbial nutrient utilization and energy transduction. *ISME J.* 2010;4(5):673-85.
24. Teeling H, Fuchs BM, Becher D, Klockow C, Gardebrecht A, Bennke CM, et al. Substrate-Controlled Succession of Marine Bacterioplankton Populations Induced by a Phytoplankton Bloom. *Science.* 2012;336(6081):608-11.
25. Louca S, Hawley AK, Katsev S, Torres-Beltran M, Bhatia MP, Kheirandish S, et al. Integrating biogeochemistry with multiomic sequence information in a model oxygen minimum zone. *Proc Natl Acad Sci USA.* 2016;113(40):E5925-E33.
26. Konopka A, Wilkins MJ. Application of meta-transcriptomics and -proteomics to analysis of in situ physiological state. *Front Microbiol.* 2012;3.
27. DeLong EF, Preston CM, Mincer T, Rich V, Hallam SJ, Frigaard NU, et al. Community genomics among stratified microbial assemblages in the ocean's interior. *Science.* 2006;311(5760):496-503.
28. Fuhrman JA. Microbial community structure and its functional implications. *Nature.* 2009;459:193.
29. Vogel C, Marcotte EM. Insights into the regulation of protein abundance from proteomic and transcriptomic analyses. *Nat Rev Genet.* 2012;13:227.
30. Nunn BL, Timperman AT. Marine proteomics. *Mar Ecol Prog Ser.* 2007;332:281-9.
31. VerBerkmoes NC, Denev VJ, Hettich RL, Banfield JF. Systems Biology: Functional analysis of natural microbial consortia using community proteomics. *Nat Rev Microbiol.* 2009;7(3):196-205.
32. Blazewicz SJ, Barnard RL, Daly RA, Firestone MK. Evaluating rRNA as an indicator of microbial activity in environmental communities: limitations and uses. *ISME J.* 2013;7:2061.
33. May DH, Timmins-Schiffman E, Mikan MP, Haryey HR, Borenstein E, Nunn BL, et al. An Alignment-Free "Metapeptide" Strategy for Metaproteomic Characterization of Microbiome Samples Using Shotgun Metagenomic Sequencing. *J Proteome Res.* 2016;15(8):2697-705.
34. Timmins-Schiffman E, May DH, Mikan M, Riffle M, Frazar C, Harvey HR, et al. Critical decisions in metaproteomics: achieving high confidence protein annotations in a sea of unknowns. *ISME J.* 2017;11(2):309-14.
35. Timmins-Schiffman E, Mikan MP, Ting YS, Harvey HR, Nunn BL. MS analysis of a dilution series of bacteria:phytoplankton to improve detection of low abundance bacterial peptides. *Sci Rep.* 2018;8(1):9276.
36. Riffle M, May DH, Timmins-Schiffman E, Mikan MP, Jaschob D, Noble WS, et al. MetaGOmics: A Web-Based Tool for Peptide-Centric Functional and Taxonomic Analysis of Metaproteomics Data. *Proteomes.* 2018;6(1).

37. Fagervold SK, Bourgeois S, Pruski AM, Charles F, Kerherve P, Vétion G, et al. River organic matter shapes microbial communities in the sediment of the Rhone prodelta. *ISME J.* 2014;8(11):2327-38.
38. Aylward FO, Eppley JM, Smith JM, Chavez FP, Scholin CA, DeLong EF. Microbial community transcriptional networks are conserved in three domains at ocean basin scales. *Proc Natl Acad Sci USA.* 2015;112(17):5443-8.
39. Kirchman DL. The ecology of Cytophaga-Flavobacteria in aquatic environments. *FEMS Microbiol Ecol.* 2002;39(2):91-100.
40. Bergauer K, Fernandez-Guerra A, Garcia JAL, Sprenger RR, Stepanauskas R, Pachiadaki MG, et al. Organic matter processing by microbial communities throughout the Atlantic water column as revealed by metaproteomics. *Proc Natl Acad Sci USA.* 2018;115(3):E400-E8.
41. Williams TJ, Long E, Evans F, DeMaere MZ, Lauro FM, Raftery MJ, et al. A metaproteomic assessment of winter and summer bacterioplankton from Antarctic Peninsula coastal surface waters. *ISME J.* 2012;6(10):1883-900.
42. Mattes TE, Nunn BL, Marshall KT, Proskurowski G, Kelley DS, Kawka OE, et al. Sulfur oxidizers dominate carbon fixation at a biogeochemical hot spot in the dark ocean. *ISME J.* 2013;7(12):2349-60.
43. Ng C, DeMaere MZ, Williams TJ, Lauro FM, Raftery M, Gibson JAE, et al. Metaproteogenomic analysis of a dominant green sulfur bacterium from Ace Lake, Antarctica. *ISME J.* 2010;4(8):1002-19.
44. Mande SS, Mohammed MH, Ghosh TS. Classification of metagenomic sequences: methods and challenges. *Brief Bioinform.* 2012;13(6):669-81.
45. Martens L, Hermjakob H. Proteomics data validation: why all must provide data. *Mol Biosyst.* 2007;3(8):518-22.
46. Nesvizhskii AI, Aebersold R. Interpretation of shotgun proteomic data - The protein inference problem. *Mol Cell Proteomics.* 2005;4(10):1419-40.
47. Huang T, Wang JJ, Yu WC, He ZY. Protein inference: a review. *Brief Bioinform.* 2012;13(5):586-614.
48. Serang O, Moruz L, Hoopmann MR, Kall L. Recognizing Uncertainty Increases Robustness and Reproducibility of Mass Spectrometry-based Protein Inferences. *J Proteome Res.* 2012;11(12):5586-91.
49. Tanca A, Palomba A, Deligios M, Cubeddu T, Fraumene C, Biosca G, et al. Evaluating the Impact of Different Sequence Databases on Metaproteome Analysis: Insights from a Lab-Assembled Microbial Mixture. *PLoS One.* 2013;8(12).
50. Saito MA, Dorsk A, Post AF, McIlvin MR, Rappe MS, DiTullio GR, et al. Needles in the blue sea: Sub-species specificity in targeted protein biomarker analyses within the vast oceanic microbial metaproteome. *Proteomics.* 2015;15(20):3521-31.
51. Muth T, Benndorf D, Reichl U, Rapp E, Martens L. Searching for a needle in a stack of needles: challenges in metaproteomics data analysis. *Mol Biosyst.* 2013;9(4):578-85.
52. Fadeev E, Salter I, Schourup-Kristensen V, Nöthig E-M, Metfies K, Engel A, et al. Microbial Communities in the East and West Fram Strait During Sea Ice Melting Season. *Front Mar Sci.* 2018;5(429).
53. Martin M. Cutadapt removes adapter sequences from high-throughput sequencing reads. *EMBnet J.* 2011;17(1):pp. 10-2.
54. Bolger AM, Lohse M, Usadel B. Trimmomatic: a flexible trimmer for Illumina sequence data. *Bioinformatics.* 2014;30(15):2114-20.

55. Zhang J, Kobert K, Flouri T, Stamatakis A. PEAR: a fast and accurate Illumina Paired-End reAd mergeR. *Bioinformatics*. 2014;30(5):614-20.
56. Mahé F, Rognes T, Quince C, de Vargas C, Dunthorn M. Swarm: robust and fast clustering method for amplicon-based studies. *PeerJ*. 2014;2:e593.
57. Pruesse E, Peplies J, Glöckner FO. SINA: accurate high-throughput multiple sequence alignment of ribosomal RNA genes. *Bioinformatics*. 2012;28(14):1823-9.
58. Wright JJ, Lee S, Zaikova E, Walsh DA, Hallam SJ. DNA extraction from 0.22 micromM Sterivex filters and cesium chloride density gradient centrifugation. *J Vis Exp*. 2009(31).
59. Kultima JR, Sunagawa S, Li J, Chen W, Chen H, Mende DR, et al. MOCAT: a metagenomics assembly and gene prediction toolkit. *PLoS One*. 2012;7(10):e47656.
60. Vizcaino JA, Csordas A, del-Toro N, Dianes JA, Griss J, Lavidas I, et al. 2016 update of the PRIDE database and its related tools (vol 44, pg D447, 2016). *Nucleic Acids Res*. 2016;44(22):11033-11033.
61. Eng JK, Jahan TA, Hoopmann MR. Comet: An open-source MS/MS sequence database search tool. *Proteomics*. 2013;13(1):22-4.
62. Granholm V, Navarro JF, Noble WS, Käll L. Determining the calibration of confidence estimation procedures for unique peptides in shotgun proteomics. *J Proteomics*. 2013;80:123-31.
63. Kall L, Canterbury JD, Weston J, Noble WS, MacCoss MJ. Semi-supervised learning for peptide identification from shotgun proteomics datasets. *Nat Methods*. 2007;4(11):923-5.
64. Deutsch EW, Mendoza L, Shteynberg D, Slagel J, Sun Z, Moritz RL. Trans-Proteomic Pipeline, a standardized data processing pipeline for large-scale reproducible proteomics informatics. *Proteomics Clin Appl*. 2015;9(7-8):745-54.
65. Ashburner M, Ball CA, Blake JA, Botstein D, Butler H, Cherry JM, et al. Gene Ontology: tool for the unification of biology. *Nat Genet*. 2000;25:25.
66. Expansion of the Gene Ontology knowledgebase and resources. *Nucleic Acids Res*. 2017;45(D1):D331-D8.
67. Georges AA, El-Swais H, Craig SE, Li WKW, Walsh DA. Metaproteomic analysis of a winter to spring succession in coastal northwest Atlantic Ocean microbial plankton. *ISME J*. 2014;8(6):1301-13.
68. Galand PE, Salter I, Kalenitchenko D. Ecosystem productivity is associated with bacterial phylogenetic distance in surface marine waters. *Mol Ecol*. 2015;24(23):5785-95.
69. Muthusamy S, Lundin D, Branca RMM, Baltar F, Gonzalez JM, Lehtio J, et al. Comparative proteomics reveals signature metabolisms of exponentially growing and stationary phase marine bacteria. *Environ Microbiol*. 2017;19(6):2301-19.
70. Alonso-Sáez L, Zeder M, Harding T, Pernthaler J, Lovejoy C, Bertilsson S, et al. Winter bloom of a rare betaproteobacterium in the Arctic Ocean. *Front Microbiol*. 2014;5(425).
71. Christie-Oleza JA, Fernandez B, Nogales B, Bosch R, Armengaud J. Proteomic insights into the lifestyle of an environmentally relevant marine bacterium. *ISME J*. 2012;6(1):124-35.
72. Ferguson RL, Buckley EN, Palumbo AV. Response of marine bacterioplankton to differential filtration and confinement. *Appl Environ Microbiol*. 1984;47(1):49-55.
73. Chin-Leo G, Kirchman DL. Unbalanced growth in natural assemblages of marine bacterioplankton. *Mar Ecol Prog Ser*. 1990;63(1):1-8.
74. Flardh K, Cohen PS, Kjelleberg S. Ribosomes exist in large excess over the apparent demand for protein synthesis during carbon starvation in marine *Vibrio* sp. strain CCUG 15956. *J Bacteriol*. 1992;174(21):6780-8.

75. Harvey HR, Tuttle JH, Bell JT. Kinetics of phytoplankton decay during simulated sedimentation - Changes in biochemical composition and microbial activity under oxic and anoxic conditions. *Geochim Cosmochim Acta*. 1995;59(16):3367-77.
76. Keil RG, Kirchman DL. Utilization of dissolved protein and amino acids in the northern Sargasso Sea. *Aquat Microb Ecol*. 1999;18(3):293-300.
77. Amon RMW, Fitznar HP, Benner R. Linkages among the bioreactivity, chemical composition, and diagenetic state of marine dissolved organic matter. *Limnol Oceanogr*. 2001;46(2):287-97.
78. Castello A, Hentze MW, Preiss T. Metabolic Enzymes Enjoying New Partnerships as RNA-Binding Proteins. *Trends Endocrinol Metab*. 2015;26(12):746-57.
79. Koebmann BJ, Westerhoff HV, Snoep JL, Nilsson D, Jensen PR. The glycolytic flux in *Escherichia coli* is controlled by the demand for ATP. *J Bacteriol*. 2002;184(14):3909-16.
80. Sun J, Steindler L, Thrash JC, Halsey KH, Smith DP, Carter AE, et al. One Carbon Metabolism in SAR11 Pelagic Marine Bacteria. *PLoS One*. 2011;6(8).
81. Higgins CF. ABC transporters: physiology, structure and mechanism - an overview. *Res Microbiol*. 2001;152(3-4):205-10.
82. Sowell SM, Abraham PE, Shah M, Verberkmoes NC, Smith DP, Barofsky DF, et al. Environmental proteomics of microbial plankton in a highly productive coastal upwelling system. *ISME J*. 2011;5(5):856-65.
83. Sowell SM, Wilhelm LJ, Norbeck AD, Lipton MS, Nicora CD, Barofsky DF, et al. Transport functions dominate the SAR11 metaproteome at low-nutrient extremes in the Sargasso Sea. *ISME J*. 2009;3(1):93-105.
84. Forchhammer K. Glutamine signalling in bacteria. *Front Biosci (Landmark Ed)*. 2007;12:358-70.
85. Berges JA, Mulholland MR. *Enzymes and Nitrogen Cycling. Nitrogen in the Marine Environment*. 2nd ed: Elsevier; 2008. p. 1385-444.
86. Jurgenson CT, Begley TP, Ealick SE. The Structural and Biochemical Foundations of Thiamin Biosynthesis. *Annu Rev Biochem*. 2009;78(1):569-603.
87. Sunagawa S, Coelho LP, Chaffron S, Kultima JR, Labadie K, Salazar G, et al. Structure and function of the global ocean microbiome. *Science*. 2015;348(6237).
88. Bermingham A, Derrick JP. The folic acid biosynthesis pathway in bacteria: evaluation of potential for antibacterial drug discovery. *Bioessays*. 2002;24(7):637-48.
89. Percudani R, Peracchi A. A genomic overview of pyridoxal-phosphate-dependent enzymes. *EMBO Rep*. 2003;4(9):850-4.
90. Kim PB, Nelson JW, Breaker RR. An Ancient Riboswitch Class in Bacteria Regulates Purine Biosynthesis and One-Carbon Metabolism. *Mol Cell*. 2015;57(2):317-28.
91. Akashi H, Gojobori T. Metabolic efficiency and amino acid composition in the proteomes of *Escherichia coli* and *Bacillus subtilis*. *Proc Natl Acad Sci U S A*. 2002;99(6):3695-700.
92. Leonhartsberger S, Korsa I, Bock A. The molecular biology of formate metabolism in enterobacteria. *J Mol Microbiol Biotechnol*. 2002;4(3):269-76.
93. Ferry JG. Formate dehydrogenase. *FEMS Microbiol Lett*. 1990;87(3-4):377-82.
94. Fuhrman JA, Cram JA, Needham DM. Marine microbial community dynamics and their ecological interpretation. *Nat Rev Microbiol*. 2015;13(3):133-46.



95. Gomez-Pereira PR, Schuler M, Fuchs BM, Bennke C, Teeling H, Waldmann J, et al. Genomic content of uncultured Bacteroidetes from contrasting oceanic provinces in the North Atlantic Ocean. *Environ Microbiol.* 2012;14(1):52-66.
96. Caffrey BE, Williams TA, Jiang XW, Toft C, Hokamp K, Fares MA. Proteome-Wide Analysis of Functional Divergence in Bacteria: Exploring a Host of Ecological Adaptations. *PLoS One.* 2012;7(4).
97. Needham DM, Fuhrman JA. Pronounced daily succession of phytoplankton, archaea and bacteria following a spring bloom. *Nat Microbiol.* 2016;1(4).
98. Moran MA, Belas R, Schell MA, Gonzalez JM, Sun F, Sun S, et al. Ecological genomics of marine roseobacters. *Appl Environ Microbiol.* 2007;73(14):4559-69.
99. Alonso-Sáez L, Sánchez O, Gasol JM, Balagué V, Pedrós-Alio C. Winter-to-summer changes in the composition and single-cell activity of near-surface Arctic prokaryotes. *Environ Microbiol.* 2008;10(9):2444-54.
100. Giovannoni SJ, Tripp HJ, Givan S, Podar M, Vergin KL, Baptista D, et al. Genome streamlining in a cosmopolitan oceanic bacterium. *Science.* 2005;309(5738):1242-5.
101. Lauro FM, McDougald D, Thomas T, Williams TJ, Egan S, Rice S, et al. The genomic basis of trophic strategy in marine bacteria. *Proc Natl Acad Sci USA.* 2009;106(37):15527-33.
102. Williams TJ, Ertan H, Ting L, Cavicchioli R. Carbon and nitrogen substrate utilization in the marine bacterium *Sphingopyxis alaskensis* strain RB2256. *ISME J.* 2009;3(9):1036-52.
103. Sañudo-Wilhelmy SA, Gómez-Consarnau L, Suffridge C, Webb EA. The Role of B Vitamins in Marine Biogeochemistry. *Ann Rev Mar Sci.* 2014;6(1):339-67.
104. Coles VJ, Stukel MR, Brooks MT, Burd A, Crump BC, Moran MA, et al. Ocean biogeochemistry modeled with emergent trait-based genomics. *Science.* 2017;358(6367):1149-54.
105. Grebmeier JM. Shifting patterns of life in the Pacific Arctic and Sub-Arctic seas. *Ann Rev Mar Sci.* 2012;4:63-78.
106. Van Pelt TI, Napp JM, Ashjian CJ, Harvey HR, Lomas MW, Sigler MF, et al. An introduction and overview of the Bering Sea Project: Volume IV. *Deep-Sea Res PT II.* 2016;134:3-12.
107. Grebmeier JM, Cooper LW, Feder HM, Sirenko BI. Ecosystem dynamics of the Pacific-influenced Northern Bering and Chukchi Seas in the Amerasian Arctic. *Prog Oceanogr.* 2006;71(2):331-61.
108. Michel C, Ingram RG, Harris LR. Variability in oceanographic and ecological processes in the Canadian Arctic Archipelago. *Prog Oceanogr.* 2006;71(2):379-401.
109. Hunt Jr GL, Stabeno P, Walters G, Sinclair E, Brodeur RD, Napp JM, et al. Climate change and control of the southeastern Bering Sea pelagic ecosystem. *Deep-Sea Res PT II.* 2002;49(26):5821-53.
110. Pomeroy LR, Deibel D. Temperature Regulation of Bacterial Activity During the Spring Bloom in Newfoundland Coastal Waters. *Science.* 1986;233(4761):359-61.
111. Azam F. Microbial Control of Oceanic Carbon Flux: The Plot Thickens. *Science.* 1998;280(5364):694-6.
112. Perovich D, Meier W, Tschudi M, Farrell S, Gerland S, Henricks S, et al. Sea Ice [in Arctic Report Card 2016]: NOAAs Arctic Program; 2016. Available from: <https://www.arctic.noaa.gov/Report-Card/Report-Card-2016/ArtMID/5022/ArticleID/286/Sea-Ice>.

113. Frey KE CJ, Cooper, LW, Gradinger, RR, Grebmeier, JM, Tremblay JE. Arctic Ocean Primary Productivity [in Arctic Report Card 2016]: NOAAs Arctic Program; 2016. Available from: <https://www.arctic.noaa.gov/Report-Card/Report-Card-2016/ArtMID/5022/ArticleID/284/Arctic-Ocean-Primary-Productivity>.
114. Kirchman DL, Hill V, Cottrell MT, Gradinger R, Malmstrom RR, Parker A. Standing stocks, production, and respiration of phytoplankton and heterotrophic bacteria in the western Arctic Ocean. *Deep-Sea Res PT II*. 2009;56(17):1237-48.
115. Han D, Ha HK, Hwang CY, Lee BY, Hur H-G, Lee YK. Bacterial communities along stratified water columns at the Chukchi Borderland in the western Arctic Ocean. *Deep-Sea Res PT II*. 2015;120:52-60.
116. Galand PE, Potvin M, Casamayor EO, Lovejoy C. Hydrography shapes bacterial biogeography of the deep Arctic Ocean. *ISME J*. 2009;4:564.
117. Comeau AM, Li WKW, Tremblay J-É, Carmack EC, Lovejoy C. Arctic Ocean Microbial Community Structure before and after the 2007 Record Sea Ice Minimum. *PLoS One*. 2011;6(11):e27492.
118. Arrigo KR, van Dijken G, Pabi S. Impact of a shrinking Arctic ice cover on marine primary production. *Geophys Res Lett*. 2008;35(19).
119. Kirchman DL, Morán XAG, Ducklow H. Microbial growth in the polar oceans — role of temperature and potential impact of climate change. *Nat Rev Microbiol*. 2009;7:451.
120. Wheeler PA, Gosselin M, Sherr E, Thibault D, Kirchman DL, Benner R, et al. Active cycling of organic carbon in the central Arctic Ocean. *Nature*. 1996;380(6576):697-9.
121. Kirchman DL, Malmstrom RR, Cottrell MT. Control of bacterial growth by temperature and organic matter in the Western Arctic. *Deep-Sea Res PT II*. 2005;52(24):3386-95.
122. Zhuang Y, Jin H, Li H, Chen J, Lin L, Bai Y, et al. Pacific inflow control on phytoplankton community in the Eastern Chukchi Shelf during summer. *Cont Shelf Res*. 2016;129:23-32.
123. Teske A, Durbin A, Ziervogel K, Cox C, Arnosti C. Microbial Community Composition and Function in Permanently Cold Seawater and Sediments from an Arctic Fjord of Svalbard. *Appl Environ Microbiol*. 2011;77(6):2008-18.
124. Logue JB, Findlay SE, Comte J. Editorial: Microbial Responses to Environmental Changes. *Front Microbiol*. 2015;6:1364.
125. Cooper LW, Whitley TE, Grebmeier JM, Weingartner T. The nutrient, salinity, and stable oxygen isotope composition of Bering and Chukchi Seas waters in and near the Bering Strait. *J Geophys Res Oceans*. 1997;102(C6):12563-73.
126. Weingartner T, Aagaard K, Woodgate R, Danielson S, Sasaki Y, Cavalieri D. Circulation on the north central Chukchi Sea shelf. *Deep-Sea Res PT II*. 2005;52(24):3150-74.
127. Anderson MJ, Walsh DCI. PERMANOVA, ANOSIM, and the Mantel test in the face of heterogeneous dispersions: What null hypothesis are you testing? *Ecol Monogr*. 2013;83(4):557-74.
128. Yager PL, Connelly TL, Mortazavi B, Wommack KE, Bano N, Bauer JE, et al. Dynamic bacterial and viral response to an algal bloom at subzero temperatures. *Limnol Oceanogr*. 2001;46(4):790-801.
129. Ortega-Retuerta E, Fichot CG, Arrigo KR, Van Dijken GL, Joux F. Response of marine bacterioplankton to a massive under-ice phytoplankton bloom in the Chukchi Sea (Western Arctic Ocean). *Deep-Sea Res PT II*. 2014;105:74-84.

130. Awasthi A, Singh M, Soni SK, Singh R, Kalra A. Biodiversity acts as insurance of productivity of bacterial communities under abiotic perturbations. *ISME J.* 2014;8:2445.
131. Fuhrman JA, Hewson I, Schwalbach MS, Steele JA, Brown MV, Naeem S. Annually reoccurring bacterial communities are predictable from ocean conditions. *Proc Natl Acad Sci USA.* 2006;103(35):13104-9.
132. Traving SJ, Rowe O, Jakobsen NM, Sorensen H, Dinasquet J, Stedmon CA, et al. The Effect of Increased Loads of Dissolved Organic Matter on Estuarine Microbial Community Composition and Function. *Front Microbiol.* 2017;8:351.
133. Girvan MS, Campbell CD, Killham K, Prosser JI, Glover LA. Bacterial diversity promotes community stability and functional resilience after perturbation. *Environ Microbiol.* 2005;7(3):301-13.
134. Williams TJ, Wilkins D, Long E, Evans F, DeMaere MZ, Raftery MJ, et al. The role of planktonic Flavobacteria in processing algal organic matter in coastal East Antarctica revealed using metagenomics and metaproteomics. *Environ Microbiol.* 2012:n/a-n/a.
135. Gomez-Pereira PR, Fuchs BM, Alonso C, Oliver MJ, van Beusekom JE, Amann R. Distinct flavobacterial communities in contrasting water masses of the north Atlantic Ocean. *ISME J.* 2010;4(4):472-87.
136. Sapp M, Schwaderer AS, Wiltshire KH, Hoppe H-G, Gerdts G, Wichels A. Species-Specific Bacterial Communities in the Phycosphere of Microalgae? *Microb Ecol.* 2007;53(4):683-99.
137. Sarmento H, Morana C, Gasol JM. Bacterioplankton niche partitioning in the use of phytoplankton-derived dissolved organic carbon: quantity is more important than quality. *ISME J.* 2016;10:2582.
138. Kirchman DL, Cottrell MT, Lovejoy C. The structure of bacterial communities in the western Arctic Ocean as revealed by pyrosequencing of 16S rRNA genes. *Environ Microbiol.* 2010;12(5):1132-43.
139. Gifford SM, Sharma S, Booth M, Moran MA. Expression patterns reveal niche diversification in a marine microbial assemblage. *ISME J.* 2013;7(2):281-98.
140. Evans R, Alessi AM, Bird S, McQueen-Mason SJ, Bruce NC, Brockhurst MA. Defining the functional traits that drive bacterial decomposer community productivity. *ISME J.* 2017;11:1680.
141. Comte J, Fauteux L, Del Giorgio PA. Links between metabolic plasticity and functional redundancy in freshwater bacterioplankton communities. *Front Microbiol.* 2013;4:112.
142. Balmonte JP, Teske A, Arnosti C. Structure and function of high Arctic pelagic, particle-associated and benthic bacterial communities. *Environ Microbiol.* 2018;20(8):2941-54.
143. Beier S, Rivers AR, Moran MA, Obernosterer I. The transcriptional response of prokaryotes to phytoplankton-derived dissolved organic matter in seawater. *Environ Microbiol.* 2015;17(10):3466-80.
144. Bates NR, Hansell DA, Moran SB, Codispoti LA. Seasonal and spatial distribution of particulate organic matter (POM) in the Chukchi and Beaufort Seas. *Deep-Sea Res PT II.* 2005;52(24-26):3324-43.
145. Deutsch C, Gruber N, Key RM, Sarmiento JL, Ganachaud A. Denitrification and N<sub>2</sub> fixation in the Pacific Ocean. *Global Biogeochem Cycles.* 2001;15(2):483-506.
146. Zeng Y-X, Zhang F, He J-F, Lee SH, Qiao Z-Y, Yu Y, et al. Bacterioplankton community structure in the Arctic waters as revealed by pyrosequencing of 16S rRNA genes. *Antonie Van Leeuwenhoek.* 2013;103(6):1309-19.

147. Wang H-l, Sun L. Comparative metagenomic analysis of the microbial communities in the surroundings of Iheya north and Iheya ridge hydrothermal fields reveals insights into the survival strategy of microorganisms in deep-sea environments. *J Marine Syst.* 2018;180:102-11.
148. González PJ, Correia C, Moura I, Brondino CD, Moura JGG. Bacterial nitrate reductases: Molecular and biological aspects of nitrate reduction. *J Inorg Biochem.* 2006;100(5):1015-23.
149. Bell T, Newman JA, Silverman BW, Turner SL, Lilley AK. The contribution of species richness and composition to bacterial services. *Nature.* 2005;436:1157.
150. Amend AS, Martiny AC, Allison SD, Berlemont R, Goulden ML, Lu Y, et al. Microbial response to simulated global change is phylogenetically conserved and linked with functional potential. *ISME J.* 2015;10:109.
151. Cadotte MW, Carscadden K, Mirotchnick N. Beyond species: functional diversity and the maintenance of ecological processes and services. *J Appl Ecol.* 2011;48(5):1079-87.
152. Salles JF, Poly F, Schmid B, Roux XL. Community niche predicts the functioning of denitrifying bacterial assemblages. *Ecology.* 2009;90(12):3324-32.
153. Hodges LR, Bano N, Hollibaugh JT, Yager PL. Illustrating the importance of particulate organic matter to pelagic microbial abundance and community structure - an Arctic case study. *Aquat Microb Ecol.* 2005;40(3):217-27.
154. Dyda RY, Suzuki MT, Yoshinaga MY, Harvey HR. The response of microbial communities to diverse organic matter sources in the Arctic Ocean. *Deep-Sea Res PT II.* 2009;56(17):1249-63.
155. Harvey HR, Macko SA. Catalysts or contributors? Tracking bacterial mediation of early diagenesis in the marine water column. *Org Geochem.* 1997;26(9-10):531-44.
156. Harvey HR, Macko SA. Kinetics of phytoplankton decay during simulated sedimentation: changes in lipids under oxic and anoxic conditions. *Org Geochem.* 1997;27(3):129-40.
157. Reed DC, Algar CK, Huber JA, Dick GJ. Gene-centric approach to integrating environmental genomics and biogeochemical models. *Proc Natl Acad Sci USA.* 2014;111(5):1879-84.
158. Reed DC, Breier JA, Jiang H, Anantharaman K, Klausmeier CA, Toner BM, et al. Predicting the response of the deep-ocean microbiome to geochemical perturbations by hydrothermal vents. *ISME J.* 2015;9:1857.
159. Harvey HR, Pleuthner RL, Lessard EJ, Bernhardt MJ, Tracy Shaw C. Physical and biochemical properties of the euphausiids *Thysanoessa inermis*, *Thysanoessa raschii*, and *Thysanoessa longipes* in the eastern Bering Sea. *Deep-Sea Res PT II.* 2012;65-70:173-83.
160. Belicka LL, Macdonald RW, Harvey HR. Trace element and molecular markers of organic carbon dynamics along a shelf-basin continuum in sediments of the western Arctic Ocean. *Mar Chem.* 2009;115(1):72-85.
161. Destailats F, Angers P. One-step methodology for the synthesis of FA picolinyl esters from intact lipids. *J Am Oil Chem Soc.* 2002;79(3):253-6.
162. Moore EK, Nunn BL, Goodlett DR, Harvey HR. Identifying and tracking proteins through the marine water column: insights into the inputs and preservation mechanisms of protein in sediments. *Geochim Cosmochim Acta.* 2012;83:324-59.
163. Cowie GL, Hedges JI. Improved amino-acid quantification in environmental-samples - Charge-matched recovery standards and reduced analysis time. *Mar Chem.* 1992;37(3-4):223-38.

164. Hill DP, Davis AP, Richardson JE, Corradi JP, Ringwald M, Eppig JT, et al. PROGRAM DESCRIPTION: Strategies for Biological Annotation of Mammalian Systems: Implementing Gene Ontologies in Mouse Genome Informatics. *Genomics*. 2001;74(1):121-8.
165. Bairoch A. The ENZYME database in 2000. *Nucleic Acids Res*. 2000;28(1):304-5.
166. Gasteiger E, Gattiker A, Hoogland C, Ivanyi I, Appel RD, Bairoch A. ExPASy: The proteomics server for in-depth protein knowledge and analysis. *Nucleic Acids Res*. 2003;31(13):3784-8.
167. Kaneda T. Iso- and anteiso-fatty acids in bacteria: biosynthesis, function, and taxonomic significance. *Microbiol Rev*. 1991;55(2):288-302.
168. Volkman JK, Jeffrey SW, Nichols PD, Rogers GI, Garland CD. Fatty acid and lipid composition of 10 species of microalgae used in mariculture. *J Exp Mar Biol Ecol*. 1989;128(3):219-40.
169. Belicka LL, Macdonald RW, Harvey HR. Sources and transport of organic carbon to shelf, slope, and basin surface sediments of the Arctic Ocean. *Deep-Sea Res PT I*. 2002;49(8):1463-83.
170. Hu J, Zhang H, Peng Pa. Fatty acid composition of surface sediments in the subtropical Pearl River estuary and adjacent shelf, Southern China. *Estuar Coast Shelf Sci*. 2006;66(1):346-56.
171. Rontani JF, Zabeti N, Wakeham SG. The fate of marine lipids: Biotic vs. abiotic degradation of particulate sterols and alkenones in the Northwestern Mediterranean Sea. *Mar Chem*. 2009;113(1):9-18.
172. Cooper LW, Savvichev AS, Grebmeier JM. Abundance and Production Rates of Heterotrophic Bacterioplankton in the Context of Sediment and Water Column Processes in the Chukchi Sea. *Oceanography*. 2015;28(3):84-99.
173. Davis J, Benner R. Seasonal trends in the abundance, composition and bioavailability of particulate and dissolved organic matter in the Chukchi/Beaufort Seas and western Canada Basin. *Deep-Sea Res PT II*. 2005;52(24):3396-410.
174. Cowie GL, Hedges JI. Sources and reactivities of amino-acids in a coastal marine-environment. *Limnol Oceanogr*. 1992;37(4):703-24.
175. Cowie GL, Hedges JI, Calvert SE. Sources and relative reactivities of amino-acids, neutral sugars, and lignin in an intermittently anoxic marine-environment. *Geochim Cosmochim Acta*. 1992;56(5):1963-78.
176. Sarmiento H, Gasol JM. Use of phytoplankton-derived dissolved organic carbon by different types of bacterioplankton. *Environ Microbiol*. 2012;14(9):2348-60.
177. Fukami K, Simidu U, Taga N. Microbial decomposition of phytoplankton and zooplankton in seawater. 1. Changes in organic matter. *Mar Ecol Prog Ser*. 1985;21(1-2):1-5.
178. Goldman JC, Caron DA, Dennett MR. Regulation of gross growth efficiency and ammonium regeneration in bacteria by substrate C: N ratio1. *Limnol Oceanogr*. 1987;32(6):1239-52.
179. Wakeham SG, Beier JA. Fatty acid and sterol biomarkers as indicators of particulate matter source and alteration processes in the Black Sea. *Deep-Sea Res*. 1991;38:S943-S68.
180. McMahon R, Mikan MP, Harvey HR. Direct analysis of amino acids across multiple marine matrices via ion pairing chromatography and tandem mass spectrometry. *Limnol and Oceanogr: Methods* (in review). 2019.

181. Meyer-Reil L-A. Seasonal and Spatial Distribution of Extracellular Enzymatic Activities and Microbial Incorporation of Dissolved Organic Substrates in Marine Sediments. *Appl Environ Microbiol.* 1987;53(8):1748-55.
182. Gajewski AJ, Chróst RJ. Production and enzymatic decomposition of organic matter by microplankton in a eutrophic lake. *J Plankton Res.* 1995;17(4):709-28.
183. Gupta R, Gupta N, Rathi P. Bacterial lipases: an overview of production, purification and biochemical properties. *Appl Microbiol Biotechnol.* 2004;64(6):763-81.
184. Bornscheuer UT. Microbial carboxyl esterases: classification, properties and application in biocatalysis. *FEMS Microbiol Rev.* 2002;26(1):73-81.
185. Sun M-Y, Shi W, Lee RF. Lipid-degrading enzyme activities associated with distribution and degradation of fatty acids in the mixing zone of Altamaha estuarine sediments. *Org Geochem.* 2000;31(9):889-902.

## APPENDICES

**Appendix 1 - Non-bacterial classes.** List of non-bacterial taxonomic classes that were assigned to peptides in the A) Bering Strait (BSt) and B) Chukchi Sea (CS) metaproteomes. BSt and CS = initial bacterial community sample. aOM = algal organic matter input treatment; POM removal = particulate organic matter removal control.

A)

Non-bacterial classes	Bering Strait						
	BS	aOM input			POM removal		
		day 1	day 6	day 10	day 1	day 6	day 10
Actinopteri	x	x	x	x	x	x	x
Anthozoa	x	x	x	x	x	x	x
Chondrichthyes	x						x
Coscinodiscophyceae		x		x			
Gastropoda		x					x
Liliopsida		x					
Mamiellophyceae	x	x	x	x			x
Mammalia							x

B)

Non-bacterial classes	Chukchi Sea						
	CS	aOM input			POM removal		
		day 1	day 6	day 10	day 1	day 6	day 10
Actinopteri	x	x	x	x		x	x
Anthozoa			x	x			
Chondrichthyes							x
Coscinodiscophyceae							
Gastropoda					NA		x
Liliopsida							
Mamiellophyceae	x	x	x	x		x	x
Mammalia			x				

**Appendix 2 - Presence of bacterial phyla and classes in metaproteome.** Bacterial taxonomic phyla and classes for A) Bering Strait (BSt) and B) Chukchi Sea (CS) with peptide assignments in the metaproteomic dataset. x = presence; n.d. = no mass spectrometry data collected; blank = class not present at that time; Initial bacterial community samples = BSt and CS; aOM input = algal organic matter input; POM removal = substrate limitation within the particulate organic matter (POM) removal control.

A)

Taxonomic phylum	Taxonomic class	Bering Strait (BSt)						
		BSt	aOM input			POM removal		
			day 1	day 6	day 10	day 1	day 6	day 10
Proteobacteria	Acidithiobacillia				x			
Proteobacteria	Alphaproteobacteria	x	x	x	x	x	x	x
Proteobacteria	Betaproteobacteria	x	x	x	x	x	x	x
Proteobacteria	Deltaproteobacteria		x	x	x	x	x	x
Proteobacteria	Epsilonproteobacteria		x	x	x			x
Proteobacteria	Gammaproteobacteria	x	x	x	x	x	x	x
Proteobacteria	Zetaproteobacteria					x		
Bacteroidetes	Bacteroidia	x	x	x	x	x	x	x
Bacteroidetes	Chitinophagia	x	x	x	x	x	x	x
Bacteroidetes	Cytophagia	x	x	x	x	x	x	x
Bacteroidetes	Flavobacteriia	x	x	x	x	x	x	x
Bacteroidetes	Sphingobacteriia	x	x	x	x	x	x	x
Firmicutes	Bacilli		x				x	
Firmicutes	Clostridia			x		x	x	
Firmicutes	Negativicutes		x			x	x	x
Actinobacteria	Acidimicrobiia	x	x	x	x	x	x	x
Actinobacteria	Actinobacteria	x	x	x	x	x	x	x
Chlorobi	Chlorobia							x
Chlorobi	Ignavibacteria		x	x	x	x	x	x
Planctomycetes	Phycisphaerae			x				
Planctomycetes	Planctomycetia		x	x		x		
Aquificae	Aquificae					x		
Deferribacteres	Deferribacteres	x						
Deinococcus–Thermus	Deinococci	x						
Gemmatimonadetes	Gemmatimonadetes		x					x
Lentisphaerae	Lentisphaeria							x
Nitrospinae	Nitrospina	x	x	x	x	x	x	x
Nitrospirae	Nitrospira	x	x					x
Opitutales	Opitutae	x	x	x	x		x	x
Verrucomicrobi	Verrucomicrobiae	x				x	x	x



## Appendix 2 – Continued.

B)

		Chukchi Sea (CS)						
Taxonomic phylum	Taxonomic class	CS	aOM input			POM removal		
			day 1	day 6	day 10	day 1	day 6	day 10
Proteobacteria	Acidithiobacillia				x			
Proteobacteria	Alphaproteobacteria	x	x	x	x	x		x
Proteobacteria	Betaproteobacteria	x	x	x	x	x		x
Proteobacteria	Deltaproteobacteria	x		x	x	x		x
Proteobacteria	Epsilonproteobacteria	x		x	x	x		
Proteobacteria	Gammaproteobacteria	x	x	x	x	x		x
Proteobacteria	Zetaproteobacteria							
Bacteroidetes	Bacteroidia	x		x	x	x		x
Bacteroidetes	Chitinophagia	x		x	x			x
Bacteroidetes	Cytophagia	x	x	x	x	x		x
Bacteroidetes	Flavobacteriia	x	x	x	x	x		x
Bacteroidetes	Sphingobacteriia	x	x	x	x	x		x
Firmicutes	Bacilli							x
Firmicutes	Clostridia	x		x			x	x
Firmicutes	Negativicutes					n.d.		
Actinobacteria	Acidimicrobiia	x	x	x	x		x	x
Actinobacteria	Actinobacteria	x	x	x	x		x	x
Chlorobi	Chlorobia	x					x	x
Chlorobi	Ignavibacteria			x	x			
Planctomycetes	Phycisphaerae							
Planctomycetes	Planctomycetia	x	x	x	x		x	x
Aquificae	Aquificae							
Deferribacteres	Deferribacteres	x					x	x
Deinococcus–Thermus	Deinococci							
Gemmatimonadetes	Gemmatimonadetes			x				x
Lentisphaerae	Lentisphaeria						x	x
Nitrospinae	Nitrospina	x	x	x	x		x	x
Nitrospirae	Nitrospira	x	x	x	x		x	x
Opitutales	Opitutae		x	x	x		x	x
Verrucomicrobi	Verrucomicrobiae	x			x			







## Appendix 3B – Continued.

Bacterial phylum	Bacterial Class	Chukchi Sea (CS) aOM input						POM removal						
		d0	d1	d2	d4	d6	d10	d0	d1	d2	d4	d6	d10	
Chloroflexi	Dehalococcoidia								x					
Chloroflexi	JG30-KF-CM66	x							x	x				x
Chloroflexi	KD4-96													x
Chloroflexi	SAR202_clade	x	x	x	x	x	x	x	x	x	x	x	x	x
Actinobacteria	Acidimicrobiia	x	x	x	x	x	x	x	x	x	x	x	x	x
Actinobacteria	Actinobacteria	x	x	x	x	x	x	x	x	x	x	x	x	x
Actinobacteria	Actinobacteria_unclassified		x					x	x	x	x			
Candidate_division_OP3	Candidate_division_OP3_unclassified	x	x	x	x	x		x	x	x	x	x	x	x
Candidate_division_SR1	Candidate_division_SR1_unclassified													
Candidate_division_WS6	Candidate_division_WS6_unclassified		x						x					
Firmicutes	Bacilli		x	x									x	x
Firmicutes	Clostridia	x			x				x					x
Firmicutes	Negativicutes		x											
Cyanobacteria	Cyanobacteria						x							
Cyanobacteria	ML635J-21	x	x	x		x	x	x	x	x	x	x	x	x
Bacteria_unclassified	Bacteria_unclassified	x	x	x	x	x	x	x	x	x	x	x	x	x
Chlamydiae	Chlamydiae	x	x	x	x	x	x	x	x	x	x	x	x	x
Fibrobacteres	Fibrobacteria	x	x	x	x		x	x	x	x			x	x
Fusobacteria	Fusobacteriia	x												
Gemmatimonadetes	Gemmatimonadetes	x	x	x	x	x		x	x	x	x	x	x	x
Gracilibacteria	Gracilibacteria_unclassified	x	x	x	x	x	x	x	x	x	x	x	x	x
Hydrogenedentes	Hydrogenedentes_unclassified	x	x			x	x	x						x
Marinimicrobia_(SAR406_clade)	Marinimicrobia_(SAR406_clade)_unclassified	x	x	x	x	x	x	x	x	x	x	x	x	x
Microgenomates	Microgenomates_unclassified	x												x
Nitrospirae	Nitrospira	x	x	x					x	x	x	x		
Omnitrophica	NPL-UPA2	x	x	x				x	x		x	x		
Parcubacteria	Parcubacteria_unclassified	x	x	x	x			x	x	x	x	x	x	x
PAUC34f	PAUC34f_unclassified	x	x	x				x	x	x	x	x	x	x
Saccharibacteria	Saccharibacteria_unclassified	x	x					x	x	x				x
Spirochaetae	Spirochaetes	x							x					
Tenericutes	Mollicutes	x	x	x				x	x	x	x	x		
TM6	TM6_unclassified		x											
WCHB1-60	WCHB1-60_unclassified								x					

**Appendix 4 – SIMPER analysis.** An analysis of similarity percentages (SIMPER) of free-living bacterial operational taxonomic units (OTUs) from 16S rRNA sequencing, representing 80% of the difference in taxonomic composition between microbiomes. Analysis was run with all samples. Uncl = unclassified.

SIMPER %	phylum	class	order	family	genus
11.68	Proteobacteria	Gammaproteobacteria	Oceanospirillales	Oceanospirillaceae	Balneatrix
11.39	Bacteroidetes	Flavobacteriia	Flavobacteriales	Flavobacteriaceae	Polaribacter
10.48	Proteobacteria	Gammaproteobacteria	Oceanospirillales	Oceanospirillales_uncl	Oceanospirillales_uncl
6.20	Proteobacteria	Alphaproteobacteria	SAR11_clade	Surface_1	Surface_1_uncl
4.59	Proteobacteria	Alphaproteobacteria	Rhodobacterales	Rhodobacteraceae	Sulfitobacter
3.24	Bacteroidetes	Flavobacteriia	Flavobacteriales	Cryomorphaceae	Owenweeksia
3.04	Proteobacteria	Gammaproteobacteria	Cellvibrionales	Porticocceae	SAR92_clade
2.75	Proteobacteria	Gammaproteobacteria	Alteromonadales	Colwelliaceae	Colwelliaceae_uncl
2.49	Proteobacteria	Alphaproteobacteria	Rhodobacterales	Rhodobacteraceae	Rhodobacteraceae_uncl
2.36	Proteobacteria	Gammaproteobacteria	Alteromonadales	Colwelliaceae	Colwellia
1.55	Bacteroidetes	Flavobacteriia	Flavobacteriales	Flavobacteriaceae	Flavobacteriaceae_uncl
1.44	Proteobacteria	Gammaproteobacteria	Oceanospirillales	OM182_clade	OM182_clade_uncl
1.44	Proteobacteria	Deltaproteobacteria	SAR324_clade(Marine_group_B)	SAR324_clade(Marine_group_B)_uncl	SAR324_clade(Marine_group_B)_uncl
1.31	Bacteroidetes	Flavobacteriia	Flavobacteriales	Flavobacteriaceae	Ulvibacter
1.02	Bacteroidetes	Flavobacteriia	Flavobacteriales	Flavobacteriaceae	NS4_marine_group
0.98	Proteobacteria	Deltaproteobacteria	Desulfobacterales	Nitrospinaceae	Nitrospina
0.87	Bacteroidetes	Flavobacteriia	Flavobacteriales	Flavobacteriaceae	Formosa
0.77	Proteobacteria	Gammaproteobacteria	Oceanospirillales	SAR86_clade	SAR86_clade_uncl
0.74	Bacteroidetes	Flavobacteriia	Flavobacteriales	NS9_marine_group	NS9_marine_group_uncl
0.73	Proteobacteria	Gammaproteobacteria	Oceanospirillales	Oceanospirillaceae	Reinekea
0.72	Proteobacteria	Gammaproteobacteria	Oceanospirillales	Oceanospirillaceae	Pseudospirillum
0.69	Bacteroidetes	Flavobacteriia	Flavobacteriales	Flavobacteriaceae	NS5_marine_group
0.57	Bacteroidetes	Sphingobacteriia	Sphingobacteriales	NS11-12_marine_group	NS11-12_marine_group_uncl
0.51	Proteobacteria	Alphaproteobacteria	Rhodobacterales	Rhodobacteraceae	Planktomarina
0.49	Proteobacteria	Gammaproteobacteria	Alteromonadales	Pseudoalteromonadaceae	Pseudoalteromonas
0.46	Proteobacteria	Proteobacteria_uncl	Proteobacteria_uncl	Proteobacteria_uncl	Proteobacteria_uncl
0.44	Proteobacteria	Alphaproteobacteria	SAR11_clade	SAR11_clade_uncl	SAR11_clade_uncl
0.41	Bacteroidetes	Flavobacteriia	Flavobacteriales	Flavobacteriaceae	NS3a_marine_group
0.39	Proteobacteria	Epsilonproteobacteria	Campylobacteriales	Campylobacteraceae	Arcobacter

## Appendix 4 – Continued.

SIMPER %	phylum	class	order	family	genus
0.34	Actinobacteria	Acidimicrobiia	Acidimicrobiales	Sva0996_marine_group	Sva0996_marine_group_uncl
0.32	Proteobacteria	Gammaproteobacteria	Pseudomonadales	Moraxellaceae	Acinetobacter
0.32	Proteobacteria	Betaproteobacteria	Methylophilales	Methylophilaceae	Methylothera
0.31	Proteobacteria	Gammaproteobacteria	Oceanospirillales	Oceanospirillaceae	Oceanospirillaceae_uncl
0.28	Proteobacteria	Gammaproteobacteria	Order_Incertae_Sedis	Family_Incertae_Sedis	Marinicella
0.27	Proteobacteria	Gammaproteobacteria	Thiotrichales	Piscirickettsiaceae	Piscirickettsiaceae_uncl
0.26	Proteobacteria	Gammaproteobacteria	Alteromonadales	Alteromonadaceae	Paraglacicola
0.26	Planctomycetes	OM190	OM190_uncl	OM190_uncl	OM190_uncl
0.23	Proteobacteria	Alphaproteobacteria	SAR11_clade	Surface_2	Surface_2_uncl
0.22	Bacteroidetes	Flavobacteriia	Flavobacteriales	Flavobacteriaceae	Wenylingzhuangia
0.22	Proteobacteria	Gammaproteobacteria	Oceanospirillales	Oceanospirillaceae	Oleispira
0.21	Bacteroidetes	Flavobacteriia	Flavobacteriales	Flavobacteriaceae	NS2b_marine_group
0.21	Bacteria_uncl	Bacteria_uncl	Bacteria_uncl	Bacteria_uncl	Bacteria_uncl
0.21	Marinimicrobia (SAR406_clade)	Marinimicrobia (SAR406_clade)_uncl	Marinimicrobia (SAR406_clade)_uncl	Marinimicrobia (SAR406_clade)_uncl	Marinimicrobia (SAR406_clade)_uncl
0.21	Proteobacteria	Alphaproteobacteria	Rhodospirillales	Rhodospirillaceae	AEGEAN-169_marine_group
0.21	Proteobacteria	Alphaproteobacteria	Rhodospirillales	Rhodospirillaceae	Defluviococcus
0.19	Proteobacteria	Alphaproteobacteria	Rhodospirillales	Rhodospirillaceae	Rhodospirillaceae_uncl
0.17	Proteobacteria	Gammaproteobacteria	Chromatiales	Chromatiaceae	Rheinheimera
0.15	Proteobacteria	Betaproteobacteria	Methylophilales	Methylophilaceae	OM43_clade
0.14	Proteobacteria	Alphaproteobacteria	Rickettsiales	SAR116_clade	SAR116_clade_uncl
0.14	Proteobacteria	Alphaproteobacteria	SAR11_clade	Chesapeake-Delaware_Bay	Chesapeake-Delaware_Bay_uncl
0.13	Bacteroidetes	Flavobacteriia	Flavobacteriales	Cryomorphaceae	NS10_marine_group
0.13	Proteobacteria	Betaproteobacteria	Burkholderiales	Comamonadaceae	BAL58_marine_group
0.13	Proteobacteria	Alphaproteobacteria	SAR11_clade	Surface_4	Surface_4_uncl
0.13	Proteobacteria	Gammaproteobacteria	Thiotrichales	Thiotrichaceae	Thiothrix
0.12	Bacteroidetes	Cytophagia	Cytophagales	Flammeovirgaceae	Fabibacter
0.12	Bacteroidetes	Cytophagia	Cytophagales	Flammeovirgaceae	Marinoscillum
0.11	Proteobacteria	Alphaproteobacteria	OCS116_clade	OCS116_clade_uncl	OCS116_clade_uncl
0.11	Actinobacteria	Acidimicrobiia	Acidimicrobiales	Acidimicrobiaceae	Illumatobacter
0.10	Actinobacteria	Actinobacteria	Micrococcales	Microbacteriaceae	Candidatus_Aquiluna
0.09	Proteobacteria	Alphaproteobacteria	SB1-18	SB1-18_uncl	SB1-18_uncl
0.09	Proteobacteria	Alphaproteobacteria	Rhodobacterales	Rhodobacteraceae	Asciadiaceihabitans
0.07	Chloroflexi	SAR202_clade	SAR202_clade_uncl	SAR202_clade_uncl	SAR202_clade_uncl
0.07	Proteobacteria	Gammaproteobacteria	Alteromonadales	Alteromonadaceae	Alteromonas
0.06	Proteobacteria	Gammaproteobacteria	Oceanospirillales	ZD0405	ZD0405_uncl
0.06	Proteobacteria	Gammaproteobacteria	BD7-8_marine_group	BD7-8_marine_group_uncl	BD7-8_marine_group_uncl
0.06	Actinobacteria	Actinobacteria	PeM15	PeM15_uncl	PeM15_uncl

**Appendix 5 - Bray-Curtis dissimilarity matrix.** Bray-Curtis dissimilarity matrix comparing the free-living bacterial community compositions of each microbiome, Bering Strait (BSt) and Chukchi Sea (CS), under both organic perturbations (particulate organic matter removal (POMr) or algal organic matter input (aOM)) on each day (d0, d1, d2, d4, d6, d10). Comparisons were based on normalized 16S rRNA operational taxonomic units (OTUs).

	BSt_d0_ POMr	BSt_d1_ POMr	BSt_d2_ POMr	BSt_d4_ POMr	BSt_d6_ POMr	BSt_d10_ POMr
BSt_d0_POMr	0	0.229877964	0.307468899	0.513042768	0.323761393	0.328396283
BSt_d1_POMr	0.229877964	0	0.156080472	0.525846147	0.21550968	0.245519044
BSt_d2_POMr	0.307468899	0.156080472	0	0.501297051	0.191583637	0.242197493
BSt_d4_POMr	0.513042768	0.525846147	0.501297051	0	0.400623405	0.384979517
BSt_d6_POMr	0.323761393	0.21550968	0.191583637	0.400623405	0	0.134853218
BSt_d10_POMr	0.328396283	0.245519044	0.242197493	0.384979517	0.134853218	0
BSt_d0_aOM	0.115894102	0.237866279	0.324115112	0.544321982	0.347762241	0.355333023
BSt_d1_aOM	0.201312916	0.142527898	0.205964021	0.475199096	0.211163541	0.231142286
BSt_d2_aOM	0.381602862	0.224370905	0.146659037	0.491828413	0.210857274	0.262881519
BSt_d4_aOM	0.436614563	0.283127287	0.223912445	0.500537259	0.26553018	0.300900291
BSt_d6_aOM	0.486225044	0.331323184	0.279405862	0.491123836	0.291467002	0.322368173
BSt_d10_aOM	0.4788129	0.336778315	0.287390299	0.492244582	0.285133158	0.306358466
CS_d0_POMr	0.550083258	0.655968064	0.720147989	0.821975014	0.731975654	0.725747062
CS_d1_POMr	0.55349765	0.658332174	0.72115743	0.825374661	0.734852857	0.729162145
CS_d2_POMr	0.527598105	0.628356653	0.692604032	0.788155038	0.701539743	0.695488845
CS_d4_POMr	0.508318267	0.60900924	0.671457631	0.764539783	0.679789813	0.673178465
CS_d6_POMr	0.506855309	0.604418768	0.666573521	0.764116166	0.674921143	0.666967777
CS_d10_POMr	0.664229151	0.685118397	0.679897489	0.596743568	0.664207913	0.662318541
CS_d0_aOM	0.54246095	0.649231771	0.713878548	0.813338545	0.723582228	0.715663568
CS_d1_aOM	0.535011112	0.639019942	0.708069329	0.806437935	0.717060381	0.709643706
CS_d2_aOM	0.501172063	0.602417033	0.668036505	0.761625439	0.67751054	0.670874798
CS_d4_aOM	0.703075604	0.639945246	0.61516597	0.758856139	0.638657324	0.663478217
CS_d6_aOM	0.713846631	0.641077829	0.614463634	0.746746783	0.638695249	0.659712279
CS_d10_aOM	0.698413501	0.62415299	0.59893509	0.732029619	0.621197347	0.643226006



## Appendix 5 – Continued.

	BSt_d0_ aOM	BSt_d1_ aOM	BSt_d2_ aOM	BSt_d4_ aOM	BSt_d6_ aOM	BSt_d10_ aOM
BSt_d0_POMr	0.115894102	0.201312916	0.381602862	0.436614563	0.486225044	0.4788129
BSt_d1_POMr	0.237866279	0.142527898	0.224370905	0.283127287	0.331323184	0.336778315
BSt_d2_POMr	0.324115112	0.205964021	0.146659037	0.223912445	0.279405862	0.287390299
BSt_d4_POMr	0.544321982	0.475199096	0.491828413	0.500537259	0.491123836	0.492244582
BSt_d6_POMr	0.347762241	0.211163541	0.210857274	0.26553018	0.291467002	0.285133158
BSt_d10_POMr	0.355333023	0.231142286	0.262881519	0.300900291	0.322368173	0.306358466
BSt_d0_aOM	0	0.223685728	0.400221515	0.456794647	0.496980273	0.494583218
BSt_d1_aOM	0.223685728	0	0.25333392	0.318522922	0.356683666	0.36034554
BSt_d2_aOM	0.400221515	0.25333392	0	0.15174701	0.204542467	0.216851824
BSt_d4_aOM	0.456794647	0.318522922	0.15174701	0	0.119748141	0.179245368
BSt_d6_aOM	0.496980273	0.356683666	0.204542467	0.119748141	0	0.154356912
BSt_d10_aOM	0.494583218	0.36034554	0.216851824	0.179245368	0.154356912	0
CS_d0_POMr	0.533788936	0.640304967	0.766824889	0.820235356	0.842500342	0.822829583
CS_d1_POMr	0.53709832	0.64362785	0.766448645	0.819833872	0.843710308	0.825098701
CS_d2_POMr	0.51290577	0.612965407	0.739046058	0.79260334	0.81576768	0.797341467
CS_d4_POMr	0.497519629	0.591692423	0.717501454	0.770491646	0.791945144	0.7753631
CS_d6_POMr	0.488945922	0.589220377	0.714087018	0.76811408	0.790394336	0.769451305
CS_d10_POMr	0.677232118	0.673030791	0.683024326	0.691008344	0.700464362	0.710031558
CS_d0_aOM	0.526727408	0.632812697	0.760803095	0.813728399	0.83626755	0.815379944
CS_d1_aOM	0.518012766	0.62183509	0.754098968	0.806890176	0.828562221	0.808806313
CS_d2_aOM	0.488119527	0.58500191	0.705890114	0.755214873	0.7765378	0.760496195
CS_d4_aOM	0.692400977	0.666663602	0.590012616	0.556518868	0.567006109	0.559921042
CS_d6_aOM	0.702919786	0.672248999	0.58495704	0.542642939	0.531123316	0.547261367
CS_d10_aOM	0.68944404	0.657328315	0.568601004	0.52564779	0.52366664	0.529189216

## Appendix 5 – Continued.

	CS_d0_ POMr	CS_d1_ POMr	CS_d2_ POMr	CS_d4_ POMr	CS_d6_ POMr	CS_d10_ POMr
BSt_d0_POMr	0.550083258	0.55349765	0.527598105	0.508318267	0.506855309	0.664229151
BSt_d1_POMr	0.655968064	0.658332174	0.628356653	0.60900924	0.604418768	0.685118397
BSt_d2_POMr	0.720147989	0.72115743	0.692604032	0.671457631	0.666573521	0.679897489
BSt_d4_POMr	0.821975014	0.825374661	0.788155038	0.764539783	0.764116166	0.596743568
BSt_d6_POMr	0.731975654	0.734852857	0.701539743	0.679789813	0.674921143	0.664207913
BSt_d10_POMr	0.725747062	0.729162145	0.695488845	0.673178465	0.666967777	0.662318541
BSt_d0_aOM	0.533788936	0.53709832	0.51290577	0.497519629	0.488945922	0.677232118
BSt_d1_aOM	0.640304967	0.64362785	0.612965407	0.591692423	0.589220377	0.673030791
BSt_d2_aOM	0.766824889	0.766448645	0.739046058	0.717501454	0.714087018	0.683024326
BSt_d4_aOM	0.820235356	0.819833872	0.79260334	0.770491646	0.76811408	0.691008344
BSt_d6_aOM	0.842500342	0.843710308	0.81576768	0.791945144	0.790394336	0.700464362
BSt_d10_aOM	0.822829583	0.825098701	0.797341467	0.7753631	0.769451305	0.710031558
CS_d0_POMr	0	0.115048176	0.179959662	0.261054363	0.207442572	0.675634844
CS_d1_POMr	0.115048176	0	0.159069849	0.257345763	0.213104097	0.69128317
CS_d2_POMr	0.179959662	0.159069849	0	0.183316337	0.139915946	0.644839297
CS_d4_POMr	0.261054363	0.257345763	0.183316337	0	0.197592382	0.601225801
CS_d6_POMr	0.207442572	0.213104097	0.139915946	0.197592382	0	0.619411043
CS_d10_POMr	0.675634844	0.69128317	0.644839297	0.601225801	0.619411043	0
CS_d0_aOM	0.086613506	0.127689317	0.184481911	0.265942967	0.213156239	0.659716202
CS_d1_aOM	0.110032245	0.145350369	0.188016868	0.263559048	0.191913374	0.660774348
CS_d2_aOM	0.172959249	0.184646622	0.145450796	0.204088252	0.164752024	0.600394769
CS_d4_aOM	0.683585297	0.690932166	0.628282518	0.602829753	0.607640299	0.632192915
CS_d6_aOM	0.732882445	0.736596742	0.69071955	0.666092734	0.669231936	0.655350184
CS_d10_aOM	0.719277789	0.725358784	0.686786071	0.662182131	0.662075799	0.646761493

## Appendix 5 – Continued.

	CS_d0_aOM	CS_d1_aOM	CS_d2_aOM	CS_d4_aOM	CS_d6_aOM	CS_d10_aOM
BSt_d0_POMr	0.54246095	0.535011112	0.501172063	0.703075604	0.713846631	0.698413501
BSt_d1_POMr	0.649231771	0.639019942	0.602417033	0.639945246	0.641077829	0.62415299
BSt_d2_POMr	0.713878548	0.708069329	0.668036505	0.61516597	0.614463634	0.59893509
BSt_d4_POMr	0.813338545	0.806437935	0.761625439	0.758856139	0.746746783	0.732029619
BSt_d6_POMr	0.723582228	0.717060381	0.67751054	0.638657324	0.638695249	0.621197347
BSt_d10_POMr	0.715663568	0.709643706	0.670874798	0.663478217	0.659712279	0.643226006
BSt_d0_aOM	0.526727408	0.518012766	0.488119527	0.692400977	0.702919786	0.68944404
BSt_d1_aOM	0.632812697	0.62183509	0.58500191	0.666663602	0.672248999	0.657328315
BSt_d2_aOM	0.760803095	0.754098968	0.705890114	0.590012616	0.58495704	0.568601004
BSt_d4_aOM	0.813728399	0.806890176	0.755214873	0.556518868	0.542642939	0.52564779
BSt_d6_aOM	0.83626755	0.828562221	0.7765378	0.567006109	0.531123316	0.52366664
BSt_d10_aOM	0.815379944	0.808806313	0.760496195	0.559921042	0.547261367	0.529189216
CS_d0_POMr	0.086613506	0.110032245	0.172959249	0.683585297	0.732882445	0.719277789
CS_d1_POMr	0.127689317	0.145350369	0.184646622	0.690932166	0.736596742	0.725358784
CS_d2_POMr	0.184481911	0.188016868	0.145450796	0.628282518	0.69071955	0.686786071
CS_d4_POMr	0.265942967	0.263559048	0.204088252	0.602829753	0.666092734	0.662182131
CS_d6_POMr	0.213156239	0.191913374	0.164752024	0.607640299	0.669231936	0.662075799
CS_d10_POMr	0.659716202	0.660774348	0.600394769	0.632192915	0.655350184	0.646761493
CS_d0_aOM	0	0.101781246	0.164064575	0.678018511	0.727348325	0.714208869
CS_d1_aOM	0.101781246	0	0.166339176	0.667795855	0.71509757	0.705603989
CS_d2_aOM	0.164064575	0.166339176	0	0.588958096	0.637489996	0.632084806
CS_d4_aOM	0.678018511	0.667795855	0.588958096	0	0.203802958	0.208026164
CS_d6_aOM	0.727348325	0.71509757	0.637489996	0.203802958	0	0.114430533
CS_d10_aOM	0.714208869	0.705603989	0.632084806	0.208026164	0.114430533	0

**Appendix 6 – Shannon diversity index.** Shannon diversity index values per microbiome (BSt = Bering Strait; CS = Chukchi Sea), treatment (POM removal = control where particulate organic matter was removed without subsequent addition of algal substrates; aOM = treatment where algal organic matter was added (aOM input)), and time (days 0, 1, 2, 4, 6, 10).

Microbiome	Treatment	Day	Shannon Diversity
BSt	POM removal	0	4.75
BSt	POM removal	1	4.76
BSt	POM removal	2	4.78
BSt	POM removal	4	4.82
BSt	POM removal	6	4.64
BSt	POM removal	10	4.84
BSt	aOM input	0	4.75
BSt	aOM input	1	4.67
BSt	aOM input	2	4.61
BSt	aOM input	4	4.46
BSt	aOM input	6	4.47
BSt	aOM input	10	4.67
CS	POM removal	0	4.18
CS	POM removal	1	4.33
CS	POM removal	2	4.38
CS	POM removal	4	4.47
CS	POM removal	6	4.58
CS	POM removal	10	4.68
CS	aOM input	0	4.21
CS	aOM input	1	4.20
CS	aOM input	2	4.42
CS	aOM input	4	3.68
CS	aOM input	6	4.23
CS	aOM input	10	4.33

## SUPPLEMENTAL MATERIALS

**Supplementary text 1 - Materials and Methods.** A complete description of all materials and methods that were used in Chapter 2, however separated from the main text due to space limitations for a manuscript submission to The ISME Journal: Multidisciplinary Journal of Microbial Ecology.

**Dataset 1 – Complete taxonomic inventory of peptide spectra for Bering Strait, algal organic matter (aOM) inputs.** Each Excel Workbook file represents the metaproteomic data collected for all time points (initial, T0, T1, T6 & T10; separated by worksheets within workbook) from a particular experimental incubation (i.e., Bering St aOM, ChukSea aOM, Bering St particulate organic matter control (POM removal), ChukSea POM removal). Each worksheet contains the total number of spectra that correlate to each Gene Ontology term as broken down by taxonomic level. Column headers: GO Accession: Gene Ontology accession number (e.g., GO:0016887), GO Name: given name of the Gene Ontology category (e.g., ATPase activity), GO Aspect: 1 of 3 GO broad categories: molecular function, biological process, cellular component, Taxonomy ID: Uniprot defined taxonomic identification number (i.e., 135619 = Oceanospirillaceae), Taxonomy Name: Uniprot defined taxonomic name at defined taxonomic rank (i.e., Oceanospirillaceae; rank= order), Taxonomy Rank: taxonomic rank, Taxonomy PSM Count: total number of peptide spectral matches that correlate to defined gene ontology term at the defined taxonomic level (rank) (i.e., integers 1-*n*), Taxonomy PSM Ratio: the ratio of PSMs for the defined GO term at the specified taxonomic rank to the total number of PSMs for all taxonomic ranks (i.e.,  $\leq 1$ ). The taxonomic name “root” is a term that indicates it represents all taxonomic levels (superkingdom through species) and is listed as “no rank” under Taxonomic rank. Example: ATPase activity has 91 PSMs at the no rank Taxonomic rank, and of those, 12 PSMs correlate to Oceanospirillaceae (rank= order). The Taxonomy PSM ratio for Oceanospirillaceae is  $12/91 = 0.14$ , or 14% of the ATPase activity peptide spectral matches can be correlated to the order Oceanospirillaceae. Unambiguous taxonomic classification per GO function at each taxonomic level is reported. Some peptides had a least common ancestor assignment at a less granular classification or had no taxonomic information; when the sum of PSM Ratios for any taxonomic level (e.g., class) per function was less than 1, the difference makes up the Unclassified taxonomic category.

**Dataset 2 - Complete taxonomic inventory of peptide spectra for Bering Strait, particulate organic matter (POM) removal.** Legend description is identical to Dataset 1.

**Dataset 3- Complete taxonomic inventory of peptide spectra for Chukchi Sea, algal organic matter (aOM) inputs.** Legend description is identical to Dataset 1.

**Dataset 4 - Complete taxonomic inventory of peptide spectra for Chukchi Sea, particulate organic matter (POM) removal.** Legend description is identical to Dataset 1.

**Dataset 5 – Relative abundance of 16S rRNA sequences to the level of genus.** BSt = Bering Strait microbiome; CS = Chukchi Sea microbiome; Days 0-10 (T0, T1, T2, T4, T6, T10); Organic matter perturbations (POMr = particulate organic matter removal; aOM = algal organic matter input).

## VITA

Molly P. Mikan

Department of Ocean, Earth & Atmospheric Sciences, Old Dominion University  
406 Oceanography & Physical Sciences Building, Norfolk, VA 23529

Education

- 
- Ph.D.**, Oceanography Expected May, 2019  
 Ocean, Earth and Atmospheric Sciences  
*Old Dominion University* *Norfolk, VA*  
 Dissertation title: Coupling metaproteomics with taxonomy to determine responses of  
 bacterioplankton to organic perturbations in the Western Arctic Ocean
- M.S.**, Marine Organic Geochemistry 2012  
 Marine, Earth and Atmospheric Sciences  
*North Carolina State University* *Raleigh, NC*  
 Thesis title: Characterization of seasonal and tidal cycling of dissolved and particulate organic  
 matter fluorescence in a coastal salt marsh ecosystem in Eastern North Carolina using parallel  
 factor (PARAFAC) analysis
- B.S.**, Natural Resource Management 2004  
 Concentration in Conservation Biology  
*Colorado State University* *Fort Collins, CO*

Peer Reviewed Publications

- 
- Timmins-Schiffman, E., **M. P. Mikan**, Y. S. Ting, H. R. Harvey and B. L. Nunn (2018). MS  
 analysis of a dilution series of bacteria:phytoplankton to improve detection of low  
 abundance bacterial peptides. *Scientific Reports*, 8(1): 9276.
- Riffle, M., May, D. H., Timmins-Schiffman, E., **Mikan, M. P.**, Jaschob, D., Noble, W. S., &  
 Nunn, B. L. (2018). MetaGomics: A Web-Based Tool for Peptide-Centric Functional  
 and Taxonomic Analysis of Metaproteomics Data. *Proteomes*, 6(1).
- Timmins-Schiffman, E., May, D. H., **Mikan, M.**, Riffle, M., Frazar, C., Harvey, H. R., . . .  
 Nunn, B. L. (2016). Critical decisions in metaproteomics: achieving high confidence  
 protein annotations in a sea of unknowns. *Isme Journal*, 11(2), 309-314.
- May, D. H., Timmins-Schiffman, E., **Mikan, M. P.**, Harvey, H. R., Borenstein, E., Nunn, B. L.,  
 & Noble, W. S. (2016). An Alignment-Free "Metapeptide" Strategy for Metaproteomic  
 Characterization of Microbiome Samples Using Shotgun Metagenomic Sequencing.  
*Journal of Proteome Research*, 15(8), 2697-2705.
- Osburn, C. L., **Mikan, M. P.**, Etheridge, J. R., Burchell, M. R., & Birgand, F. (2015). Seasonal  
 variation in the quality of dissolved and particulate organic matter exchanged between a  
 salt marsh and its adjacent estuary. *Journal of Geophysical Research-Biogeosciences*,  
 120(7), 1430-1449.
- Osburn, C. L., Handsel, L. T., **Mikan, M. P.**, Paerl, H. W., & Montgomery, M. T. (2012).  
 Fluorescence Tracking of Dissolved and Particulate Organic Matter Quality in a River-  
 Dominated Estuary. *Environmental Science & Technology*, 46(16), 8628-8636.